

T 1591

THERMODYNAMIC AND KINETIC
CONSIDERATIONS IN THE HYDROGEN REDUCTION
OF NICKEL FROM AMMONIACAL SOLUTIONS

by

Victor M. Perez

ProQuest Number: 10781866

All rights reserved

INFORMATION TO ALL USERS

The quality of this reproduction is dependent upon the quality of the copy submitted.

In the unlikely event that the author did not send a complete manuscript and there are missing pages, these will be noted. Also, if material had to be removed, a note will indicate the deletion.



ProQuest 10781866

Published by ProQuest LLC (2018). Copyright of the Dissertation is held by the Author.

All rights reserved.

This work is protected against unauthorized copying under Title 17, United States Code
Microform Edition © ProQuest LLC.

ProQuest LLC.
789 East Eisenhower Parkway
P.O. Box 1346
Ann Arbor, MI 48106 – 1346

A thesis submitted to the Faculty and the Board of Trustees of the Colorado School of Mines in partial fulfillment of the requirements for the degree of Master of Science.

Signed: Victor M. Pérez
Victor M. Pérez

Golden, Colorado

Date: Aug. 28, 1973

ARTHUR LAKES LIBRARY
COLORADO SCHOOL OF MINES
GOLDEN, COLORADO

Approved: G. P. Martins
G. P. Martins
Thesis Advisor

J. P. Hager
J. P. Hager
Head, Department of
Metallurgical Engineering

Golden, Colorado

Date: Aug. 28, 1973

ABSTRACT

The problem of reduction of nickel from ammoniacal solutions has been examined both theoretically and experimentally. In the course of the experimental work with a rotating disc (Ni, and oxidized Ti) it was found that the precipitation reaction gives a linear relationship between total nickel in solution and time. An apparent activation energy for the reaction of 8 Kcal-mol^{-1} was calculated. It appears that adsorption of hydrogen onto the catalytic surface saturates the active sites present. Rotational speed had little or no effect on the reaction. The value of the activation energy as well as the absence of any effect of rotational speed suggests a chemical control reaction. Both the surface treatment and temperature have important effects on the reaction rate. The theoretical work was focused on the determination of the species stabilities at high temperatures by using room temperature data and extrapolated to high temperatures according to the Correspondence Principle of Criss and Cobble. Also, a mathematical simulation of hydrogen reduction was carried out both at room and high temperature. The pH prediction by this simulation did not quite agree with the room temperature measurements during the course of the experiment. However, they exhibit the same trends as the experimental runs.

TABLE OF CONTENTS

	Page
ABSTRACT.	iii
TABLE OF CONTENTS	iv
LIST OF FIGURES	vi
LIST OF TABLES.	ix
ACKNOWLEDGEMENTS.	x
CHAPTER 1 INTRODUCTION	<u>1</u>
1.1 Scope of the Problem.	3
1.2 Scope of this Study	4
1.3 Aim of this Study	5
CHAPTER 2 LITERATURE REVIEW.	<u>6</u>
2.1 Early Works	6
2.2 Recent Advances	8
CHAPTER 3 THEORETICAL CONSIDERATIONS	<u>18</u>
3.1 Metal-Hydrogen Electrode Potentials .	18
3.2 Effect of Complex Formations at Room Temperature	24
3.3 Application of Correspondence Principle	27
3.4 Pourbaix Diagrams	40
3.5 General Kinetic Considerations.	44
3.6 Transport - Control	48
3.7 Chemical Control.	50
CHAPTER 4 EXPERIMENTAL APPARATUS AND PROCEDURE . . .	<u>55</u>
4.1 Apparatus	55
4.2 Materials	64
4.3 Procedure	64
CHAPTER 5 RESULTS.	<u>67</u>
5.1 Precipitation Rate Curves	67
5.2 Effect of Disc and Disc Preparation .	68

	Page
5.3 Effect of Rotational Speed	79
5.4 Effect of Temperature.	81
5.5 Effect of Hydrogen Partial Pressure.	84
5.6 Prediction of System Behavior.	89
CHAPTER 6 CONCLUSIONS.	<u>109</u>
6.1 Discussion and Summary	109
6.2 Suggestions for Future Work.	111
APPENDIX I EQUATIONS EXPRESSING EQUILIBRIA.	113
Species Distribution	113
Simulated Hydrogen Reduction	115
APPENDIX II DERIVATIVES FOR NEWTON-RAPHSON SCHEME . .	116
Species Distribution	116
Simulated Hydrogen Reduction	117
APPENDIX III.	118
Computer Porgram to Calculate Species Distribution	118
APPENDIX IV	121
Computer Program for Simulation of Hydrogen Reduction.	121
REFERENCES.	124

LIST OF FIGURES

Figure	Page
3.1 Relationship between E and the concentration of hydrogen ions at pressures of 1,100 atm. and of nickel ions and the nickel amines $\text{Ni}(\text{NH}_3)_n^{++}$ at 25°C.	23
3.2 Fraction of nickel present in each form at different ammonia-to-nickel ratios, 25°C	28
3.3 Fraction of nickel present in each form at different ammonia-to-nickel ratios, 100°C.	34
3.4 Fraction of nickel present in each form at different ammonia-to-nickel ratios, 200°C.	35
3.5 Fraction of nickel present in each form at different ammonia-to-nickel ratios, 250°C.	36
3.6 Fraction of nickel present in each form at different ammonia-to-nickel ratios, 300°C.	37
3.7 Relationship between E and pH at hydrogen pressures of 1,100 atm. and of nickel ions and the nickel amines $\text{Ni}(\text{NH}_3)_n^{++}$, 200°C.	38
3.8 Relationship between E and pH at hydrogen pressures of 1,100 atm. and of nickel ions and the nickel-ammines $\text{Ni}(\text{NH}_3)_n^{++}$, 300°C.	39
3.9 Difference obtained by accounting for activity coefficients	41
3.10 Equilibrium diagram for the system Ni-H ₂ O-NH ₃ for 25°C, 1 atm. pressure, and activities for nickel ions and nickel hydroxide: 10 ⁻⁶ M.	42
3.11 Equilibrium diagram for the system Ni-H ₂ O-NH ₃ for 200°C, 1 atm. pressure, and activities for nickel ions and nickel hydroxide: 10 ⁻⁶ M.	43

Figure	Page
4.1 A schematic diagram of the system.	59
4.2 Photographic views of the equipment.	60
4.3 Close-up view of autoclave head showing bearing housing with disc holder and shaft in place. Thermocouple is on the right and the sampling tube is on the left.	61
4.4 Photographic view of disc holders.	62
4.5 Photographs of discs and nickel powder (a) (b) (d) - Reacted nickel disc (c) - Unreacted nickel disc (e) - Oxidized titanium disc (f) - Nickel powder.	63
5.1 Typical reduction curves obtained under different conditions	72
5.2 Precipitation rate curves for oxidized titanium discs.	73
5.3 Precipitation rate curves for nickel discs treated in hydroxide atmosphere.	74
5.4 Precipitation rate curves for nickel discs electrochemically treated	76
5.5 Precipitation rate curves for nickel discs under different conditions of rotation	77
5.6 Strip chart recording of solution temperature during run NIEH11.	83
5.7 Precipitation rate curves for nickel discs as temperature is varied.	85
5.8 Variation of precipitation rate as temperature is constantly increased	86
5.9 pH predicted and measured for concentrations between .01 M and .001 M	91

Figure	Page
5.10 Nickel ion in solution as the total nickel decreases as a result of the reduction at 25°C, 200°C for a ratio of ammonia-to-nickel of 2.2	93
5.11 Nickel ion in solution as the total nickel decreases as a result of the reduction at 25°C and 200°C for an initial ammonia-to-nickel ratio of 1.2.	94
5.12 Fraction of nickel present in each form for an ammonia-nickel ratio of 5:1, at 25°C.	99
5.13 Fraction of nickel present in each form for an ammonia-nickel ratio of 10:1, at 25°C.	100
5.14 Fraction of nickel present in each form for an ammonia-nickel ratio of 2:1, at 200°C.	101
5.15 Fraction of nickel present in each form for an ammonia-nickel ratio of 5:1, at 200°C.	102
5.16 Fraction of nickel present in each form for an ammonia-nickel ratio of 10:1, at 200°C	103
5.17 Variation of nickel ion concentration at 200°C as reduction proceeds.	106

LIST OF TABLES

Table	Page
3.1 Potentials of Ni and hydrogen, 25°C.	21
3.2 Mean activity coefficient of Ni ⁺⁺ in NiSO ₄ solution	21
3.3 Thermodynamic data for the formation of nickel complex at 25°C.	25
3.4 Potential and equilibrium constants for nickel ammines at 25°C.	26
3.5 Entropy constants at different temperatures. . .	30
3.6 Free energy of reaction at high temperatures . .	32
3.7 Equilibrium constants at high temperatures . . .	33
5.1 Runs legend.	70
5.2 Average reaction rate.	88
5.3 Predicted and measured pH values with and without activity coefficients correction	88
5.4 Values of nickel ions concentration, pH, and NH _{3(F+C)} /Ni ^{II} predicted as reduction is carries out at 25°C and initial ratio of 1.2	95
5.5 Values of nickel ions concentration, pH, and NH _{3(F+C)} /Ni ^{II} predicted as reduction is carried out at 25°C and initial ratio of 2.2	96
5.6 Values of nickel ions concentration, pH and NH _{3(F+C)} /Ni ^{II} predicted as reduction is carried out at 200°C and initial ratio of 1.2.	97
5.7 Values of nickel ions concentration, pH, and NH _{3(F+C)} /Ni ^{II} predicted as reduction is carried out at 200°C and initial ratio of 2.2.	98

ACKNOWLEDGEMENTS

The author wishes to express his appreciation and grateful thanks to Dr. G.P. Martins whose competence and zeal proved to be unmeasurable during the course of this investigation. Also, grateful acknowledgements is extended to the Colorado School of Mines Foundation for the financial assistance provided.

CHAPTER 1

INTRODUCTION

The extractive metallurgy of nickel is fairly complex and costly, although rapid changes have been occurring in the last two decades. The most important sources of the metal are the mixed sulphide ores containing pentlandite ($\text{Fe, Ni}_9\text{S}_8$, nickel bearing pyrrhotite, Fe_5S_6 to $\text{Fe}_{16}\text{S}_{17}$ and nickel bearing chalcopyrite, CuFeS_2 . An increasingly important source of the metal is the oxide ores, the most important being the hydrous magnesium silicate, garnierite, $\text{H}_4(\text{Mg, Ni})_3 \cdot \text{Si}_2\text{O}_9$ to nickel bearing iron oxide (laterite).

The silicate ores are largely treated by a matte smelting process^(1,2). The ore is fused with calcium carbonate, calcium sulphate and coke to yield a nickel-iron sulphide concentrate which is further refined by smelting to eliminate the iron in a siliceous slag, and yield ultimately fairly pure nickel metal.

Oxide, or lateritic ores can be reduced in a multiple-hearth furnace and then selectively leached with ammonia-carbon dioxide solution^(1,2). The ammonia is recovered efficiently for reuse

by steaming the solution which results from leaching, while the nickel is simultaneously precipitated as basic carbonate. This is later calcined to nickel oxide for further processing to nickel metal.

The nickel-bearing sulphide ores are first ground and carried through a series of flotation and magnetic separation giving three different concentrates: nickel-bearing iron sulphide, copper-bearing nickel sulphide is desulphurized in a fluid-bed roaster, reduced with carbon monoxide and hydrogen in a rotary kiln and then leached with ammonia-carbon dioxide solution to remove the nickel. The nickel is recovered as a basic carbonate when the final solution is treated with steam.

The copper-bearing nickel sulphide is partially desulphurized in multiple-hearth roasters, melted and cooled under specially controlled conditions which allow subsequent magnetic and flotation separation into three concentrates: nickel sulphide, copper sulphide and precious metals. The nickel sulphide is sintered for further refining, either electrolytically^(1,2), by the carbonyl^(1,2) process, or by the newly reported process of Republic Steel⁽³⁾.

Nowadays the trend in the recovery of nickel from ores is based on a selective leaching of either nickel copper matte or nickel-bearing ores in acid or ammonia under elevated

temperatures and pressures. The nickel in the resulting salt solution is recovered directly by treatment with hydrogen gas at elevated temperatures and pressures.

In the last two decades, extensive studies on the hydrogen reduction of metals have been carried out. The thermodynamics of hydrogen reduction from the electrochemical⁽⁴⁾ and physiochemical^(5,6) points of view have been widely treated on theoretical grounds. As far as practical operations are concerned, very few problems are encountered by companies which employ the hydrogen reduction of metals^(7,8).

However, the kinetics of the process has always been bypassed or treated very lightly, perhaps that is because it is heterogeneous and involves highly specific factors, such as adsorption, surface area, and mass transfer, which cannot be generalized.

1.1 Scope of the Problem

The initial objective of the kinetic study of any reaction should be to determine which step, or steps, is, or are, rate controlling, under a given set of conditions. The physical variables which may then be manipulated in order to effectively increase the rate, will depend on the nature of the rate controlling step. For example, increased agitation is effective in increasing the rate when the rate of external mass transfer

is controlling. An increase in temperature will bring about an increase in rate, irrespective of which is the controlling mechanism.

The simplest case will be considered, and is one in which the reaction takes place on a smooth, clean surface. The rate controlling step is then either a surface process, or a chemical process, or the mass transfer to, or from, the bulk of the solution, or a combination of these.

The plane rotating disc, which will be used in the experiments, is the only geometry which definitely gives a uniformly accessible surface area and a hydrodynamically defined flow pattern. Also, results obtained with a rotating disc may be easily reproduced, and can be readily compared by different investigators.

1.2 Scope of this Study

In order to make this investigation meaningful, it is believed that, the introduction of seed powders to provide a catalytic surface would only serve to add an additional complexity to the problem since the hydrodynamic behavior of such systems are difficult to analyze.

As mentioned previously, the rotating disc, will provide an equally accessible area for the reactants in solutions as

well as known hydrodynamics. By this means it will be possible to both qualitatively and quantitatively analyze the kinetics of the system.

1.3 Aim of this Study

The aim of this study is to obtain a better understanding of:

a) the mechanism and kinetics of the hydrogen reduction of nickel solutions, and b) the effects of various parameters on the reaction rates.

Theoretical aspects of the work will include:

- 1) Prediction of the ammine distribution at high temperatures.
- 2) Construction of E-pH diagram for the system Ni-H₂O-NH₃ at high temperatures.
- 3) Theoretical prediction of solution behavior during hydrogen reduction.

Experiments will be designed to study the following:

- 1) Effect of initial Ni⁺⁺ concentration.
- 2) Effect of temperature.
- 3) Effect of hydrogen pressure.
- 4) Effect of hydrodynamics.

CHAPTER 2

LITERATURE REVIEW

In the review presented here the historical development of the use of hydrogen gas for the precipitation of metals from solution is first introduced. Recent works in this area are presented next, with the emphasis being confined to nickel. In many of the studies which have been presented, apart from covering the industrial practice associated with the process of hydrogen reduction of metals, both kinetics as well as chemical/electrochemical thermodynamics are covered by the various authors. By and large, the kinetic study of the ammoniacal systems have been rather superficial, due largely to the complexity of these systems.

2.1 Early Works

Precipitation by reducing a metal salt solution with hydrogen has been known for more than one hundred years. As early as 1859, Beketoff⁽⁹⁾ at the Sorbonne had reduced silver salts to metal in this way.

Ipatiew⁽¹⁰⁾ was the one, who perhaps made the major contribution to the development of the process by recovering metals such as

platinum, iridium, copper and nickel , from cobaltous and cobaltic ammoniacal chloride and sulphate solutions with hydrogen. The reactions were carried out in sealed unagitated tubes and the metallic products, when formed, were contaminated with stable oxides and basic salts which precipitated at the high temperatures used before the hydrogen could diffuse into solution and effect reduction. Although the products from this work were too impure to warrant further development, the demonstration of the feasibility of using hydrogen under pressure to achieve reduction must be considered as the corner stone of the development of the hydrogen reduction process.

In 1926, Muller, Schlecht, and Schubardt⁽¹¹⁾ obtained a patent in the United States on a process of selective metal reduction from ammoniacal solution. Their method allegedly permits separation of silver, copper, nickel, cobalt, and zinc from ammoniacal solution by applying progressively higher temperatures and hydrogen pressures. Metals produced by this technique were not pure, since no attempt was made to remove the precipitated metal between different reductions. Furthermore, it is doubtful that the zinc product contained any metallic zinc since it may be calculated that the pressure and temperature needed to reduce zinc far exceed that used in these experiments.

In the U.S.S.R., the pioneer work of Ipatievs was continued over the period of 1930-1948 by Tronev and his co-workers⁽¹²⁾,

primarily in the hydrogenation of aqueous salts of the precious metals and the precipitation of silver, gold, platinum, etc. The work on the reduction of nickel, cobalt and copper amines, led to the erroneous conclusion that nickel and cobalt could not be separated, by preferential reduction. Excessive hydrolysis, and the use of unbuffered solutions, could account for the lack of selectivity in the reduction.

2.2 Recent Advances

In the mid 1950's, a further important advancement was the combination of a process in which nickel could be dissolved from its sulphides ores, using ammonia and oxygen, with another in which precipitation of nickel from the solution with hydrogen gas at an elevated temperature and moderate pressure, was accomplished economically. The first stage of this process, discovered by F. Forward^(13,14), consists of an ammonia leach of sulphide concentrated conducted at 83°C with air at 100 lb/in² in which the sulphides are oxidized and the non-ferrous metals are complexed by ammonia to give ammine ions such as $\text{Me}(\text{NH}_3)_n^{2+}$, where n can vary from 1 to 6.

The second stage was carried out successfully by Schaufelberger and Roy⁽¹⁵⁾ who were able to precipitate nickel from NiSO_4 solutions. This work provided confirmation of the overall equilibrium reaction:



which indicates that when precipitation is carried out at constant hydrogen pressure and constant temperature, then there are a series of equilibria such that there is a linear relationship between $\log [\text{Ni}^{++}]_{\text{eq}}$ and the pH of the solution, and the slope of this straight line equals -2.

It can also be seen from the above equation that the yield of the reaction will be increased (more metal will be deposited) at equilibrium if the hydrogen ions are removed as soon as they are formed (maintaining the pH constant). This was achieved by Schaufelberger⁽¹⁶⁾ by adding sulphate ions to the solution to form bisulphate, according to the following reaction:



The addition of ammonium sulphate (112g/l) to the solution of nickel sulphate (0.2M Ni) increased the equilibrium yield from 10% to 50%. These experiments were conducted in acid solutions in which the minimum (final) pH was 2.75. He also studied the effect of different additives to nickel sulphate. High reductions were only obtained by mixing the nickel sulphate with ammonium acetate (100% reduction, final pH 4.1), and with a mixture of ammonia, ammonium sulphate (98% reduction, final pH 9.8). The conditions used were Ni=0.2M, 200°C, and 1000 psi of H₂ pressure. However, no indication was given as to the relative amounts of these components used.

Courtney and Schaufelberger⁽¹⁷⁾ also obtained nickel metal by using hydrogen to reduce nickel ammines dissolved in sulphate solutions. However, difficulties were encountered in initiating the new phase, and unless powdered seed material was introduced, the metal was deposited on the walls of the reaction vessel. They reported that the rate of disappearance of nickel, from an aqueous $\text{NiSO}_4\text{-NH}_3\text{-(NH}_4)_2\text{SO}_4$ solution containing nickel powder (100g/l), was constant for 80% of the reduction and that the reduction rates tended to decrease as the nickel ions (total nickel) concentration decreased below 0.03 molar. The conditions were 0.138 M NiSO_4 , 0.41 M NH_3 , 0.95 M $(\text{NH}_4)_2\text{SO}_4$, 100g/l of nickel powder and 150°C. They also reported that the values of the rate constant were independent of the agitation parameters and indicated that the rate controlling reaction in reduction was probably at the surface of the growing nickel particles. They also pointed out that by visual inspection (the autoclave had a glass inspection port) the blue solution turned green at about 150°C, indicating that few nickel ions were present as the tetra-ammine or higher ammines complexes.

The works of Forward^(13,14) and Schaufelberger^(15,16,17) were studied closely by Mackiw and co-workers⁽¹⁸⁾ who worked out the chemistry of the reductions from ammoniacal solutions in detail, and made these reactions the basis of Sherritt Gordon's nickel and cobalt program. In their paper, a detailed examination of the reaction by which nickel can be precipitated from

aqueous ammoniacal sulphate solutions by hydrogen at elevated pressures and temperatures is thoroughly reviewed. They proposed a mechanism to account for the catalytic effect of ferrous salt additions, and the effect of variables on the autocatalytic nature of the reduction are described. They also mentioned (and this has been adopted since by workers⁽⁵⁾, as well as review authors^(6,19)) that the reaction was independent of the nickel concentration in solution, and proportional to the H_2 partial pressure to approximately the first order (0.9), and to have an apparent energy of activation of between 5 and 15 Kcal. Perhaps the most important contribution of Mackiw and co-workers⁽¹⁸⁾ was the optimal ratio of ammonia to nickel concentration, which they found experimentally to be 2. This value was later confirmed by Meddings and Mackiw⁽⁵⁾.

Another important point found by Mackiw and co-workers⁽¹⁸⁾ was that the activation energy in the temperature range of $150^\circ - 175^\circ C$ was $13.7 \text{ Kcal-mol}^{-1}$, and in the temperature range of $175-200^\circ C$ it was $5.7 \text{ Kcal-mol}^{-1}$. Their plot of $\log k$ vs $1/T$ gives a curve rather than a straight line and a satisfactory explanation is not really presented. He only mentions that the rate of formation of nuclei is probably not temperature sensitive. However, it appears that from a kinetics point of view that at low temperatures the reduction is chemically controlled, and at high temperatures it is diffusion controlled.

Wimber and Wadsworth⁽²⁰⁾ reported similar results for cobalt precipitation and obtained results indicating catalysis of the reduction reaction by stainless steel and pyrex glass.

In 1964, Meddings and Mackiw⁽⁶⁾ reported the importance of additives, stressing the importance of reducing solutions which contained pre-existing nickel nuclei and nuclei other than nickel. They again reported that they found the reaction to be a zero order reaction up to 85% of the reduction, but without explaining any reaction mechanism. Also, they recalculated the apparent activation energy and reported a value of $10.2 \text{ Kcal-mol}^{-1}$. Perhaps the major contribution of the paper is the study of the effects of nuclei other than nickel and additives (anthraquinone). The surprising result of the use of anthraquinone is that without changing the apparent activation energy ($10.2 \text{ Kcal-mol}^{-1}$) the rate of reduction could be increased by a factor of twenty. The explanation for this increase is due to the fact that the anthraquinone increases the number of reaction sites i.e., "active centers" where the hydrogen molecules can be adsorbed. They also postulate that the change in the order of the reaction after 85% of the reduction has been accomplished, is due to the fact that the nickel ions (or nickel ammines) are more strongly adsorbed than the hydrogen on the surface of the seed.

In 1966, W. Kunda, D.J.I. Evans, and V.N. Mackiw⁽²⁶⁾ studied extensively the effects of additives on the hydrogen reduction

of nickel from its aqueous ammine-ammonium carbonate solutions. They found that besides the effects of anthraquinone, which were mentioned previously, polyacrylamines of high molecular weight (flocculating agents) produce loose, fluffy nickel powders. Wetting agents, such as sulphonated fatty acids and alkyl-aryl sulphonates, promote agglomeration. These are, in general, a few of the most important properties. Also, it is worthwhile mentioning that in this system (nickel carbonate) there is no need for ferrous sulphate catalyst, and the nickel powder produced has a lower sulphur and iron content than the powder produced from ammonium sulphate systems.

In 1968, D.J.I. Evans, in his review paper, Production of Metals by Gaseous Reduction from Solution, made a good general compilation of all those independent papers dealing in the subject, without adding anything new.

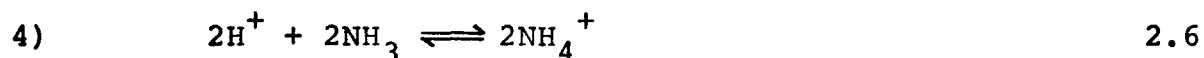
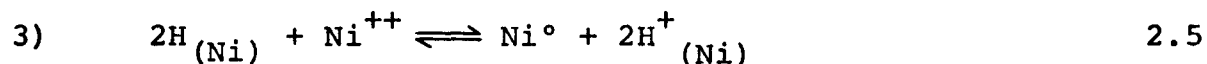
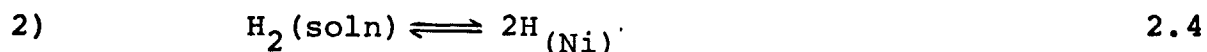
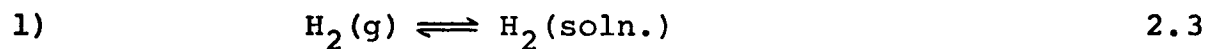
In his brief review of precipitation of metal from solutions by gases, F. Habashi⁽²²⁾, has an extensive list of bibliography of authors that have dealt with the subject in reference. Among these references appear several papers published by Russian researchers, which he does not actually review, but merely lists them in his bibliography.

Aside from early works mentioned previously, G.N. Dobrokhotov and G.N. Onuchkina⁽²³⁾, in 1962 published what might be con-

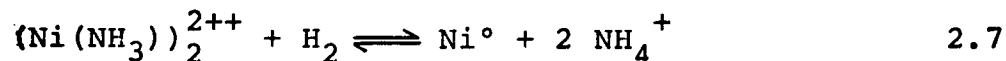
sidered one of the few serious and thorough investigations which deals with the kinetics of hydrogen reduction of nickel sulphate-ammonium system. This work has been very helpful to the investigation presented in this thesis. In their paper, they present the usual steps associated with heterogeneous reactions in solutions to show that the kinetics of hydrogen reduction is carried out in four different steps:

- 1) Solution of hydrogen gas in the solution, which is a fast reaction.
- 2) Adsorption of the hydrogen in solution onto the nickel metal, which is also fast.
- 3) Reaction of the hydrogen adsorbed with nickel ions, which is the controlling step (slow).
- 4) Discharge (*diffusion*) of the reaction products into the total mass of the solution which is also fast.

If these four steps are put in the form of chemical equations, we obtain:



The paper stated that the reaction is either governed by the rate of the chemical reaction, or by the diffusion of hydrogen into solution. Also, it was pointed out that the agitation of the system has a very striking character in relation to the activation energy. For vigorous mixing (Reynolds no. $\geq 18,000$), the reduction has a "strict kinetic character" (activation energy of $17.7 \text{ Kcal-mol}^{-1}$), and when the mixing rate is slowed, the reaction becomes diffusion controlled (activation energy of 4 Kcal-mol^{-1}). Dobrokhotov also gives a relationship for depletion of nickel with time which indicates an apparent first order reaction with respect to total nickel and a half order reaction with respect to hydrogen partial pressure. Furthermore, he mentions that the whole reduction is in fact controlled by the diammine reduction according to:



The work done on hydrogen reduction of nickel under acid conditions should also be mentioned, even though the corrosive conditions encountered are severe enough so that in commercial practice alkaline conditions are always preferred when using stainless steel equipment. As mentioned previously, Schaufelberger and Roy⁽¹⁵⁾ obtained precipitated nickel at a pH of 2.75.

Recently, S.C. Sircar, and D.R. Wiles⁽²⁴⁾ devised a way of avoiding corrosive conditions by using the anion of a weak

acid. Their system consisted of a nickel ion solution in an ammonium acetate solution. The pH was buffered between 3.5 and 4.25. They report that the rate of the reaction was of the first order with respect to both nickel concentration and surface area, independent of the agitation and proportional to the square root of hydrogen pressure up to 15 atm. Above this pressure the rate fails to increase proportionately.

The later work by Sato⁽²⁵⁾, using the same solutions as Sicar, considered kinetic and electrochemical studies of the system. He found that the reaction was proportional to both the surface area, and to the square root of the hydrogen partial pressure (as mentioned by Sicar) but without any restriction as far as pressure was concerned (maximum pressure - 25 atm.). The reaction rate was also dependent on the nickel concentration, and was found to be of one-half order. The effect of temperature as given by the Arrhenius plot of the reaction indicated an activation energy of 28.8 Kcal-mol⁻¹.

Pourbaix diagrams for the system Ni-H₂O-NH₃-H₂SO₄ at various activities of NH₄⁺ + NH₃ were constructed by Letowski and Niemiec⁽²⁶⁾. They found that at 25°C and pH values less than 7, the ammonium nickel sulphate Ni(NH₄)₂(SO₄)₂·6H₂O precipitates as a solid phase at high activities of the reactants.

Malmstrons⁽²⁷⁾ extrapolated the values of Letowski and Niemic at 150°C. He found that at this temperature, the solubility of sulphates as well as metal ammonium sulphates are not exceeded even at 1 molar solution of nickel. The only effect was that the equilibrium lines of nickel, nickel hydroxide, and the nickel amines are shifted toward lower pH values. Even at concentrations of $\text{NH}_4^+ + \text{NH}_3$ of 10 molar, there is a stable hydroxide region between the metal ions and the amine complexes.

CHAPTER 3

THEORETICAL CONSIDERATIONS

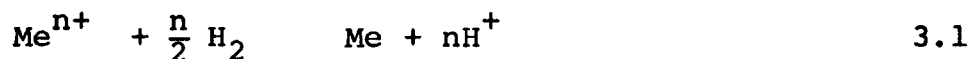
The present chapter deals with both thermodynamic and kinetic considerations appropriate to the investigation undertaken. Ionic equilibria at high temperature has been extrapolated for the Ni-H₂O-NH₃ system using the Correspondence Principle of Criss and Cobble⁽³²⁾. Stability diagrams for nickel ions and nickel ammines as well as Pourbaix diagrams were thereby constructed. Finally, the usual kinetic aspects of both mass-transfer in rotating disc systems as well as heterogeneous chemical kinetics is presented.

3.1 Metal-Hydrogen Electrode Potentials

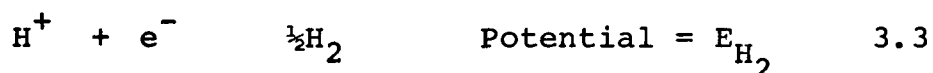
If metals are to be precipitated by hydrogen from aqueous solutions of their ions, the thermodynamic factors must obviously be favorable. Any assessment of how successfully metals can be produced in this way must therefore involve considerations of the free energy changes associated with the various possible reactions. In dealing with aqueous systems, however, it has become customary to express the thermodynamics of the possible reactions in terms of reversible electrode

potentials, instead of free energies. The principles involved are exactly the same, but since the relevant data are normally tabulated in terms of electrode potentials instead, these will be used in the following discussion of hydrogen and metals in aqueous solution.

In general, the reduction of metal ions by hydrogen in solution can be written as:



Now this reaction can be viewed as two half-cell reactions, each with their own potential:



If E_{Me} exceeds E_{H_2} , then the metal will liberate hydrogen from water and pass into solution. However if E_{H_2} exceeds E_{Me} , the reverse reaction (Eq. 3.2) will occur and metal Me will be precipitated from solution. The potentials denoted by E_{Me} and E_{H_2} are single electrode potentials and are defined in the usual electrochemical nomenclature by:

$$E_{\text{H}^+, \frac{1}{2}\text{H}_2} = E^\circ_{\text{H}^+, \frac{1}{2}\text{H}_2} - \frac{2.303 RT}{F} \log \frac{1}{a_{\text{H}^+}} -$$

$$\frac{2.303 RT}{2F} \log p_{\text{H}_2} \quad 3.4$$

Bearing in mind that the activity of hydrogen gas is the fugacity of hydrogen, and that at moderate pressures the error involved in using partial pressure instead of fugacity is negligible (at 100 atm. partial pressure, the fugacity is 106.1 atm., which introduces an error of about 1% in the log term⁽⁶⁾). On the other hand, by definition of pH as $\log \frac{1}{a_{H^+}}$, and since the standard electrode potential of hydrogen, $E^{\circ}_{H^+, \frac{1}{2}H_2}$ is defined as zero, equation 3.4 is reduced to:

$$E_{H^+, \frac{1}{2}H_2} = -0.0591 \text{ pH} - 0.0295 \log p_{H_2} \quad 3.5$$

where p_{H_2} is the partial pressure of hydrogen expressed in atmospheres.

In the case of the metal electrode potential, Equation 2, we have:

$$E_{Me^{n+}, Me} = E^{\circ}_{Me^{n+}, Me} + \frac{RT}{nF} \log a_{Me^{n+}} \quad 3.6$$

By definition:

$$a_{Me^{n+}} = [Me^{n+}] \cdot \gamma \quad 3.7$$

where γ is the activity coefficient of the ion and $[Me^{n+}]$ is the analytical concentration. Then Equation 3.6 becomes:

$$E_{\text{Me}^{n+}, \text{Me}} = E^{\circ}_{\text{Me}^{n+}, \text{Me}} + \frac{0.05916}{n} \cdot \log [\text{Me}^{n+}] + \frac{0.05916}{n} \log \gamma \quad 3.8$$

In our specific case, the metal to be reduced is nickel; in order to represent these potentials graphically as a function of concentration of the metal in solution and pH, data has been taken from Latimer⁽³⁰⁾. The data obtained was mean activity coefficients of nickel sulphate and the standard potential (25°C) for Ni⁺⁺/Ni, and H⁺/H which are shown below:

Table 3.1: Potentials of Ni and hydrogen at 25°C.

Species in Equilibrium	E° (volt)
Ni ⁺⁺ /Ni	-0.250
H ⁺ /H	0

Table 3.2: Mean activity coefficient of Ni⁺⁺ in NiSO₄ solution.

Molality:	0.001	0.005	0.05	0.10	0.30	0.5	.10
Activity Coefficients:	-----	-----	----	0.150	0.084	0.063	0.043

With the potential and mean activity coefficients, we can now plot graphically potentials as functions of concentration and pH, as can be seen in Figure 3.1.

It should be emphasized that the point at which the hydrogen line crosses the line referring to a metal ion, is unique only to the concentration of the metal ion at that point, since the pH and the metal ion concentration scales are independent. The most important factor in interpreting the relative positions of the line for hydrogen and those for the metal ion is the pH of the solution. Reduction will become more favorable at high pH values. In basic solutions, the pH term in Equation 3.5 will produce a larger negative value of E for this half cell reaction, thus with decreasing hydrogen ion concentration, the reduction potential of the ion becomes more positive and the reducing power increases.

From Figure 3.1 it can be seen that either an increase in ^{pressure?} pH of about one unit or about a hundred fold increases in hydrogen pressure produce about the same increase in the expected hydrogen reduction potential. Therefore, the use of excessive pressure is rarely justified, although in some cases it may be desirable to increase the hydrogen pressure for kinetic reasons.

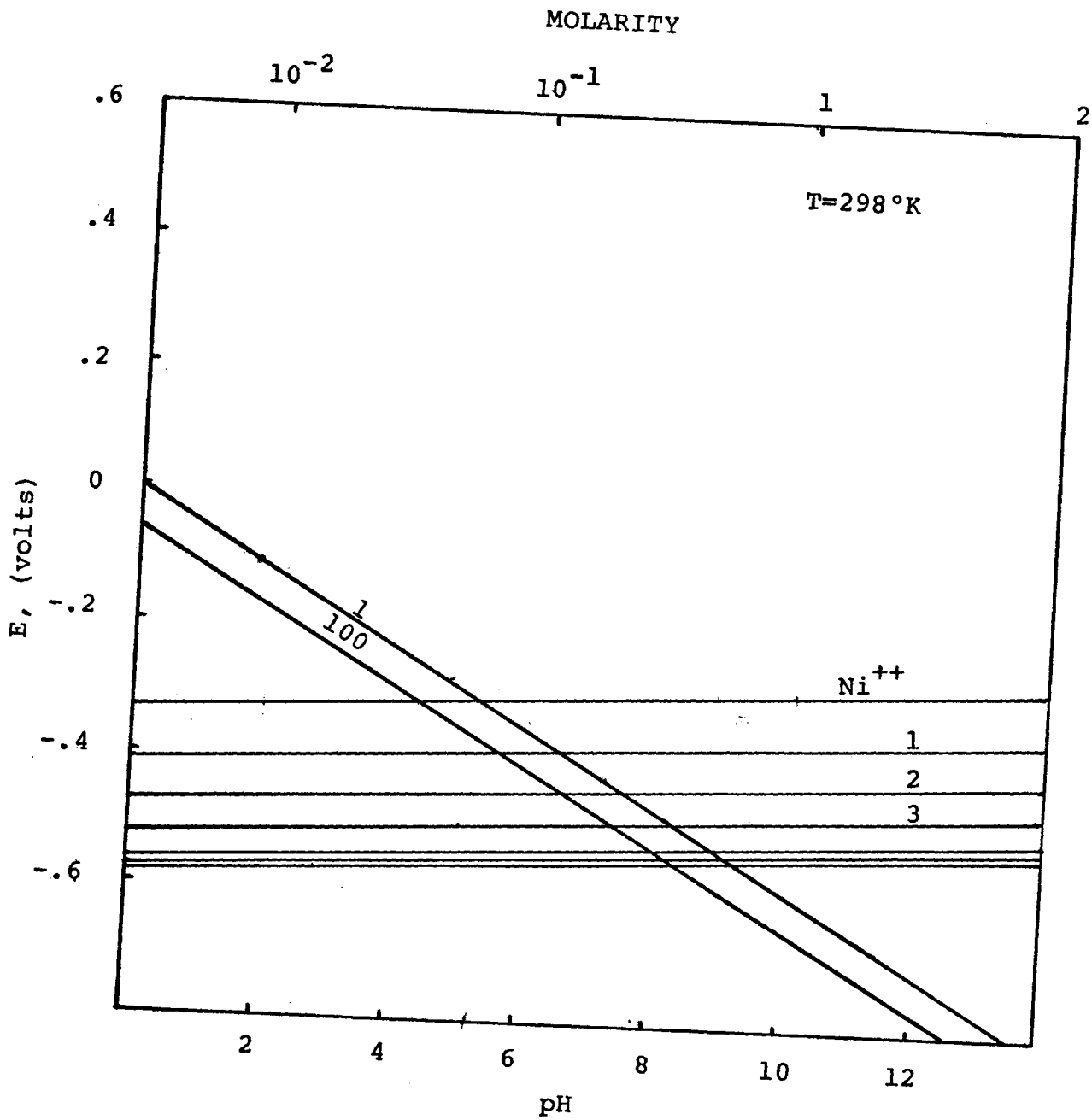


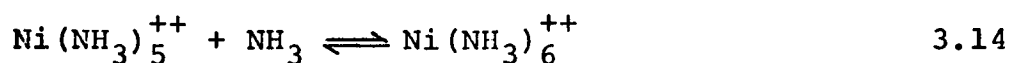
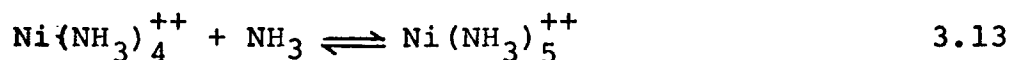
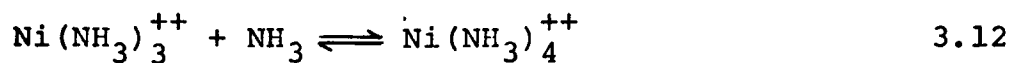
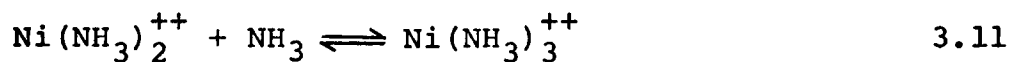
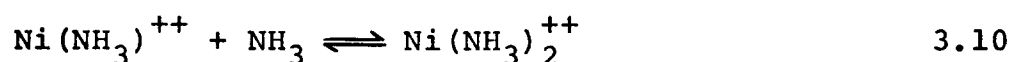
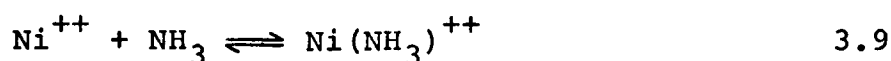
Figure 3.1 Relationship between E and pH at pressures of 1 and 100 atm. and of nickel ions and the nickel ammines $\text{Ni}(\text{NH}_3)_n^{++}$, 25°C .

3.2 Effect of Complex Formations at Room Temperature

It can be seen from Figure 3.1 that the "driving force" for the reduction increases as the pH increases, and on this basis the condition for reduction become more favorable as the solutions become more alkaline. However, above pH7 the hydrolysis of transition metal cations becomes important, and in order to prevent precipitation from solution, it is necessary to complex these ions.

For nickel, the simplest method of both raising the pH and complexing the metal ions is the addition of ammonia, which causes the formation of the metal ammines.

The addition of ammonia to a solution containing nickel ions, results in the sequential formation of ammines as follows:



The standard free energies, enthalpies and entropies of the various nickel ammine complexes are given in Table 3.3.

Table 3.3: Thermodynamic data for the formation of nickel complex at 25°C. (Reference 31)

n	1	2	3	4	5	6
ΔG°	-3860.9	-3108.9	-2418.1	-1679.9	-1079.7	-97.55
ΔH°	-4010	-3580	-4500	-3120	-2970	-4400
ΔS°	-.5	-1.58	-6.98	-4.83	-6.34	-14.43
$\log K$	2.84	2.29	1.78	1.24	0.79	0.072

For each of these step equilibria, there is a corresponding equilibrium constant given by:

$$K = \frac{a_{\text{Ni}(\text{NH}_3)_m^{++}}}{a_{[\text{Ni}^{++}]} a_{\text{NH}_3}^m} \quad K_i = \frac{a_{\text{Ni}(\text{NH}_3)_m^{++}}}{a_{[\text{Ni}^{++}]} a_{\text{NH}_3}^m} \quad 3.15$$

These equilibrium constants have been calculated by various authors (Bjerrum⁽²⁹⁾, Yatsimishy⁽³⁰⁾, Schulz⁽³¹⁾). In this thesis we will take the latest ones. Since it is the most recent, we will assume that it is the most reliable; in any case, the difference between them is only about 2% in log K.

The values of E° for all the complex species can be calculated from the equilibrium constants, and with these values we can construct a similar diagram -- E vs pH for the amines represented in Figure 3.1. The standard electrode potentials for the reduction of amines to metallic nickel are given in Table 3.4.

Table 3.4: Potential and equilibrium constants for nickel amines at 25°C.

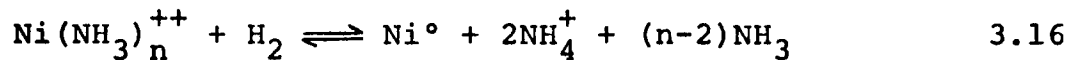
n	1	2	3	4	5	6
-E°.v	.333	.401	.453	.489	.513	.515
log K	2.840	2.278	1.779	1.236	.794	.072

Figure 3.1 makes the following points clear: the nickel amines can be reduced to metal from simple ions by hydrogen, only at somewhat higher pH values than those for nickel ions, depending on hydrogen pressure and the nickel ion and/or ammine concentration.

In the presence of ammonia, the thermodynamic considerations change on two points:

- 1) The ammine complex ions are more stable than those of simple metal ions, and therefore, harder to reduce with hydrogen at an equivalent pH value.
- 2) For a ratio of ammonia (added as NH_4OH) to nickel of 2, the hydrogen reduction process itself generates ammonium salts instead of free acid, therefore, preventing the decrease of pH associated with simple salt reduction.

The last point can be pursued farther by considering the stoichiometric equation for reduction of metal ammine complex given by the equations⁽¹⁹⁾:



Then depending on whether n is greater or less than two (for divalents metal ions complex), the solution may either rise in pH due to the production of free ammonia, or fall in pH due to the production of free acid. This fact was calculated (on the basis of hydrogen and nickel potentials) by Meddings and Mackiw⁽⁵⁾, who found that the largest driving force for hydrogen reduction of nickel is near an NH_3/Ni ratio of 2.

With the values of the equilibrium constants, a distribution diagram for all species present can be constructed. Figure 3.2 shows the distribution as the fraction of each independent species for different ammonia-nickel ratios, and where the ammonia refers to the total ammonia complexed in the system. It should be emphasized that all the remarks pertaining to this section cover only room temperature systems.

3.3 Application of Correspondence Principle

Since working temperatures of over 150°C are encountered for the hydrogen pressure reduction in commercial practice, it was necessary to obtain free energy changes with temperature, using the Entropy Correspondence Principle of Criss and Cobble⁽³²⁾.

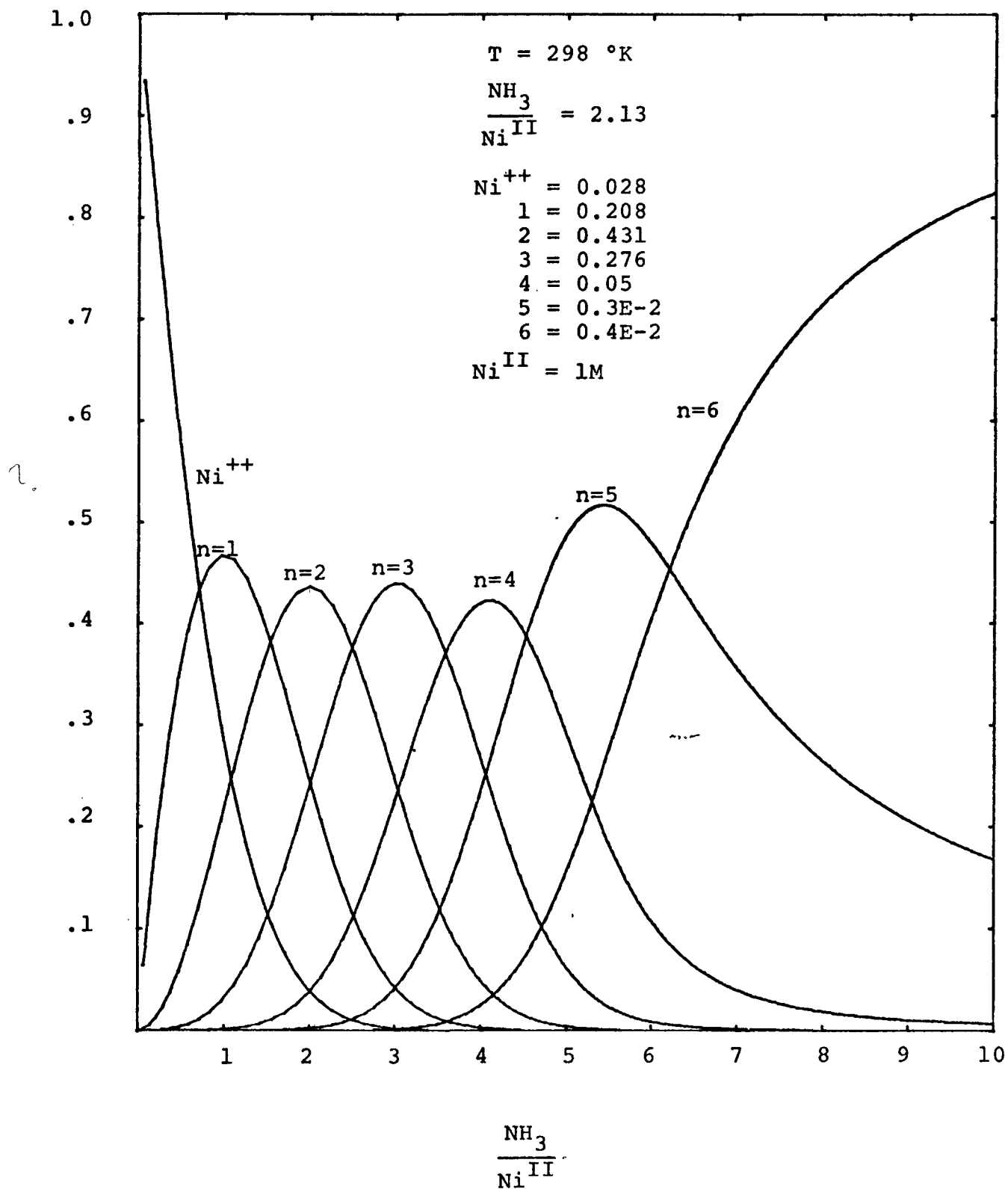


Figure 3.2. Fraction of nickel present in each form at different ammonia-to-nickel ratios, 25°C.

The correspondence principle states that a standard state can be chosen at every temperature such that the partial molar entropies of one class of ions at that temperature are linearly related to the corresponding entropies at some reference temperature. The entropy standard state at 25°C is a hydrogen ion entropy of $-5 \text{ cal-mol}^{-1}\text{-}^\circ\text{K}^{-1}$, and the general relationship can be written as:

$$\bar{S}_\theta^\circ = a_\theta + b_\theta \bar{S}_{25}^\circ \text{ (abs.)} \quad 3.18$$

where a_θ and b_θ are temperature dependent constants for each class of ions (cations, anions, oxyanions, and acidoxyanions), and where:

$$\bar{S}_{25}^\circ \text{ (abs.)} = \bar{S}_{25}^\circ \text{ conventional} - 5.0z \quad 3.19$$

z being the ionic charge.

The average value of the partial molar heat capacity between 25°C and $\theta^\circ\text{C}$ is given as:

$$\bar{C}_{p25}^\circ \theta = \frac{\bar{S}_\theta^\circ - \bar{S}_{25}^\circ}{\text{Ln } T/298.2} \quad 3.20$$

or

$$\bar{C}_{p25}^\circ \theta = \frac{a_\theta - \bar{S}_{25}^\circ (1.0 - b_\theta)}{\text{Ln } T/298.2} \quad 3.21$$

where T is the temperature θ in degrees Kelvin.

With the above formulae, Criss and Cobble⁽³²⁾ proposed that the change in free energy of a reaction at T°K is related to the change in free energy at 298°K by the equation:

$$\Delta G_T^\circ = \Delta G_{298}^\circ - (T - 298)\Delta S_{298}^\circ + (T - 298) \bar{C}_P^{\circ T} - T \bar{C}_P^{\circ T} \ln T/298 \quad 3.22$$

So that ΔG_T° can be calculated from ΔG_{298}° , ΔS_{298}° , and the heat capacity data.

The term $\bar{C}_P^{\circ T}$ is an average value of the heat capacity change for the reaction between 298°K and T and involves both solid and solute species.

Table 3.5 gives the values of a_θ and b_θ for cations at different temperatures. In the application of the formulae, it was considered as a first approximation that the nickel amines behave like divalent cations.

Table 3.5: Entropy constants at different temperatures.

$\theta^\circ\text{C}$	a_θ	b_θ
25	0	1.00
100	10.3	.876
150	16.3	.792

Table 3.5 Continued

$\theta^\circ\text{C}$	a_θ	b_θ
200	23.3	.711
250	29.9	.630
300	36.6	.548

$$C_{P_{25}}^\circ = A + B \bar{S}_{25}^\circ \quad 3.23$$

$$A = 41.6$$

$$B = -.523$$

The correspondence principle has been used by Robbins⁽³³⁾ to calculate E-pH diagrams of various systems. He shows for the system $\text{HSO}_4^- = \text{SO}_4^{2-} + \text{H}^+$ the change of free energy for this reaction at high temperatures predicted by both the correspondence principle and the Van't Hoff equation and compared with experimental data. Very good agreement between the correspondence principle and experimental data is obtained. However, the values predicted by Van't Hoff equations are lower by a maximum of about 4 Kcal-mol⁻¹ than the experimental value of approximately 10 Kcal-mol⁻¹.

The influence of pressure in the chemical equilibrium was also taken into consideration by Criss and Cobble⁽³³⁾ in their correspondence principle, and they conclude that its effect

can be ignored up to a temperature of 300°C, since the magnitude of the errors introduced are within the limits of accuracy of the data used in the correspondence principle.

The values of the free energies and equilibrium constants respectively by this method are shown in Tables 3.6 and 3.7.

Table 3.6: Free energy of reaction at high temperatures.

$$\text{Ni}^{++} + n\text{NH}_3 \leftarrow \text{Ni}(\text{NH}_3)_n^{++} \quad 3.24$$

$\Delta G_{\theta}^{\circ}$ (Kcal)

	0	25	100	150	200	250	300
n							
1		3.86	3.37	2.59	1.46	.02	-1.74
2		6.96	5.92	4.30	2.01	-.9	-4.45
3		9.38	7.04	4.72	1.07	-3.5	-8.97
4		11.04	8.29	4.64	-.29	-6.4	-13.78
5		12.15	8.48	3.80	-2.50	-10.3	-19.51
6		12.25	7.11	10.74	-6.83	-16.5	-27.88

Table 3.7: Equilibrium constants at high temperatures.

$$K = \frac{a_{\text{Ni}(\text{NH}_3)_n^{++}}}{a_{\text{Ni}^{++}} \cdot a_{\text{NH}_3}^n} \quad 3.25$$

n	1	2	3	4	5	6	T°C
log K	2.84	2.29	1.78	1.24	.79	.07	25
	1.98	1.49	.87	.52	.11	-.8	100
	1.34	.89	.22	.04	-.44	-1.4	150
	.68	.25	-.43	-.63	-1.01	-2.02	200
	.006	-.39	-1.1	-1.23	-1.6	-2.62	250
	-.660	-1.03	-1.7	-1.8	-2.19	--3.2	300

With these new constants an additional set of stability diagrams were drawn. From the graphs - Figures 3.3, 3.4, 3.5, 3.6-it is clear that at a $\text{NH}_3/\text{Ni}^{++}$ ratio of 2, as the temperature is increased, the first two nickel complexes become the most important species. Above 200°C the concentration of nickel ions start increasing until at a temperature of 300°C, its abundance for the same $\text{NH}_3/\text{Ni}^{++}$ ratio is almost three times as much as the amount complexed with ammonia. This is to be expected because generally with increasing temperature, the dissociation of the complex also increases.

Furthermore, making an additional plot for E-pH, the slope for the reaction, $\text{H}_2 = 2\text{H}^+ + 2\text{e}^-$, increases continuously as we increase

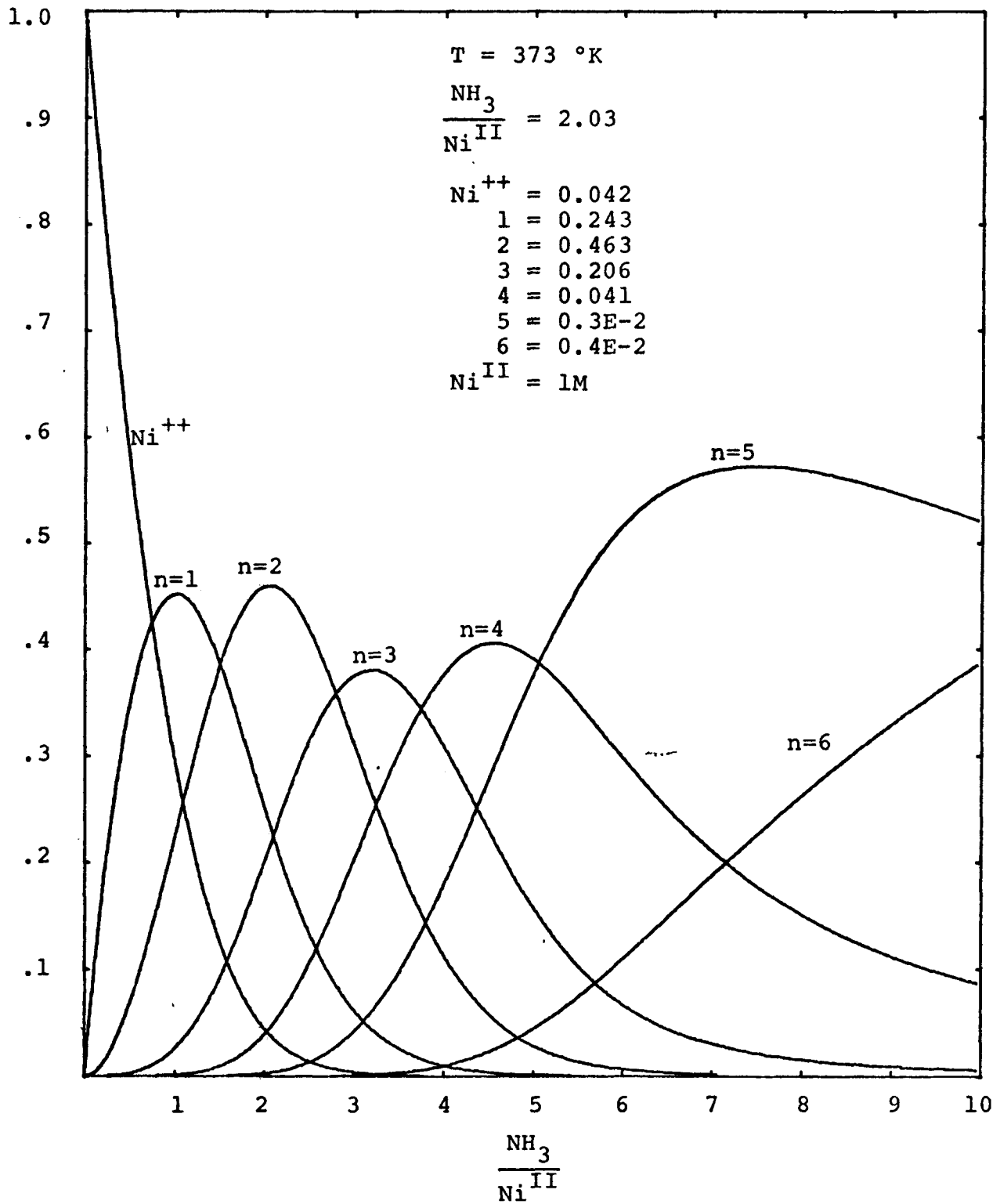


Figure 3.3. Fraction of nickel present in each form at different ammonia-to-nickel ratios, 100°C.

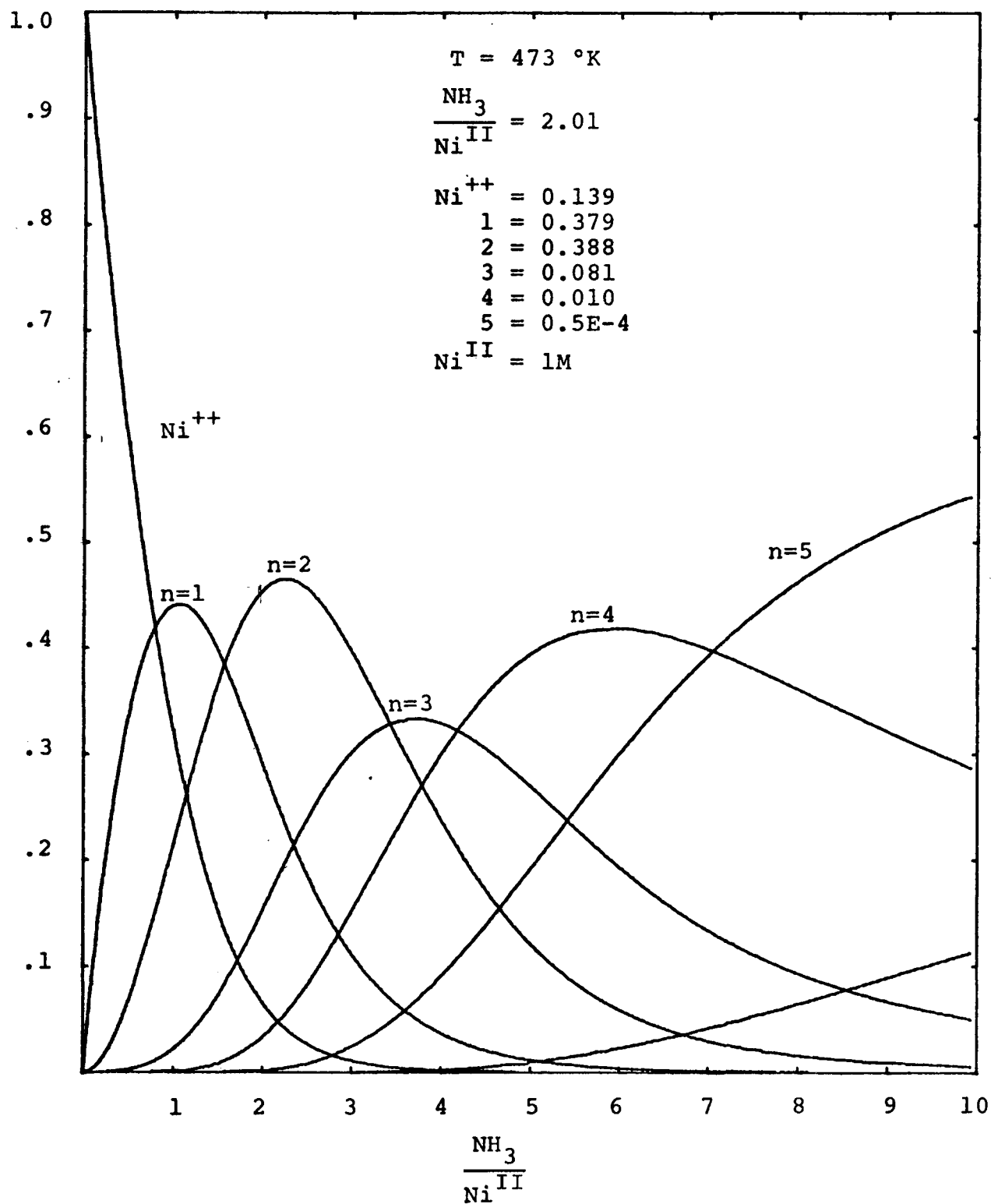


Figure 3.4. Fraction of nickel present in each form at different ammonia-to-nickel ratios, 200°C.

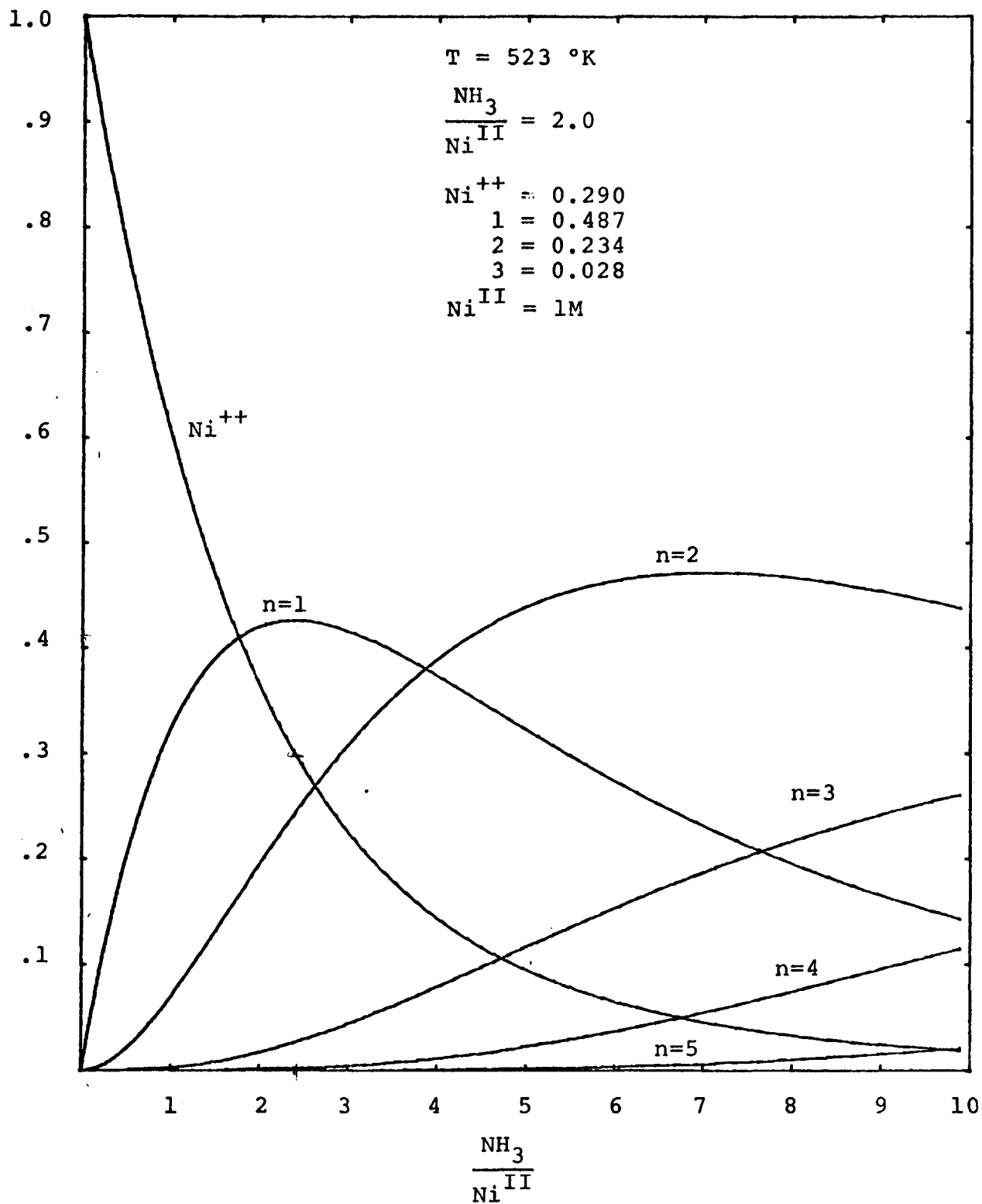


Figure 3.5. Fraction of nickel present in each form at different ammonia-to-nickel ratios, 250°C.

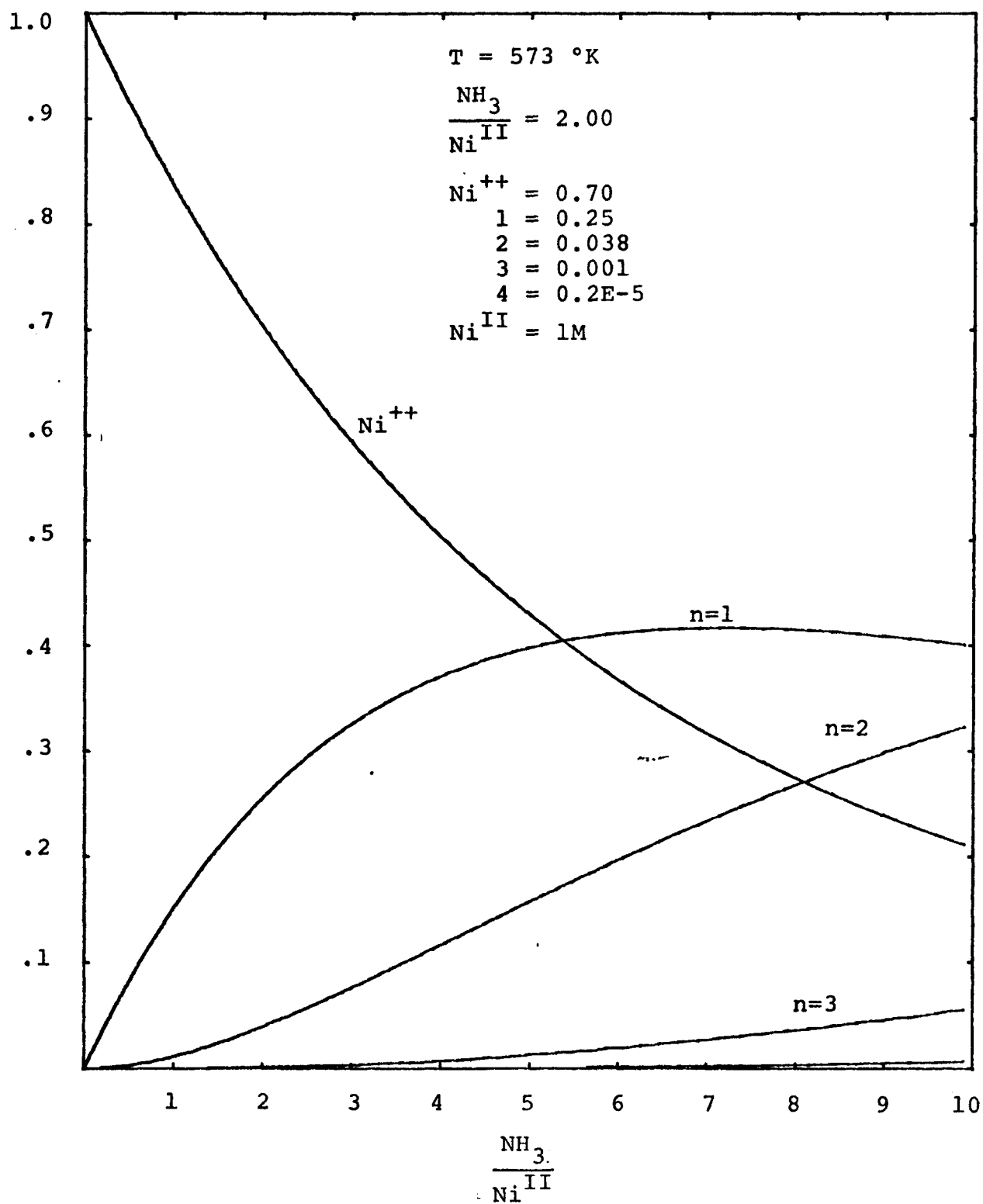


Figure 3.6. Fraction of nickel present in each form at different ammonia-to-nickel ratios, 300°C.

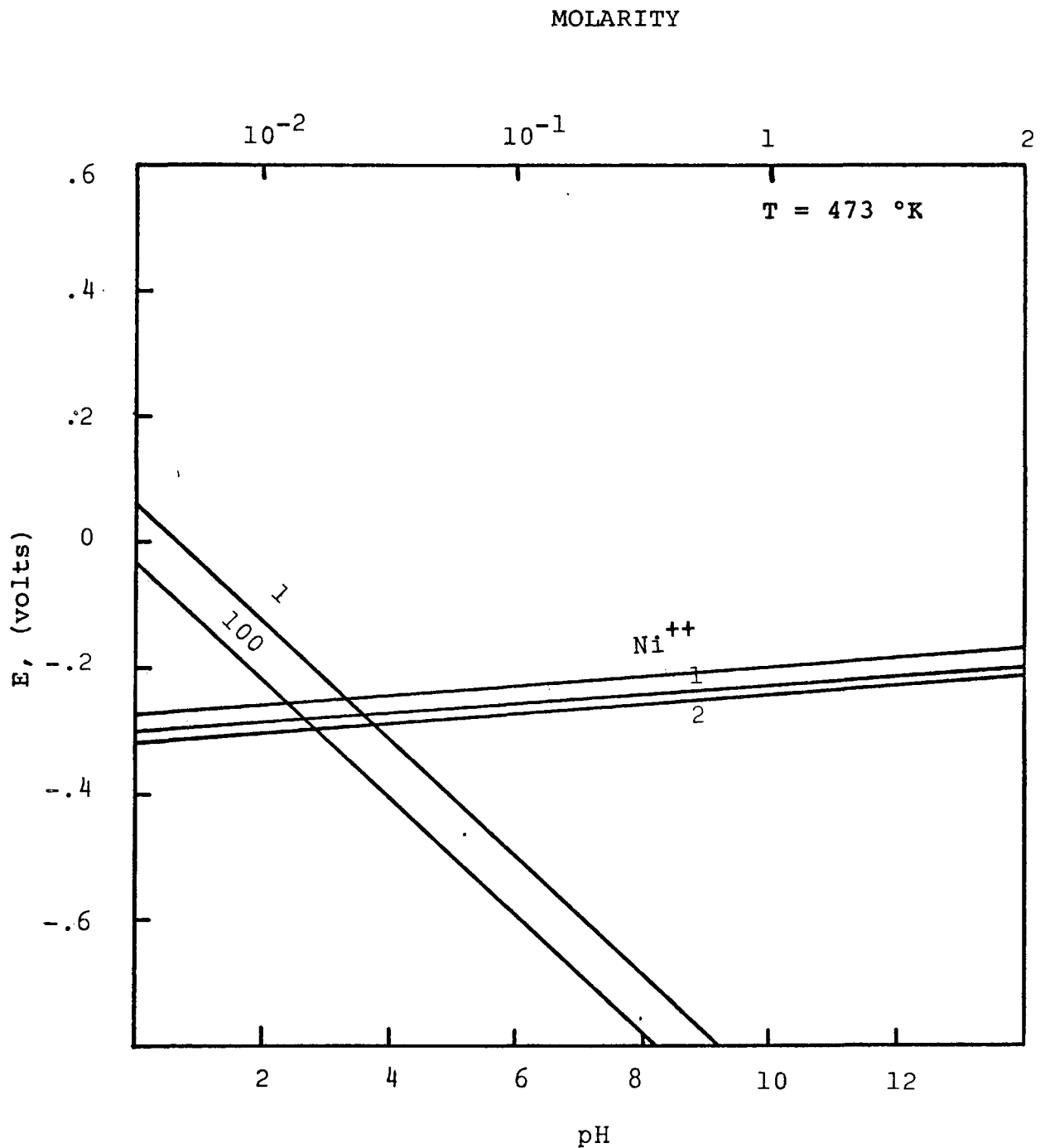


Figure 3.7. Relationship between E and pH at hydrogen pressures of 1 and 100 atm, and of nickel ions and the nickel-ammines $\text{Ni}(\text{NH}_3)_n^{++}$, 200°C .

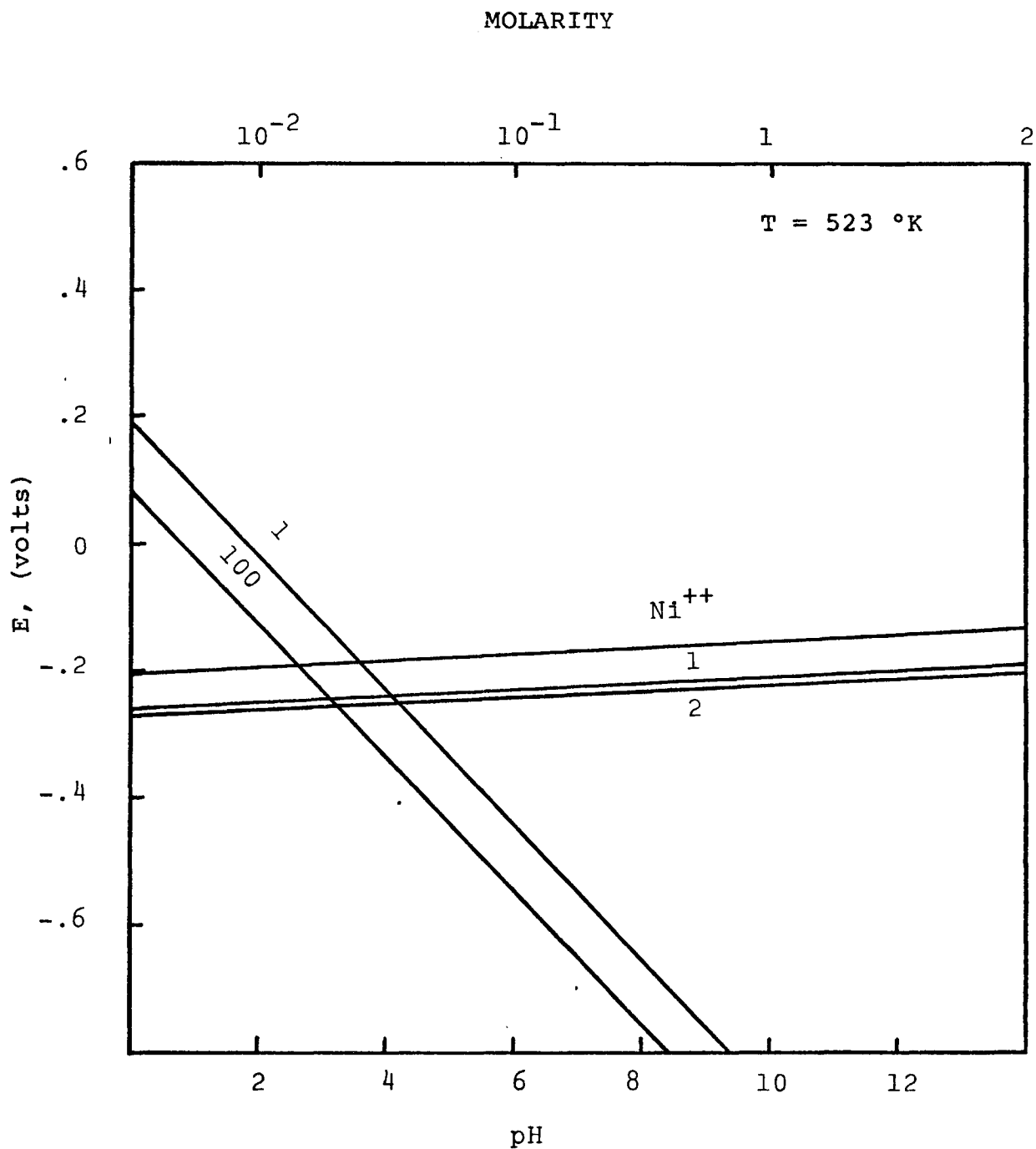


Figure 3.8. Relationship between E and pH at hydrogen pressures of 1 and 100 atm. and of nickel ions and the nickel-ammines $\text{Ni}(\text{NH}_3)_n^{++}$, 300°C.

the temperature, making the reduction more favorable. The reduction is then possible at much lower pH. Figures 3.7 and 3.8 show these plots.

It is worthwhile mentioning that these diagrams were constructed assuming activities equal to 1. Similar plots were constructed by making the corrections for activity coefficients following Criss and Cobble's⁽³³⁾ correspondence principle, and making the approximation that activities for the nickel ammines were the same as those for copper given by Butler⁽³⁴⁾. The effect of including activity coefficients may be interpreted such that the distribution of species obtained at a given temperature corresponds to a lower temperature (approximately 25°C lower) when the activity coefficient is set equal to unity. Figure 3.9 shows one such corrected plot.

3.4 Pourbaix Diagrams

For the thermodynamic study of the equilibrium phenomena of a metal in an aqueous solution, it is convenient to represent the various equilibria by a Pourbaix diagram where the abscissa represents the pH of the solution and the ordinate the equilibrium potential of each of the reactions considered.

Essentially, Pourbaix diagrams are isothermal phase diagrams which represent metal-ion-oxide equilibria, in which each of the components have a limited domain of stability.

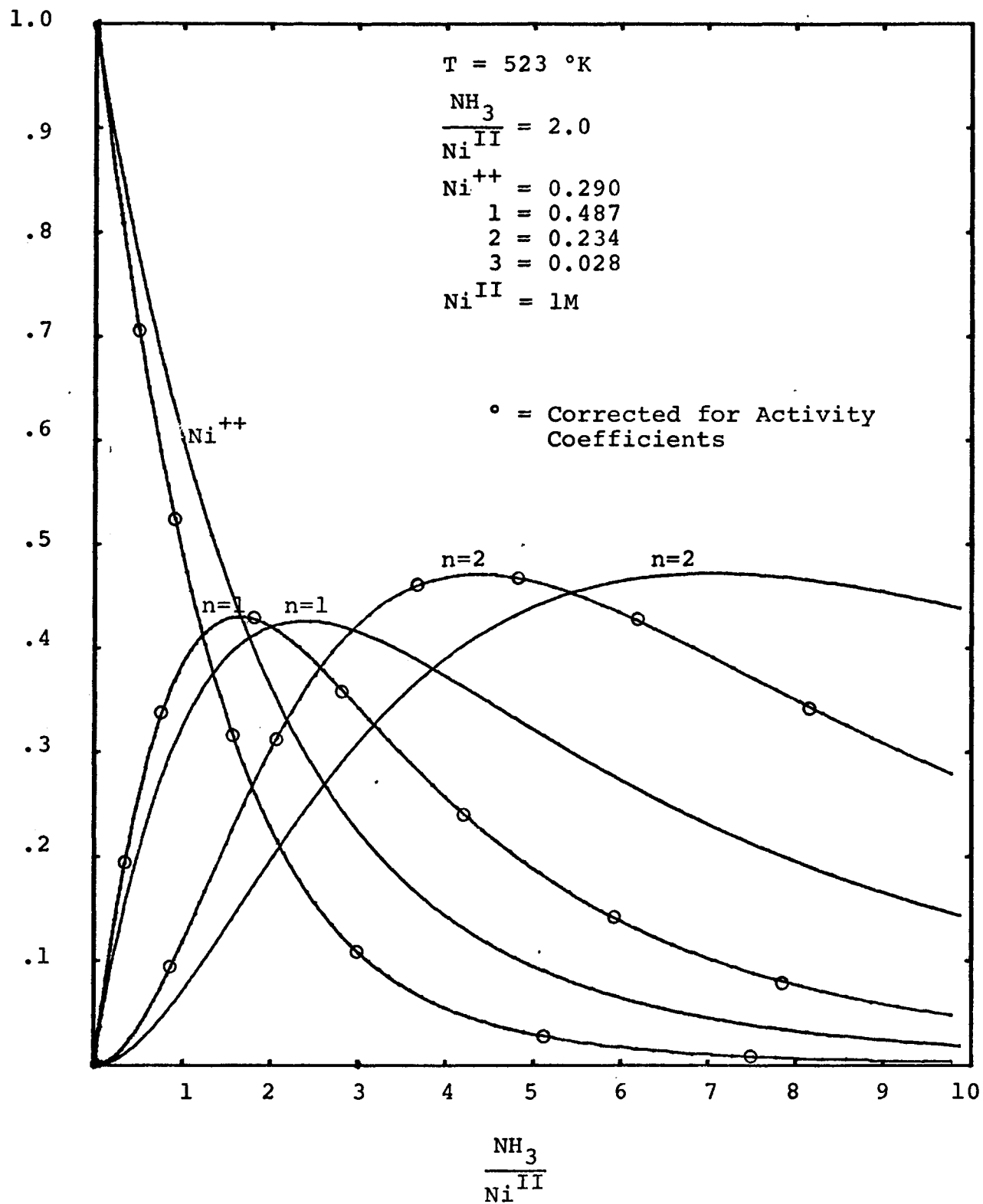


Figure 3.9. Difference obtained by accounting for activity coefficients at 250°C.

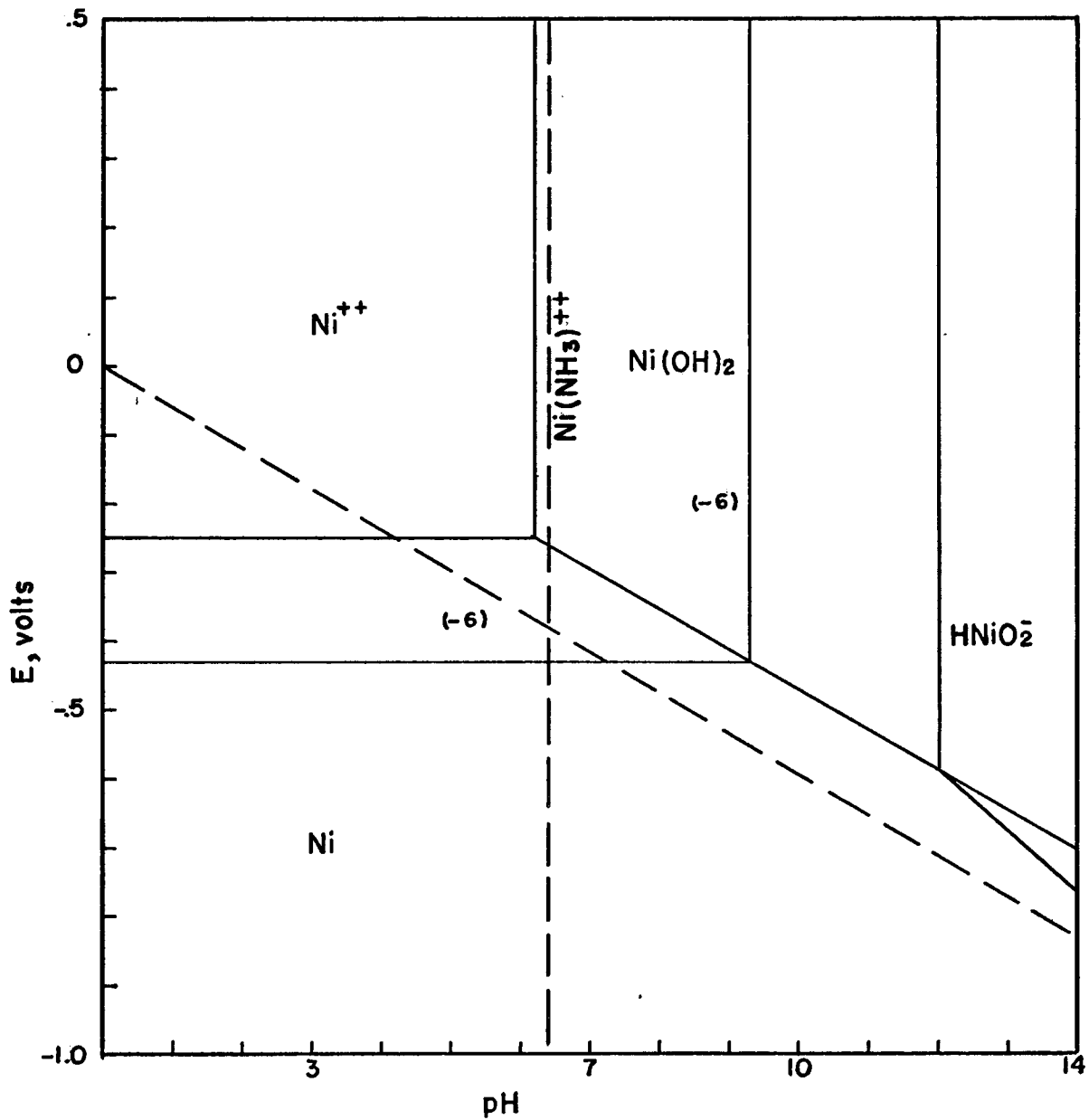


Figure 3.10. Equilibrium diagram for the system Ni-NH₃ for 25°C, 1 atm. pressure, and activities for nickel ions and nickel hydroxide: 10^{-6} M.

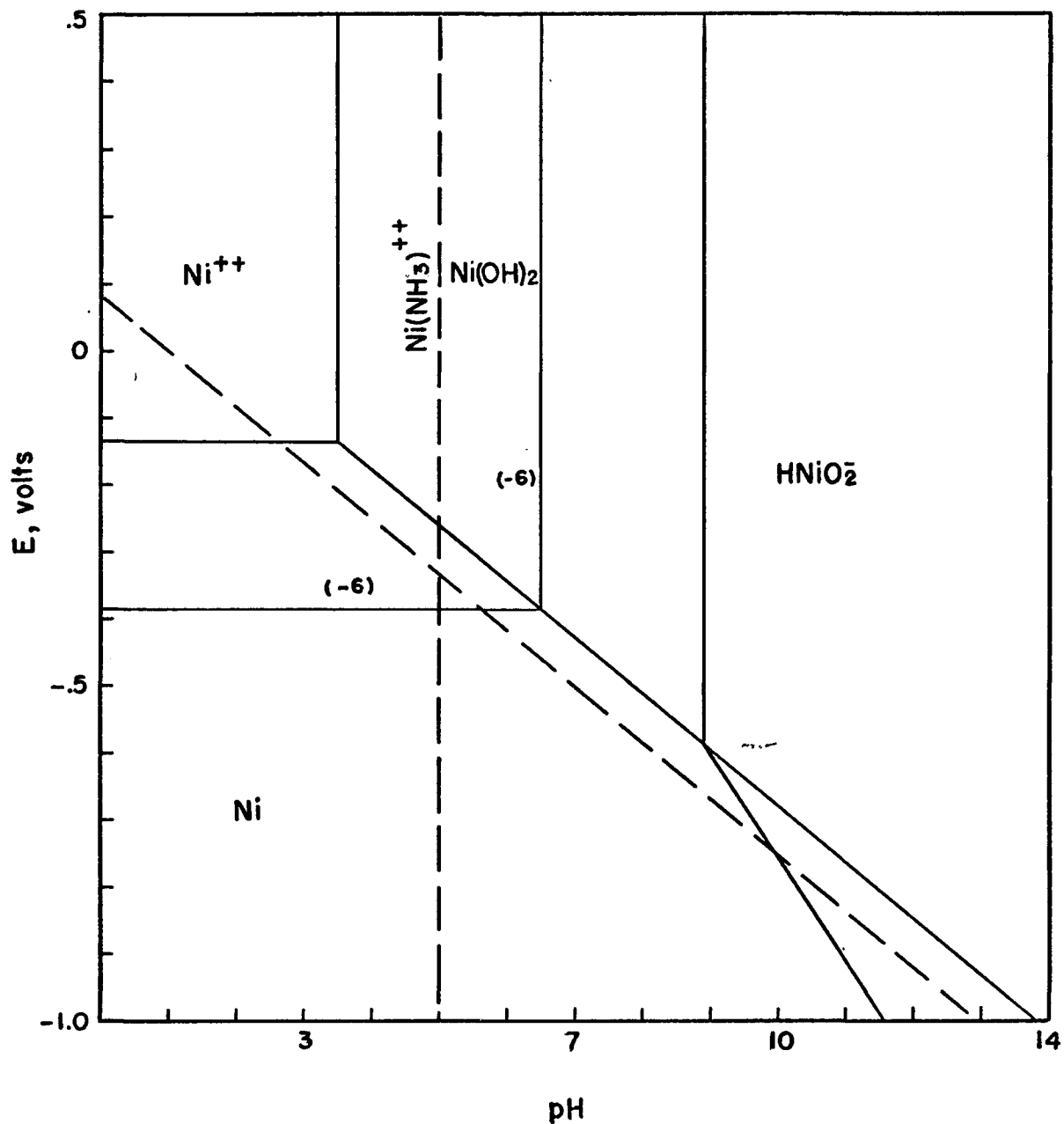


Figure 3.11. Equilibrium diagram for the system $\text{Ni-H}_2\text{O-NH}_3$ for 200°C , 1 atm. pressure, and activities for nickel ions and nickel hydroxide: 10^{-6}M .

In the present study, a series of such diagrams were drawn for different temperatures, for the system Ni-H₂O-NH₃. Graphical representations are shown in Figures 3.10 and 3.11. These diagrams represent a static situation. In practice the system is in fact dynamic and the lines representing the equilibria for the nickel-ammonia-complexes are no longer valid during next instance in time, due to continuously changing nickel-ammonia-complexes to nickel-ions ratio and concentration of ammonium in solution. In Figures 3.10 and 3.11 the stability region of the nickel-ammonia-complexes were drawn fixing the ratio and concentration of ammonium equal to 1 and 1 molar respectively.

The thermodynamic considerations presented so far is adequate in indicating the feasibility of the reduction of nickel solutions, but they do not explain the mechanism of most processes used commercially. As a simple case in point, it would appear from Figure 3.1 that nickel can be reduced from solutions at room temperature, using a hydrogen partial pressure of one atmosphere, provided the pH is high enough. In practice, reduction is not achieved and factors affecting the kinetics must also be taken into consideration.

3.5 General Kinetic Considerations

All chemical reactions are divided into two categories: homogeneous, which proceed in a bulk phase, and hetero-

geneous, which proceeds at the surface of separation between phases. The rate of a homogeneous reaction is defined as: *the amount of a particular species reacting in unit volume per unit time*. This quantity also represents the change in the concentration of the substance in unit time should the reaction be taking place at constant volume. The rate of heterogeneous reaction is defined as: *the amount of a particular species reacting per unit surface in unit time*. This quantity is no longer directly related to the change in concentration of the bulk phase. In both cases the reaction rates are functions of the temperature and the concentration of the species participating in the reaction.

In the system being studied (heterogeneous) two substances in solution (hydrogen and nickel ions) react with one another at a solid surface, the solid being itself unaltered, the overall reaction process may be broken down into the following steps:

a) Gas Absorption: In which the gas is absorbed into the solution to give a dissolved or solution species. Henry's Law Constant, H_e , relates the amount of dissolved gas to its partial pressure in the gas phase. This constant itself depends on the nature of the solvent and the temperature.

b) Transport of Reactants in Solution to the Solid-Liquid Interphase: For the reaction to occur, the reacting

species have to be transported from one phase to the surface of the other. The easiest way to accomplish such a transfer is by stirring the solution. In this manner the species can be convectively transported within the solution, maintaining its bulk concentration uniform. In the region close to the surface, where the velocity field is such that the solution velocity is small and decreases to zero at the solid surface, the reactants are transferred to the surface by molecular diffusion within the solution.

c) Molecular Diffusion to the Reaction Site: The mass transfer of reactants across a laminar boundary layer may be described using Fick's law of diffusion for the case of a steady concentration profile.

$$\frac{dn}{dt} = - DA \frac{dC}{dx} \quad 3.26$$

where $\frac{dn}{dt}$ is the rate at which the species diffuses (in the positive direction) through the cross-sectional area A , in a direction from high concentration to that of low concentration. The rate is proportional to the concentration gradient in the direction of diffusion, $-\frac{dC}{dx}$, and to the cross-sectional area A . D is the diffusion coefficient of the species in the solution and is a measure of the quantity diffusing in unit time through unit cross-section when the concentration gradient is unity.

d) Chemical Reaction: In heterogeneous systems where the chemical reaction takes place in a surface, three steps are occurring successively:

1) Adsorption: Two categories of molecular adsorption on surfaces may be distinguished - physical adsorption and chemical adsorption. Reactions of this type have been calculated by models called adsorption isotherms. It should be remarked that these have been essentially developed for gas/solid systems.

2) Chemical Reaction: In which the species adsorbed reacts either with other species on the surface or with each other.

3) Desorption: Products are desorbed from the surface, which gives the site further opportunity to adsorb fresh reactants.

e) Molecular Diffusion of the Soluble Reaction Products: In the same manner that the reactants arrive at the reaction surface, any solution product must also take the opposite route, with the same considerations of Fick's law of diffusion.

On the basis of the rate determining step, heterogeneous reactions are divided into three categories:

1) The rate of chemical reaction at the interface is much faster than the rate of transport of reactants to,

or products from, the surface. The observed rate is therefore determined solely by the rate of the slowest transport process. It is preferable to term these "transport-controlled" process rather than "diffusional-controlled", since mass-transfer occurs both by diffusion and by convection.

2) The rate of chemical reaction at the interface is much slower than the rate of either of the transport process, and hence determines the observed rate. This process is termed as "chemical control reaction".

3) Both rates are of comparable magnitude, and the observed rate is determined by some function of the two. These have been termed reactions of intermediate type, mixed control and the like. In fact it is the general case where coupling between the various processes are present. Since only the two limiting cases, 1) and 2), are usually considered (see Dobrokhotov et al⁽²³⁾) these will be discussed further.

3.6 Transport - Control

In such a situation, the chemical reaction between the solid and the ion would occur extremely rapid and the equilibrium would be obtained instantaneously. As a result, the concentration of ion, say at the interface would be close to the equilibrium value (if the reaction is irreversible, this value

is approximately zero). Therefore, further reaction can take place at a rate at which the consumed species would be replenished from the bulk of the solution. In other words, the reaction rate would be controlled by the transport of ions to the interface.

For a reaction controlled by convection or molecular diffusion, any mathematical treatment should be aimed at the developing expression of the mass flux. Such equations are obtained from a knowledge of the fluid flow or the hydrodynamics of the geometry concern.

Levich⁽³⁵⁾ has solved the transport equations for the case of rotating disc geometry. The solution for the final mass-flux equation is given by (the concentration of the diffusing species at the surface assumed to be zero):

$$j = 0.62 D^{2/3} \nu^{-1/6} \omega^{1/2} C \quad 3.27$$

where j = the mass flux ($ML^{-2}t^{-1}$)

D = the diffusivity (L^2t^{-1})

ν = the kinematic viscosity (L^2t^{-1})

ω = the angular velocity of the disc (t^{-1})

C = the mass concentration of the diffusing species (ML^{-3})

and the diffusion boundary layer (the region over which concentration changes are considered to occur) is given by:

$$\delta = \frac{DC}{j} = 1.61 (D/\nu)^{1/3} (\nu/\omega)^{1/2} \quad 3.28$$

This diffusion boundary layer (the region over which velocity changes are considered to occur) thickness is given also in terms of the hydrodynamic boundary layer thickness δ_0 , as:

$$\delta = .5 (D/\nu)^{1/3} \delta_0 \quad 3.29$$

where $\delta_0 = 3.6 (\nu/\omega)^{1/2} \quad 3.30$

This solution is strictly applicable to a disc rotating in an infinite environment only and under laminar flow conditions. Also, steady state is an assumption in the solution.

In principle the above equations can be used to predict reaction rates (j) when the process is transport controlled. Hence, this requires knowledge of the transport properties (D and ν) of the system. Since these are not always readily available, it is usual to group these terms together and investigate the effect of rotational speed on the system and instead measure an effective "rate constant" which contains these parameters.

3.7 Chemical Control

For chemical control reactions, we have the conditions that the concentration of the solute is uniform throughout the fluid body. Using the definition for the heterogeneous chemical

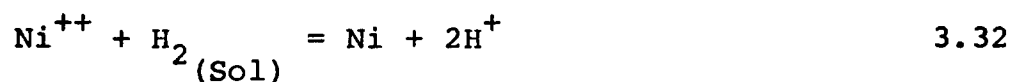
reaction rate then for a constant volume reaction

$$r_i'' \equiv \frac{V}{A} \frac{dC_i}{dt} \quad 3.31$$

where V is the solution volume

A is the surface area on which the reaction is occurring
 C_i is the bulk concentration of the species i .

Heterogeneous chemical reactions may be subdivided into two categories - non-catalytic and catalytic. The following reaction which is pertinent to this thesis, will be used to demonstrate the manner in which these two cases are treated theoretically:



Non-catalytic Heterogeneous Chemical Reaction: The approach is similar to the methods for homogeneous reaction and the following heterogeneous rate expression may be used if the reaction can be considered to be irreversible:

$$r_{\text{Ni}^{++}}'' = -k C_{\text{Ni}^{++}}^a C_{\text{H}_2}^b \quad 3.33$$

where $C_{\text{Ni}^{++}}$ and C_{H_2} are the concentrations of nickel ions and hydrogen gas in solution respectively.

The objective is then to find the values of k , a , and b .

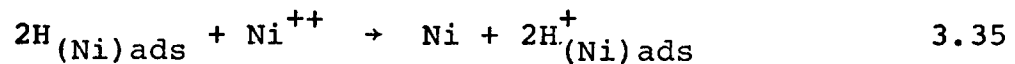
Should the reaction be elementary (i.e. equation 3.32 represents

the actual kinetic mechanism) then a and b would both be equal to 1. In general, however, this is seldom true.

Catalytic Heterogeneous Chemical Reaction: If one extends the theory of gas/solid catalysis to the case of liquid/solid system, then the reaction given by equation 3.32 can be visualized as occurring in the following steps:



where hydrogen is adsorbed onto the nickel surface,



where the adsorbed hydrogen reacts with the nickel ions to produce nickel metal and hydrogen ions. This reaction is in fact electrochemical in nature and involves an electron transfer between two hydrogen atoms on the surface and the nickel ion. The simultaneous de-electronation of the two hydrogen atoms on the nickel surface and the electronation of the nickel ion (reduction) takes place in the solution within close proximity of the surface; the reduced nickel atom being deposited on the nickel surface. Finally, the hydrogen ions are desorbed off the surface according to:



This is the so called active-site theory and will be discussed further in the interpretation of the results.

In general three types of rate expressions can be written depending on whether adsorption, surface reaction, or desorption is rate controlling. Texts dealing with gas/solid catalysis include those by Smith⁽³⁶⁾ and Levinspiel⁽³⁷⁾. The expressions are obtained by now considering the surface concentration of the species in a manner similar to homogeneous systems. These surface concentrations are then related to the bulk phase (gas) concentration by the adsorption isotherms. Again evaluation of unknown constants in the rate equations is the goal. This is accomplished by analysis of the experimental results. It should be mentioned that the description presented here on the catalytic behaviors are along the lines suggested by Dobrokhotov et al⁽²³⁾.

An important characteristic of chemical control reactions is their high sensitivity to temperature changes. This temperature response of the reaction mechanism is characterized by a high value of activation energy of the order of 10 to 15 Kcal-mol⁻¹ for a purely chemical controlled process.

Also, chemically controlled heterogeneous reactions are extremely sensitive to the nature and the extent of the surface

available for the reaction. Once again, this is in contrast to a pure transport-controlled reaction.

CHAPTER 4

EXPERIMENTAL APPARATUS AND PROCEDURE

The salient features of the apparatus used together with modification to standard equipment are covered in this chapter. The chemicals used and procedure followed are also reported here.

4.1 Apparatus

General. The reaction vessel consisted of a modified one liter - 316 stainless steel autoclave (Parr Instruments, Model 4641). A one liter pyrex liner was provided in order to avoid contact of the solution with the walls of the autoclave. The unit was able to operate at pressures up to 2000 psi and 300°C temperature.

Modifications in the head of the autoclave were made in order to eliminate the thermowell and replace it by a sensitive 1/16" Inconel sheathed iron-constant (Omega Engineering, Inc.) ungrounded thermocouple coated with teflon and jacketed in a 1/16" i.d. teflon tubing in order to avoid possible reaction between the thermocouple sheath and the solution.

A .025 bore, 1/16" o.d., 316 stainless steel tube was used as the sampling tube. The total length of the tube was approximately 2 feet and it was sealed through the autoclave head using a Swagelok fitting. A 316 stainless steel Nupro diaphragm valve was located above the head (see Figure 4.3). The hold-up of the sampling tube was measured and found to be approximately 1.0 ml. The heat transfer from the tube was adequate enough so that a flush and sample could be taken without the final solution being greater than 50-60°C.

The head was counter-bored in order to support a bearing housing (thrust-bearing and ball-bearings) which carries the shaft of the disc holder (see Figure 4.4). A stainless steel spring coupling was used to couple the standard drive shaft to the disc holder shaft; in this way the eccentricity was reduced to a minimum.

Heating of the autoclave was provided by a set of four heating elements (Watlow, 3.6 KW total rating) around an aluminum jacket of internal diameter equal to the outside diameter of the autoclave bomb. The aluminum jacket with heaters was assembled to the furnace shell and ends, the Fiberfax wool was used as insulation. A thermocouple was clamped to the heating elements and provided the sensor signal for the temperature controller. Temperature control was achieved by

Leeds and Northrup Electromax III temperature controller with proportional, reset, rate, and approach actions.

The autoclave could be quenched (200°C to 60°C) using a water cooled copper jacket. Typical quench times were of the order of 20 minutes.

The drive to the disc holder was provided by a General-Electric DC Statrotol motor with a SCR motor controller modified by replacing the standard one-turn potentiometer with a ten-turn one.

The rotational speed of the shaft was measured with a General-Radio 1531-AB Strobotac. The motor had a speed range of 0 to 1725 rpm.

Pre-purified hydrogen (99.95% purity) from a type E tank, regulated by a Matheson Model 2-350 regulator, was supplied to the autoclave. The pressure was measured with a Matheson 63-561, 316 stainless steel bourdon tube pressure gage. Valves were provided in the line for isolation and for flushing the system. All tube fittings were Swagelok and of 316 stainless steel.

The temperature of the solution was continuously recorded on a Honeywell Electronik 194 potentiometric recorder. The

range used was 10mV. and the thermocouple was provided with a 0°C cold junction. It was thus possible to measure the temperature of the solution to $\pm .5^\circ\text{C}$. Zero suppression was used to measure thermocouple outputs in excess of 10mV.

Figure 4.1 shows a schematic diagram of the whole system, and Figure 4.2 is a photograph of the equipment. Figure 4.3 shows the autoclave with the bomb and furnace removed.

Disc-Holders and Discs. The early experiments were carried out using a stainless-steel bell-shaped disc holder. The disc holder and shaft were sprayed with teflon over the region exposed to the solution. Experimental difficulties with these holders led to the use of all-Teflon holders screwed onto stainless-steel shafts. The final holder used was of Teflon and of conical shape; the choice of this shape was influenced by the work of Blurton and Riddiford⁽³⁸⁾. The discs were made from commercially pure nickel rod, 1/2" diameter and approximately 1/8" thick. They were pressed into the Teflon coated stainless-steel holders and in the case of the all-Teflon holders were held in place by a small stainless-steel Allen cap-screw, which screwed into a threaded blind-hole in the back of the disc. Photographs of the disc holders and discs are shown in Figures 4.4 and 4.5 respectively.

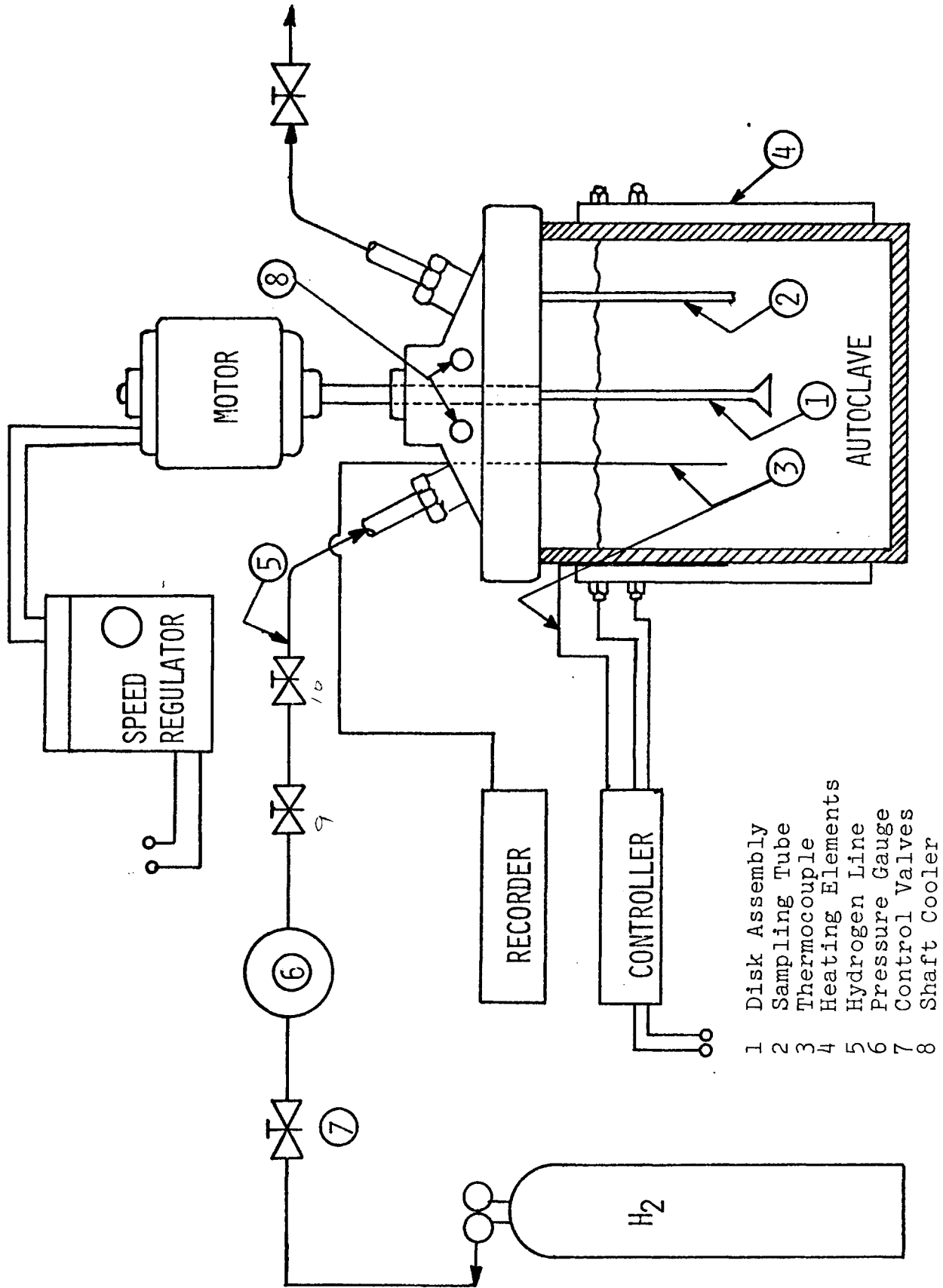


Figure 4.1. A schematic diagram of the system.

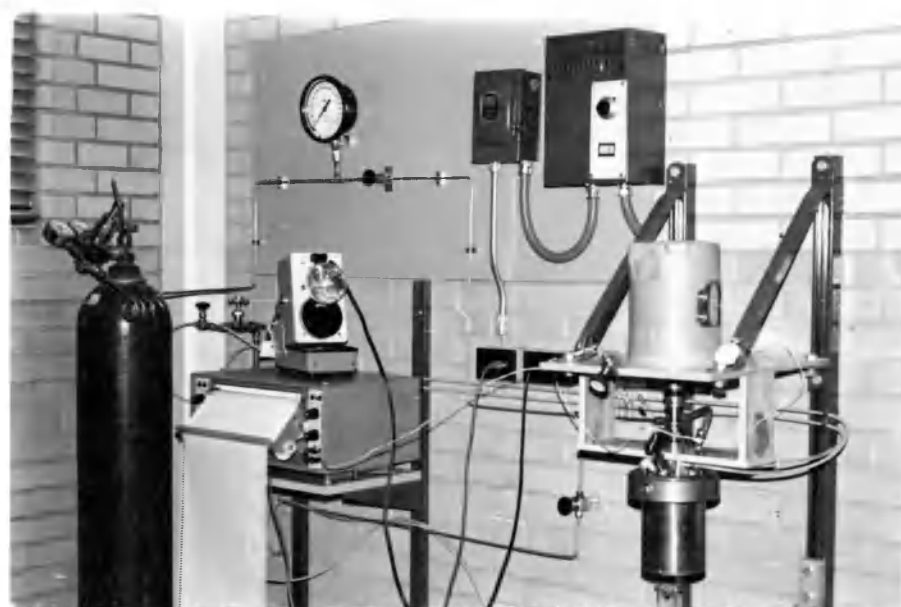


Figure 4.2. Photographic views of the equipment.

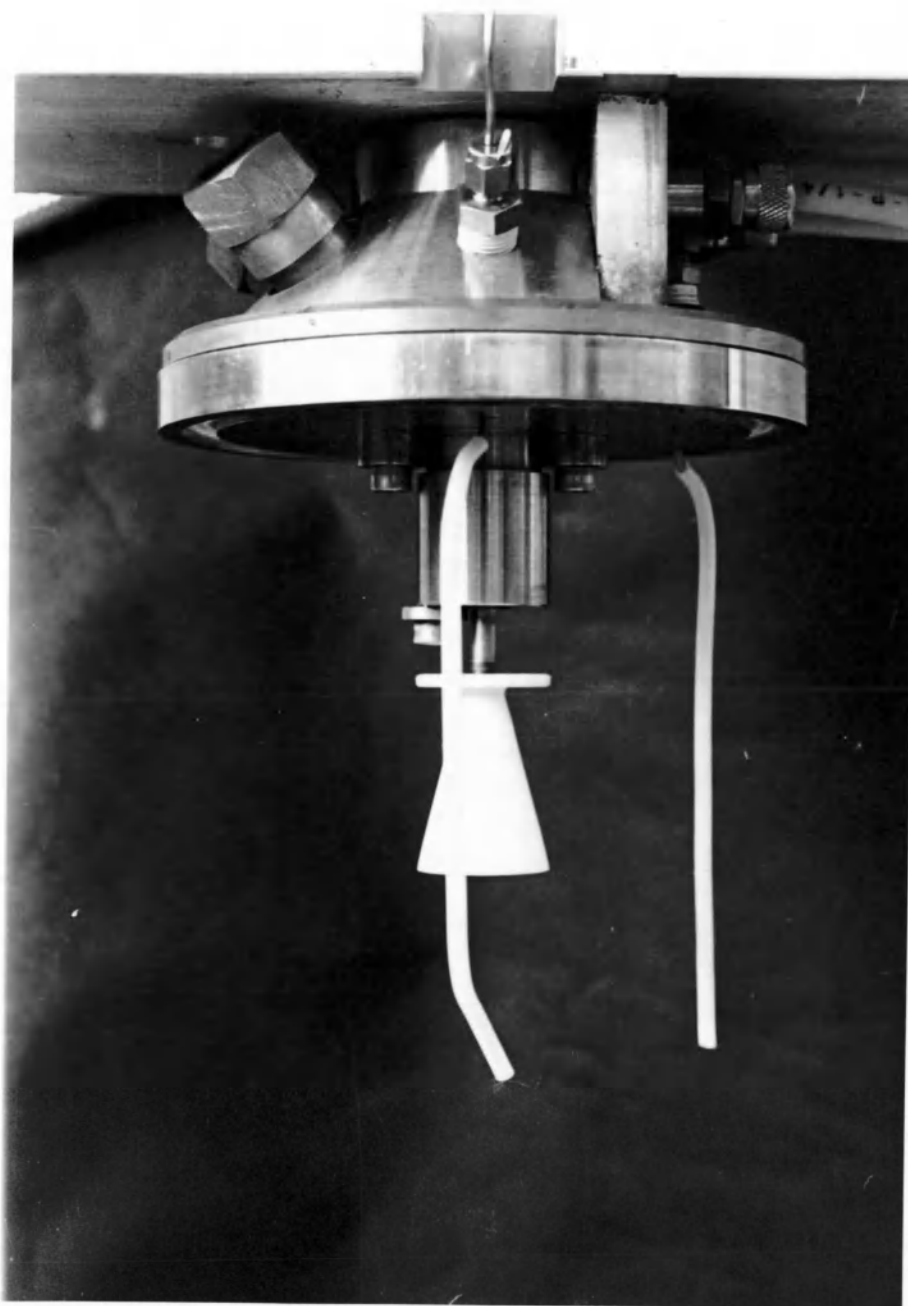


Figure 4.3. Close-up of autoclave head showing bearing housing with disc holder and shaft in place. Thermocouple is on the right and the sampling tube is on the left.

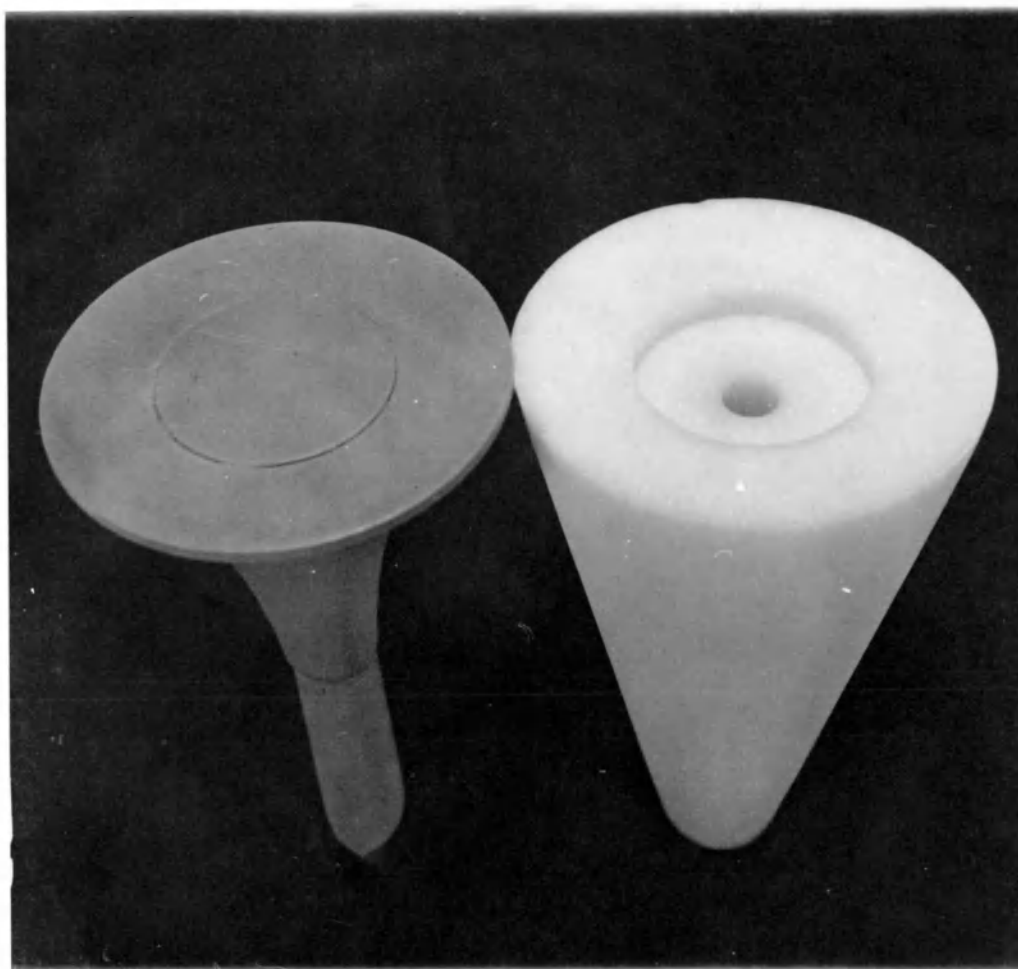


Figure 4.4. Photographic view of the disc holder.

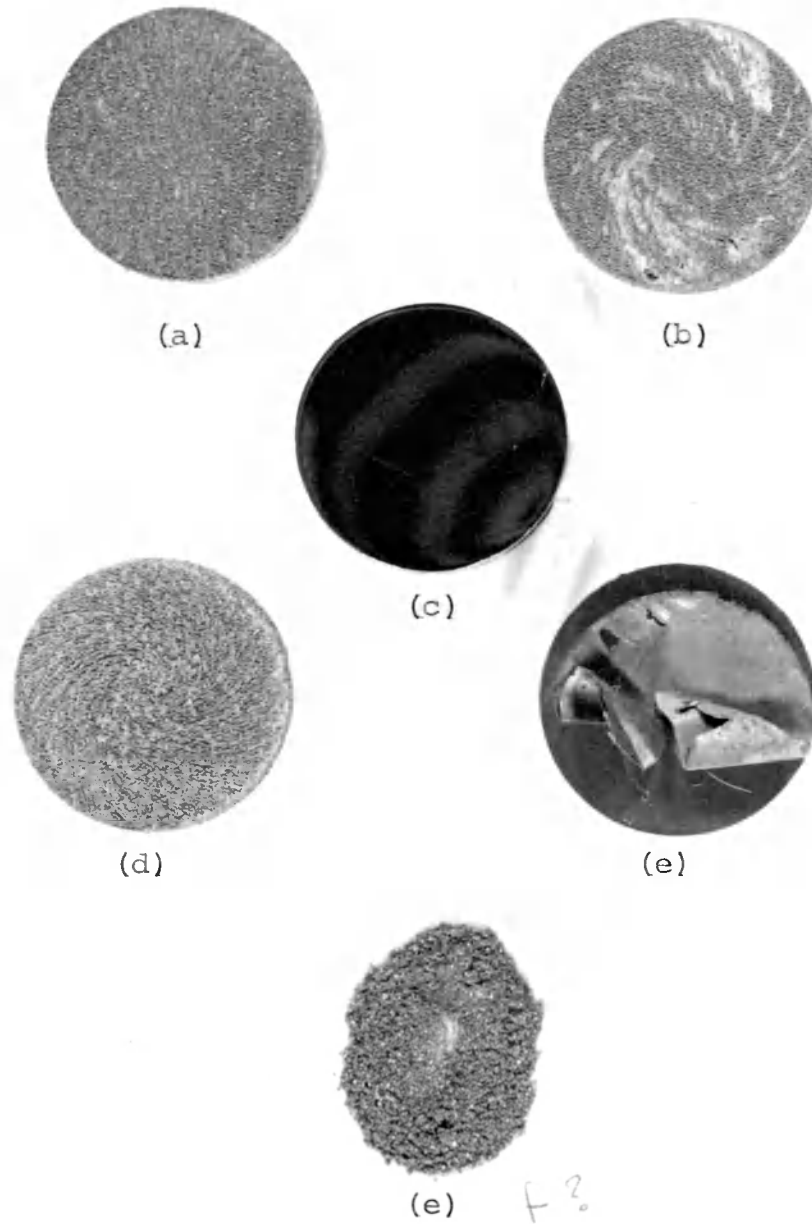


Figure 4.5. Photographs of discs and nickel powder
(a) (b) (d) - Reacted nickel disc
(c) - Unreacted nickel disc
(e) - Oxidized titanium disc
(f) - Nickel powder
Refer to section 5.3.

4.2 Materials

The synthetic solutions were prepared with reagent grade ammonium hydroxide (NH_4OH) (DuPont), ammonium sulfate (NH_4)₂ SO_4 and nickel sulfate (NiSO_4) (Mallinckrodt). The conductivity of the distilled water was approximately 20 μmho .

Titration of the free ammonia in the ammonium hydroxide was done using a one normal solution of hydrochloric acid with methyl-orange 1%, as an indicator.

The discs were of commercially pure nickel (nickel 200, supplied by INCO - 99.54Ni, .01Cu, .04Si, .005S, .03Fe, .27Mn, and .08C. Hydrogen used was high-purity (99.95% provided by NCG.

4.3 Procedure

The exposed surface of the disc was ground with silicon carbide abrasive paper from 1/0 to 4/0 grit. After this, a final polish was given with a one micron alumina oxide. The disc in this condition was treated electrochemically with one normal solution of sulfuric acid in order to eliminate any oxide remaining on the surface, the conditions were 1mA cathodically for about five minutes. The disc was then washed with distilled water and methyl-alcohol and either pressed into the holder or screwed into place.

A volume of 400 cc of synthetic sample was poured into the pyrex liner, placed inside the autoclave, which was now assembled. The valves in the system were now closed and the system was heated to approximately 100°C. At this stage the sampling tube was flushed and a sample taken (volume of flush and sample, between 3 and 4 ml) and the hydrogen gas was admitted into the system at a total pressure close to the predetermined value for that run. During the course of the investigation it was discovered that the hydrogen dissolution was quite exothermic, and it was therefore necessary to start admitting hydrogen at a temperature lower than the actual value for a particular run. The working temperature was attained in approximately 30 to 45 minutes. During this time, and also during the actual run, samples (including flushing to eliminate the hold-up in the sampling tube) were continuously drawn out of the system at 10 to 15 minute intervals.

The samples, stoppered in 6 ml. flint vials, were allowed to cool and the pH measured using a Beckman Zeromatic II. They were then diluted within a range of lower than 5 parts per million (linear calibrated region of absorption versus concentration) and analyzed for nickel on a Perkin-Elmer 107 AA Spectrophotometer. The samples were diluted in a 10 to 1 ratio with a solution of 5% hydrochloric acid (using a Fisher Model 250 diluter) in order to avoid interference with sulfate ions which were always present in the solution. These analyses were carried out after the completion of the run.

At the end of each run, the disc holder and liner were washed with a concentrated solution of nitric acid in order to dissolve any traces of nickel that might be remaining on the glass. The same solution was used to wash the tips of the sampling tube and thermocouple. After the nitric acid wash, the liner was thoroughly rinsed with distilled water, followed by a final methyl alcohol rinse. A rinse with the run-solution preceded the filling of the liner.

CHAPTER 5

RESULTS

The results presented here covers both the experimental investigation as well as theoretical attempts at predicting the experimental results obtained. The experimental investigation covered numerous preliminary runs not reported here. Problems were first encountered with the Teflon coated stainless steel disc holders, in that nickel precipitated on the Teflon coating. Similar behavior was obtained with an oxidized titanium disc holder. Microscopic examination showed that the coating was in fact porous and nickel precipitation initiated at these points on the holder. The final disc holder of pure Teflon was successful in eliminating this problem. No appreciable deposit was obtained on the glass liner nor the thermocouple sheath and sampling tube. Reproducibility of the results were tested by repeating several runs at random.

5.1 Precipitation Rate Curves

Typical reduction curves, depicting the amount of nickel remaining in solution as a function of time are shown in Figure 5.1 to 5.6, and were obtained using synthetic solutions

in which the amount of nickel was fixed at .01 M. The ordinate represents the concentration of total nickel (in all forms) remaining in solution, expressed as parts per million, the abscissa represents time measured from the instant the hydrogen was admitted.

The plots are seen to be quite different as far as disc, disc preparation, and procedure were concerned. Except for the discs of surface oxidized titanium and the nickel discs thermally treated in hydrogen atmosphere, a characteristic plateau is observed during the precipitation. In general the reduction appears to be linear with time. The presence of the plateau will be discussed in the section (5.2) which follows. In most experiments, reduction proceeded almost to completion, the final concentration of nickel being less than 75 ppm.

5.2 Effect of Disc and Disc Preparation

These effects should be considered separately, due to the fact that in some instances discs of material other than nickel were used (electrolytically oxidized titanium). Furthermore the nickel discs themselves were exposed to different treatments (hydrogen atmosphere at high temperatures, electrochemical hydrogen treated, and no treatment at all). In some cases the discs were kept stationary until the working temperature was reached, and in other cases the disc was rotating throughout the run.

In Figure 5.1 the reduction curves for a number of cases are shown. Table 5.1 gives the legend for all runs carried out. The only feature to which attention will be drawn, is the absence of a plateau region for the oxidized titanium disc (run TI01).

Oxidized Titanium Discs: Figure 5.2 shows the reduction curves for the oxidized titanium discs, as well as the temperature and pH history during the runs. These particular discs were oxidized electrochemically in order to provide a very inert film of oxide (rutile) over the surface. It can be seen that the average rate of the reaction varies linearly with time for both of the cases considered. Also, no effects on rate of reaction are observed as the rotational speed is increased. This is clear evidence of a chemical-controlled reaction of zero order with respect to total nickel concentration. The average reaction rate, for the cases shown in Figure 5.2, has a value of 9.6×10^{-5} mol-liter⁻¹-minute⁻¹. It can be seen that there is a sudden drop in pH, after the total nickel concentration in solution falls below 400 ppm.

Nickel Discs Treated in Hydrogen Atmosphere: The results are shown in Figure 5.3. The behavior was somewhat similar to that for the oxidized titanium discs, except that they show a tendency to fall off towards the end of the reduction. The approximate rate of the reaction is lower (5.82×10^{-5} mol-liter⁻¹-minute⁻¹).

Table 5.1 Runs Legend.

RUN#	T°C	P _{Total}	RPM	TYPE	SPINNING ALWAYS AF.T°C	NITH	TREATMENT			
							NIEH	TIO	NINT	
NITH1	225	450	600	Ni	X	O	X	O	O	O
NITH2	225	450	400	Ni	X	O	X	O	O	O
TIO1	225	450	600	Ti	X	O	O	O	X	O
TIO2	227	450	1000	Ti	X	O	O	O	X	O
NINT2	225	450	600	Ni	O	X	O	O	O	X
NIEH4	225	425	1000	Ni	O	X	O	X	O	O
NIEH5	225	450	600	Ni	O	X	O	X	O	O
NIEH6	225	425	100	Ni	X	O	O	X	O	O
NIEH7	225	425	600	Ni	X	O	O	X	O	O
NIEH8	225	450	600	Ni	O	X	O	X	O	O
NIEH10	170- 230	300- 450	600	Ni	X	O	O	X	O	O
NIEH11	188	400	600	Ni	X	O	O	X	O	O
NIEH12	205	420	600	Ni	X	O	O	X	O	O
NIEH13	225	450	600	Ni	X	O	O	X	O	O

Table 5.1 Continued . .

LEGEND

- NINT → Nickel not treated
- TIO → Titanium oxidized electrochemically
- NITH → Nickel treated in hydrogen atmosphere
- NIEH → Nickel electrochemical hydrogen

- X → Yes
- O → No

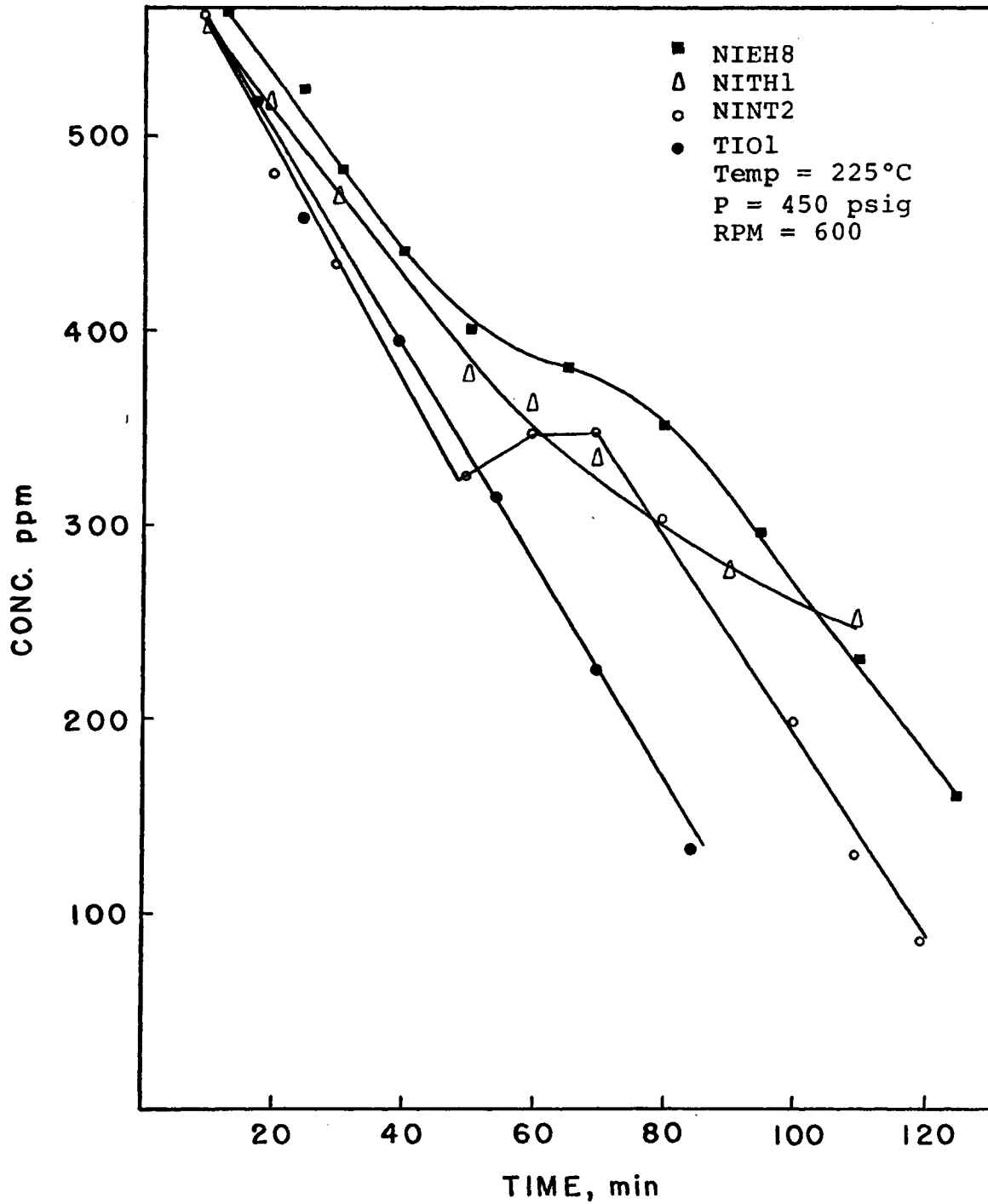


Figure 5.1. Typical reduction curves obtained under different conditions.

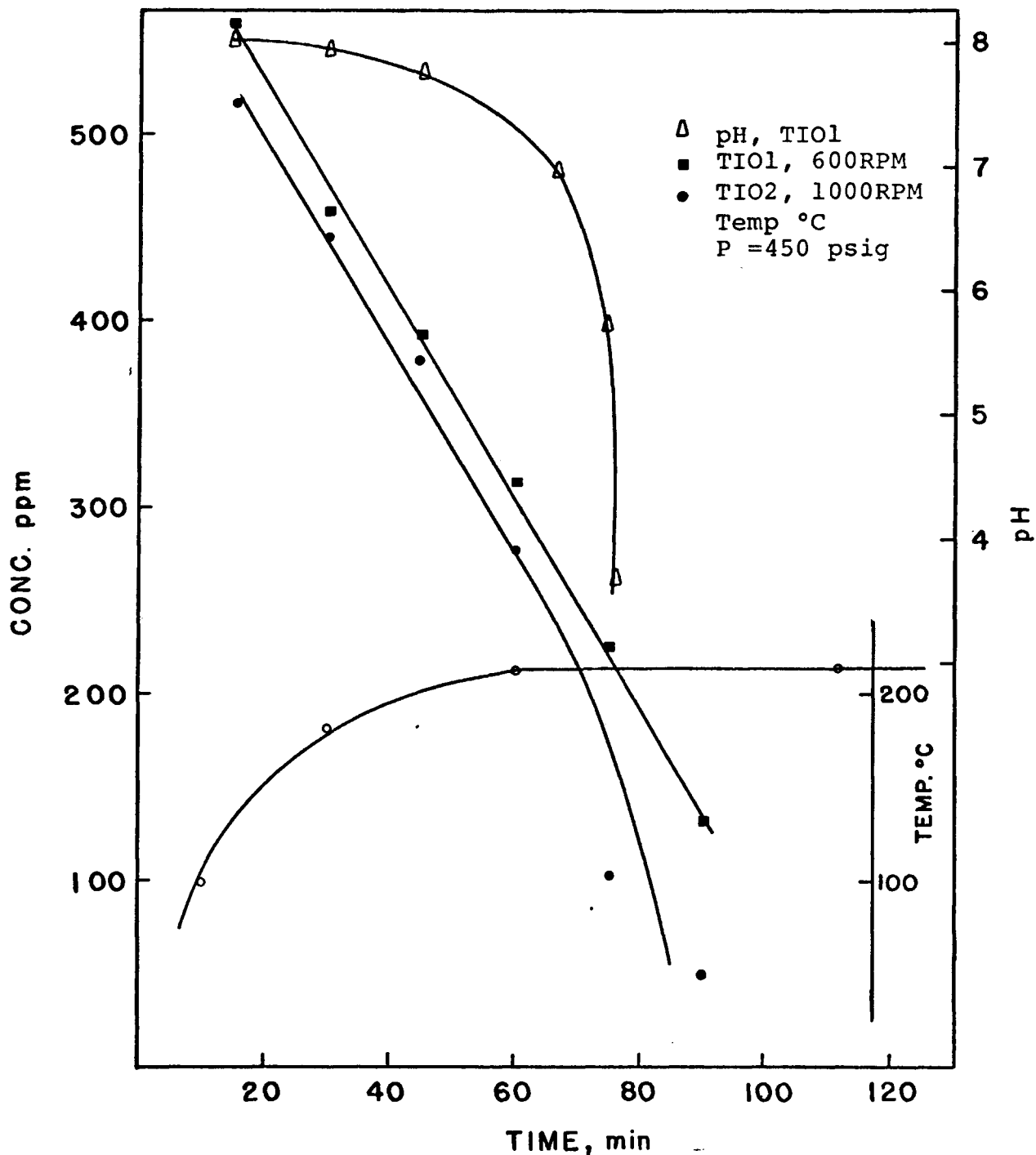


Figure 5.2. Precipitation rate curves for oxidized titanium discs.

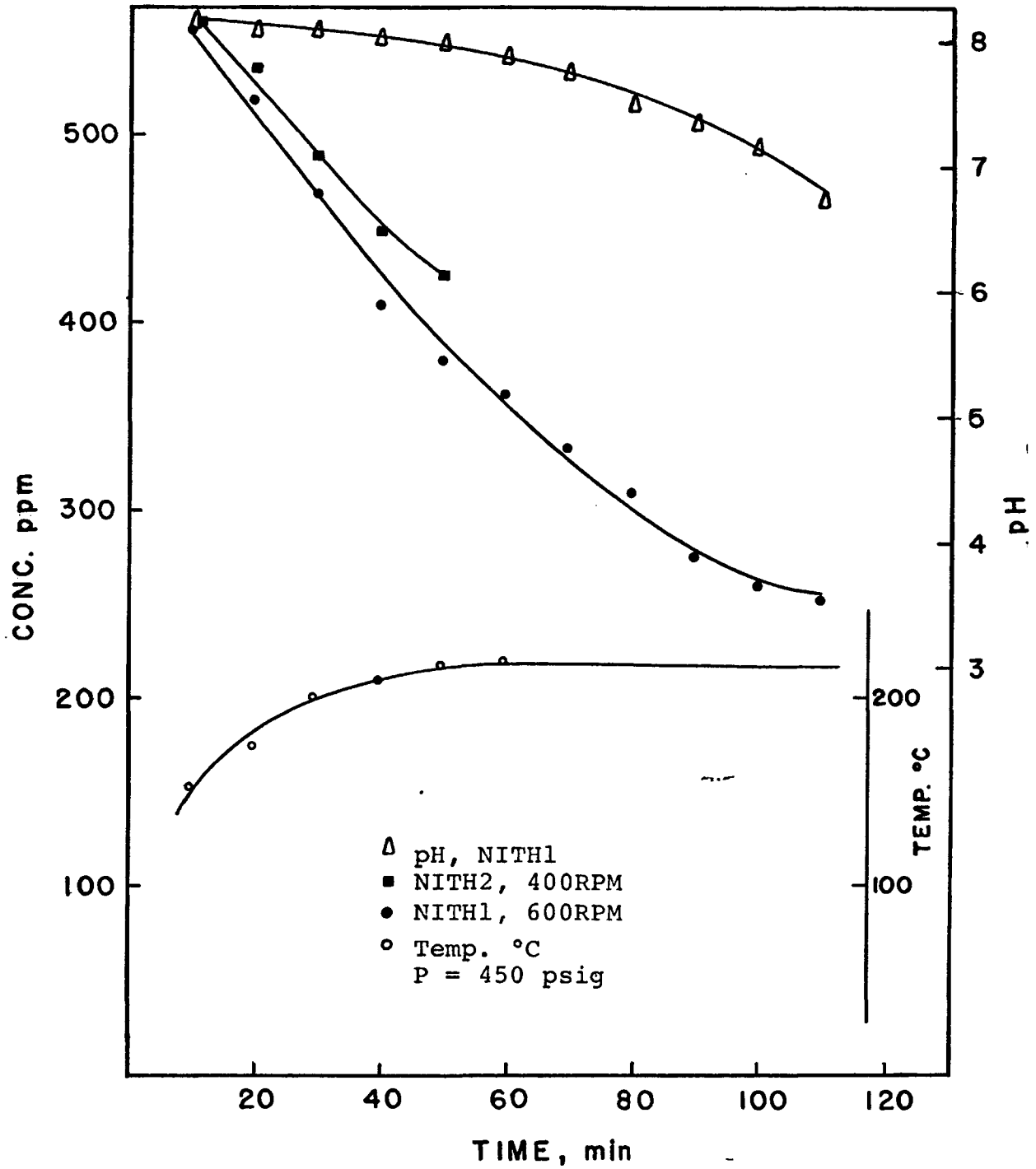


Figure 5.3. Precipitation rate curves for nickel discs treated in hydrogen atmosphere.

Nickel Discs -- Electrochemically Hydrogen Treated and No Treatment: The common feature of the reduction curves for these discs is the plateau region, mentioned previously, which occurred when the system reached the preset temperature for a particular run. The curves for the treated discs are shown in Figure 5.4. The behavior is the same for all the runs shown except that run NIEH4 was carried out with the disc stationary during the initial period. It is noted that the curves for 100 and 600 rpm have approximately the same rates during the primary and secondary reduction periods. The primary reduction rate is much higher for the case when the disc was stationary and is explained by the fact that the deposit tended to cover the entire disc surface when the disc was kept stationary. The surface area on which the reaction was occurring was therefore greater.

Figure 5.5 shows the effect of the electrochemical hydrogen treatment of the disc on the primary reduction rate for the case when the disc is kept stationary. It can be seen that basically there is very little difference. It should be mentioned that the untreated disc was not highly polished using alumina as was the case prior to the electrochemical treatment for the treated discs.

The morphology of the deposit can be observed by the photographs in Figure 4.5. In (a) the nickel disc was thermally

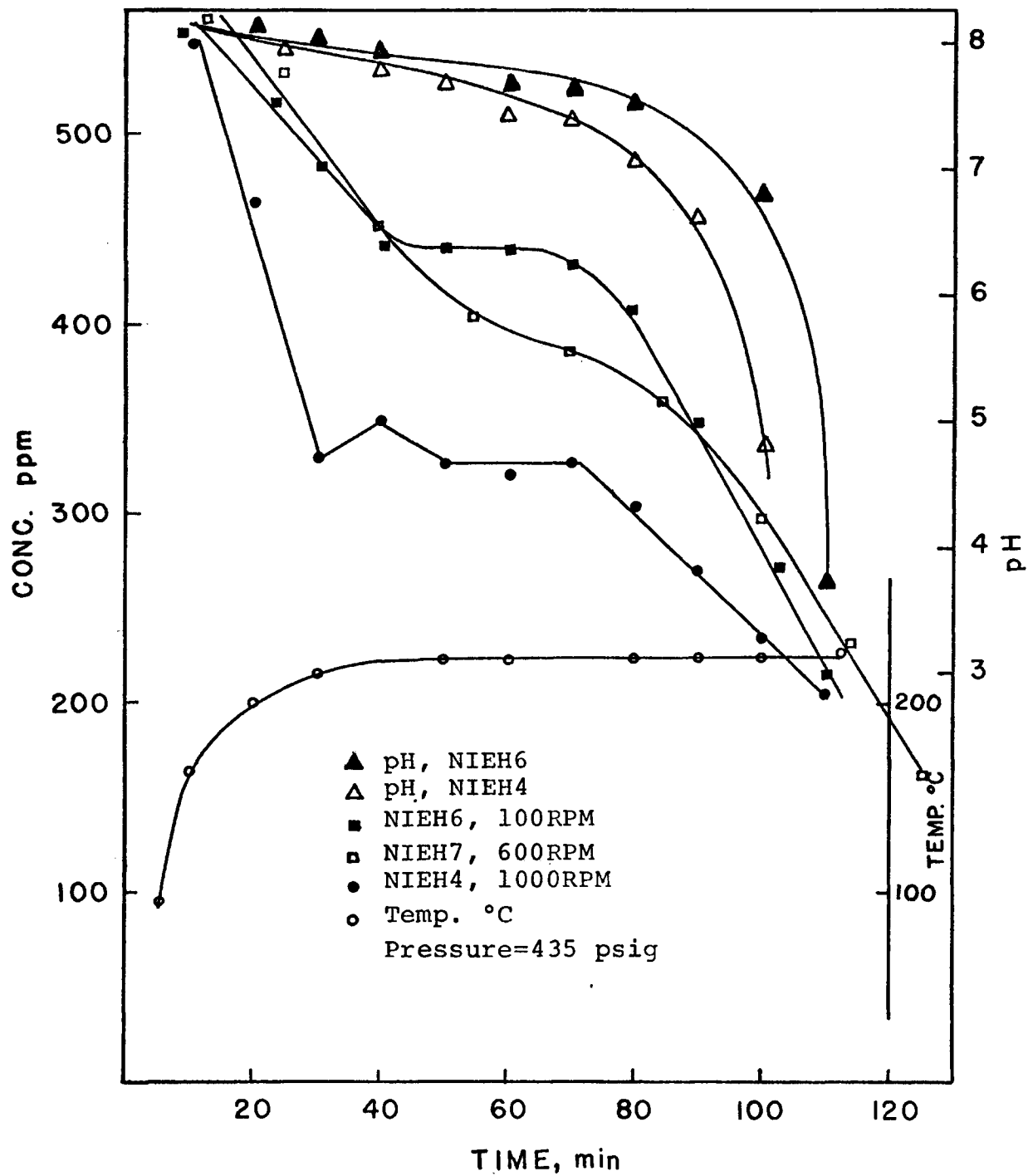


Figure 5.4. Precipitation rate curves for nickel discs electrochemically treated.

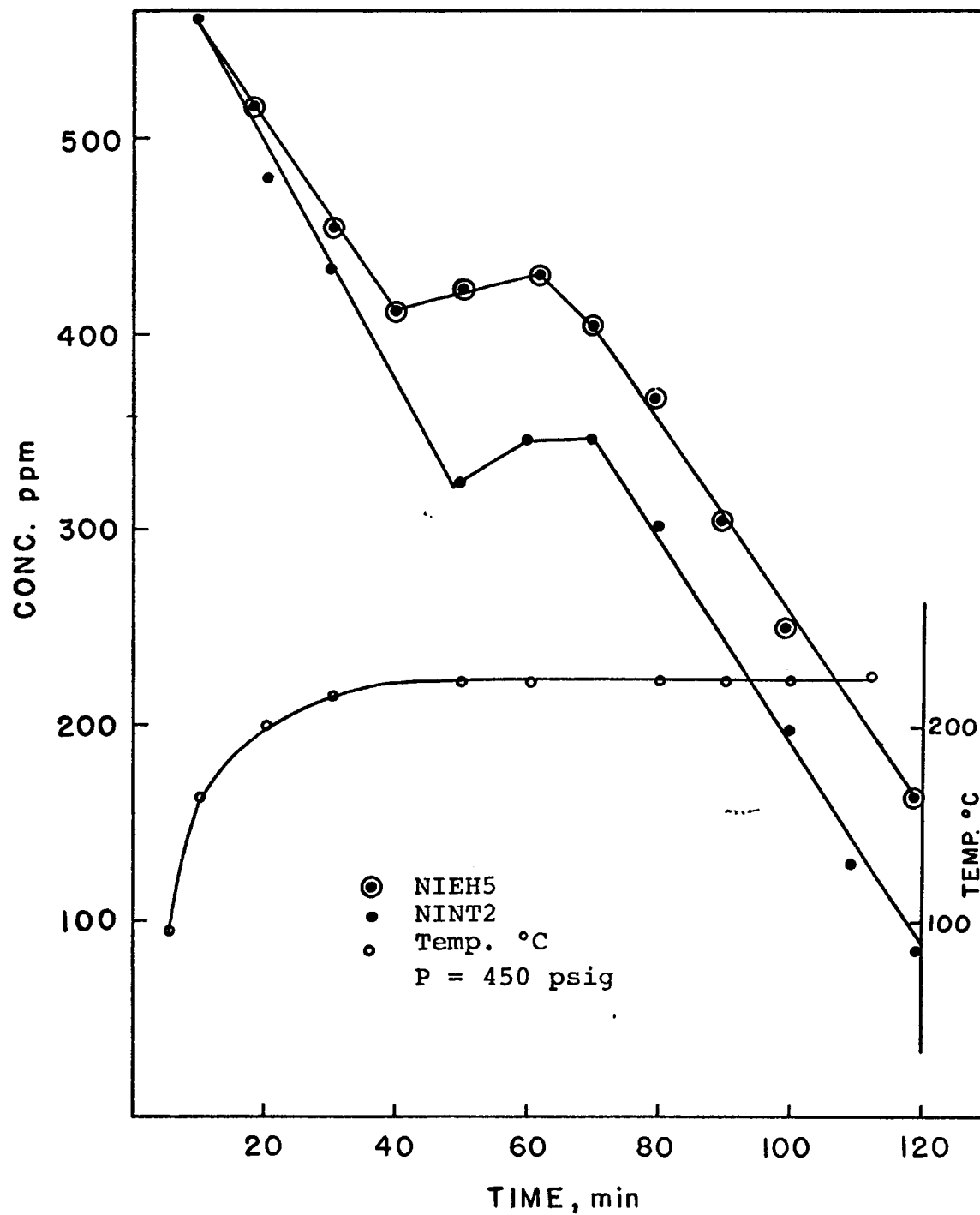


Figure 5.5. Precipitation rate curves for nickel discs under different conditions of surface preparation.

treated in hydrogen atmosphere and a uniform deposit was obtained. The nickel disc (b) was electrochemically hydrogen treated and run at a high RPM; the flow pattern of the solution can be seen on the disc with considerable bare spots. It should be pointed out that there were some discs with even larger areas of deposit-free surface. An untreated disc prior to electrochemical treatment is shown in (c); the surface was, of course, mirror like and the black color is only because of the lighting used for the photograph. In (d) another electrochemically treated nickel disc is shown which was run at a lower RPM than (b). The oxidized titanium disc with its foil like deposit peeled off is shown in (e). Powder collected on the bottom of the liner is shown in (f).

The following explanation for the plateau region which occurred in the electrochemically treated nickel disc has been advanced. It appears to fit all the "clues" available. The solution may become supersaturated with hydrogen as it is heated to the working temperature. Nucleation and growth of hydrogen gas on the surface of the disc could therefore occur when the solution temperature stabilizes. The gas bubbles thus formed can adhere to the surface and mask it from further reaction. This seems to be the only plausible explanation when one considers the behavior observed with the oxidized titanium and thermally-treated-in-hydrogen-atmosphere discs (no plateau in the reduction curves). This would indicate that

hydrogen gas is more easily nucleated on the electrochemically treated nickel disc. Once the supersaturation has been "relieved" hydrogen gas will no longer be present on the surface and the reaction can now proceed again.

5.3 Effect of Rotational Speed

Within the rotational speed investigated (100-1600 RPM) there appeared to be little effect of the rotational speed on the reduction rate for runs carried out under identical conditions (other than rotational speed). In fact with the disc stationary higher reduction rates were obtained due to the surface area taking part in the reaction as discussed in the previous section.

The effect of the rotational speed on the deposited surface taking part in the reaction may be pursued further at this stage. Referring once again to the photographs in Figure 4.5, it was observed that when the disc was rotated from the start of the run that the deposit was preferential and followed the hydrodynamic flow pattern of the solution. On the other hand, the deposit covered the entire surface when the disc was not rotated. This contrasting behavior was not observed with the thermally treated-in-hydrogen atmosphere nickel disc nor the oxidized titanium. Based on work reported on gas-solid catalysis⁽³⁶⁾, it appears that hydrogen gas is chemisorbed onto nickel, the process being unactivated. If one extends

this to this system, it is quite possible that the same remarks are true. Thus, the reaction proceeds at a higher rate once all the active sites on the surface are in use. However, it would appear that the active sites are affected during the initial rotation of the disc which were treated electrochemically with hydrogen. Consequently, preferential lines of deposit are established on the surface. This phenomenon does not appear to occur on the thermally treated discs nor oxidized titanium. It might be that these surfaces have active sites which provide much larger interaction with the hydrogen adsorbed with the result that the hydrogen is more reactive.

After the plateau region had been passed, the rate of reduction is higher for the cases where the disc had been rotating throughout the run. This may be explained by the fact that the deposit in the case of the preferentially deposited nickel grows dendritically into the solution and is sheared off by the rotation of the disc. These sheared-off deposits (powder) thereby provide additional nickel surface on which reduction may take place. This shearing action is not as severe when the nickel surface is completely covered with nickel as is the case for runs where the disc was stationary initially. Evidence for this postulate can be seen in Figure 4.5(b) where a disc which had been rotated continuously shows bare spots. In addition these runs also produced significant powder which collected on the bottom of the lines.

5.4 Effect of Temperature

The effect of temperature plays an important role in the reduction of nickel in these ammoniacal systems. It was clearly evident from the thermodynamic considerations that the equilibria amongst the various species is strongly influenced by the temperature. Two types of temperature effects have been observed and will be considered separately.

Period Before Temperature Stabilization: It was discovered during the very first runs with the system that hydrogen absorption from the gas phase into the solution proved to be a very exothermic process; a fact that has never been reported by any of the previous workers who have dealt with such systems. Henry's Law Constant is an increasing function of temperature and its relationship is given by:

$$\frac{d \ln H_e}{d(1/T)} = - \frac{\Delta H}{R} \quad 5.1$$

where T is the absolute temperature in °K

R is the gas constant

ΔH is the heat of absorption

H_e is the Henry's Law Constant for a particular gas

With the above equation and Henry's Law Constant for hydrogen given by Pray, Schweickert and Minnich⁽³⁹⁾, it was found that the heat of absorption had a value (for dissolution in

water) of $-4.95 \text{ kcal-mol}^{-1}$ between 177°C and 225°C . This exothermic effect can be seen in Figure 5.6, where a photograph of the temperature record of one of the actual experiments (run # NIEH11) is shown. The point #2 on the graph indicates the point at which hydrogen gas was admitted to the system. The increase in the temperature rise of the system is clearly observed. Confirmation was provided by carrying out an experiment using distilled water.

Because of the above mentioned phenomena, it was necessary to admit hydrogen into the autoclave, and consequently start reduction, before the preset temperature for that particular run was reached. As mentioned previously and observed in Figures 5.1 to 5.4, the concentration varied linearly with increasing temperature, until the temperature reached the preset value. In the case of the electrochemically treated nickel disc the reaction then seemed to stop at this particular point for a period varying from twenty to forty minutes. After this plateau, the reaction continued again. In the runs in which the temperature was kept at 200°C or below, several of these plateaus were evident. At higher temperatures only one plateau was detected. Interestingly enough, once the plateau region was passed the reaction proceeded at the same rate prior to the plateau.

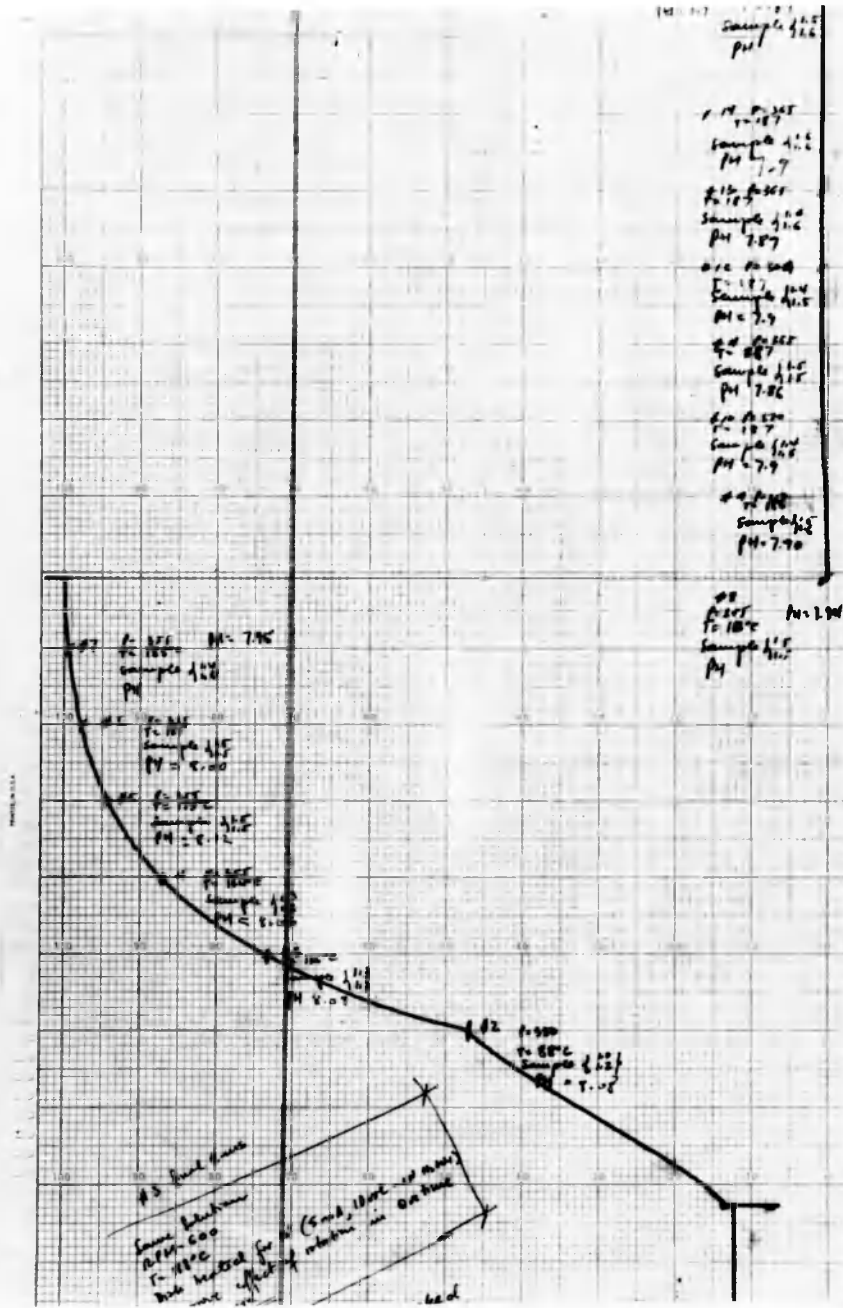


Figure 5.6. Strip chart recording of solution temperature during run NIEH11.

Period After Temperature Stabilization: Figure 5.7 shows three runs done at different temperatures, the rate of reaction increased as the temperature was increased. The approximate rate for the runs at 205°C and 225°C were 3.85×10^{-2} mol-liter⁻¹-minute⁻¹ and 7.54×10^{-5} mol-liter⁻¹-minute⁻¹ respectively. If these values are used to calculate an approximate activation energy for the reaction of a value of 8.0 Kcal-mol⁻¹ is obtained.

Figure 5.8 shows a run (NIEH10) in which reduction was started at a low temperature (170°C) and temperature increased continuously by stepping the temperature controller set point in increments of 10 deg. °C. It can be seen that the plateau is not as evident. An explanation for the plateau has already been discussed in the previous section

An Arrhenius type plot to determine the activation energy for the system was not attempted because of the difficulty in interpreting the results.

5.5 Effect of Hydrogen Partial Pressure

In the system used for the present study there was significant coupling between the final temperature achieved for a given total pressure. This was partly due to the phenomenon of the heat of absorption associated with the hydrogen solution and also to the fact that no internal cooling was available

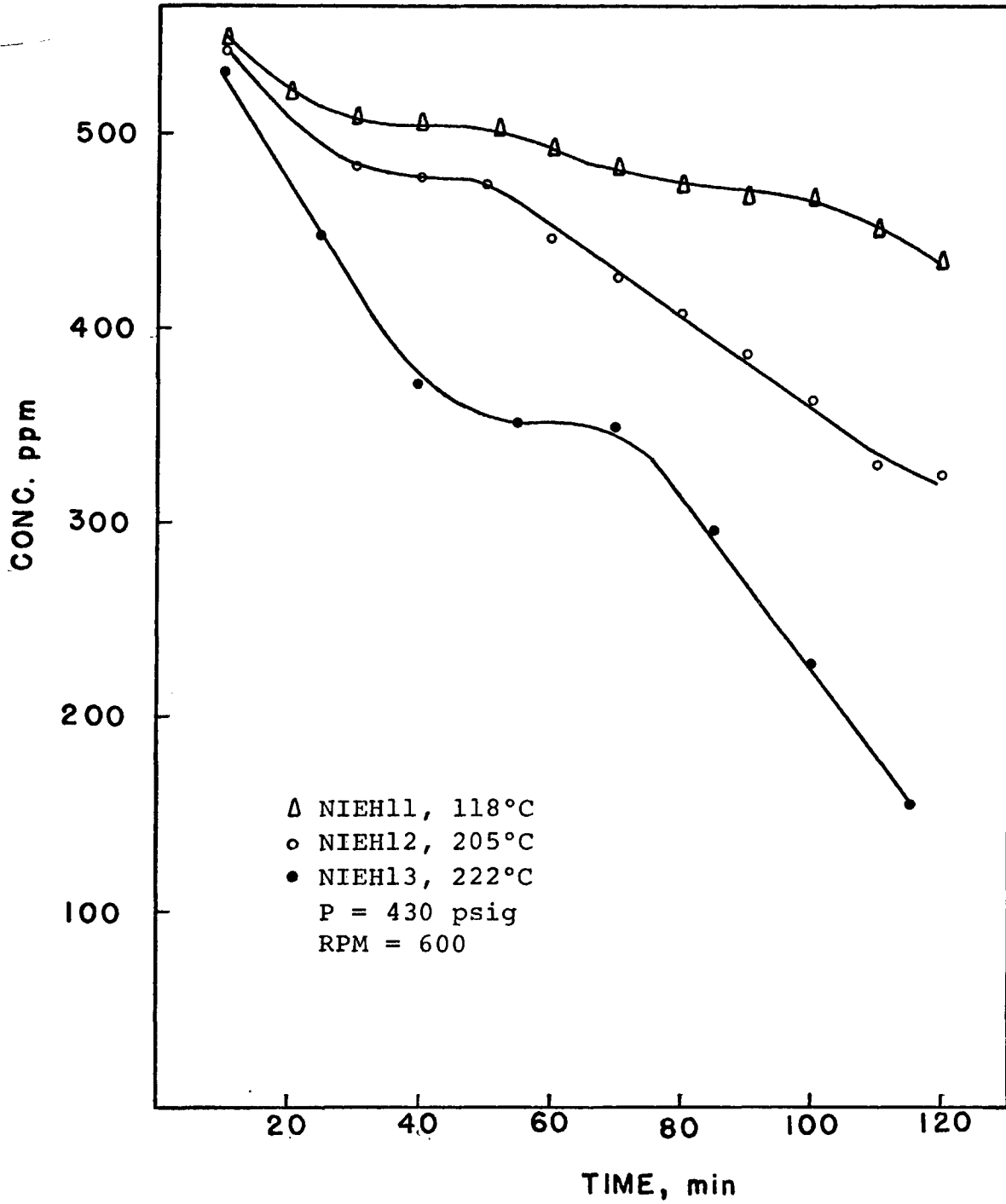


Figure 5.7. Precipitation rate curves for nickel discs as temperature is varied.

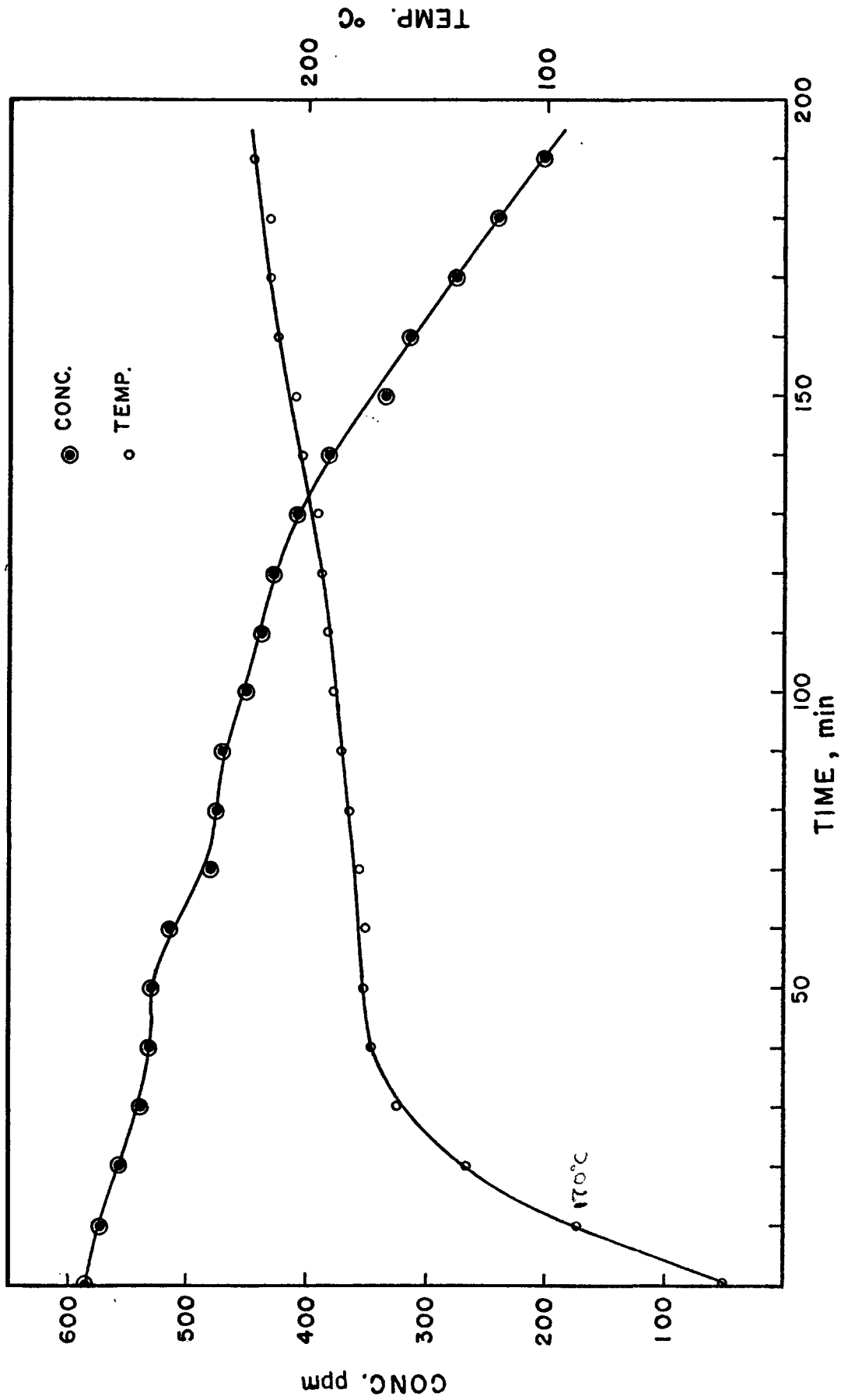


Figure 5.8. Variation of precipitation rate as temperature is constantly increased.

from within the autoclave. The partial pressures of hydrogen used in the series of runs carried out varied between 15 to 160 psia. These values were estimated using the vapor pressure data for pure water.

No influence of partial pressure of hydrogen on the reaction rate could be detected. This may be so because the active-sites are completely saturated with hydrogen within the range of partial pressures used. It should be mentioned that the pressure regulator showed a tendency to drift during a run and correction had to be made continuously. It might have been possible to avoid this by having a small leak of hydrogen (to an extraction load) from the supply line.

Finally, in connection with the Arrhenius type plots mentioned in the last section, it is realized that the concentration (activity) of the hydrogen gas in solution should be kept constant as the temperature is varied, in order to be able to measure the activation energy for the reaction. This requires compensation for both the vapor pressure of the components other than hydrogen at the new temperature as well as the change in the Henry's Law Constant.

Table 5.2 Average Reaction Rate

RUN	AVERAGE RATE (mol-liter ⁻¹ -minute ⁻¹)
NIEH4	5.50·10 ⁻⁵
NIEH5	8.00·10 ⁻⁵
NIEH6	7.49·10 ⁻⁵
NIEH7	9.08·10 ⁻⁵
NIEH12	3.85·10 ⁻⁵
NIEH13	7.54·10 ⁻⁵
NITH1	5.82·10 ⁻⁵
NINT0	8.57·10 ⁻⁵
NINT2	8.85·10 ⁻⁵
TI02	9.59·10 ⁻⁵

Table 5.3 Predicted and measured pH values with and without activity coefficients correction

[Ni ^{II}] x 10 ³ (m)	1	3	5	7	9	10
pH Predicted	8.17	8.00	7.90	7.83	7.77	7.74
pH Measured	8.18	8.18	8.20	8.19	8.19	8.19
pH Corrected for Activity Coefficient	8.31	8.15	8.05	7.97	7.91	7.88

5.6 Prediction of System Behavior

It became apparent that in order to be able to describe the kinetic behavior of the system in terms of the mechanism which might be occurring, the equilibria between the species (other than hydrogen) in solution would have to be predicted at high temperature. The assumption would then be made that these reactions were fast. Investigators in the past have tried to postulate mechanisms based on the system equilibria at room temperature.

It was therefore decided to attempt prediction of the system behavior (species distribution) under conditions of hydrogen reduction. In essence this consisted of first of all predicting the species distribution of a solution of known composition. The reduction was then simulated by decreasing the nickel concentration while at the same time observing the conservation of the mass balance change in hydrogen ions in the system as a result of reduction as well as redistribution in the system. The effect was to keep the positive and negative charges constant in the solution thereby preserving its electroneutrality. The resulting equations are given in Appendix I. The derivatives of the relevant equations used in a Newton-Raphson scheme for their solution is given in Appendix II. The programs, in BASIC, are given in Appendix III.

pH Prediction at Room Temperature: In order to test the equation proposed for describing the equilibria in the system, species distribution for a series of artificially prepared solutions was predicted. These solutions were prepared such that the ratio of NiSO_4 to $(\text{NH}_4)_2\text{SO}_4$ was constant at 4, and the ratio of ammonia, from ammonium hydroxide, to nickel was also constant at 2. The total nickel concentration in the solution was then varied between .01 M and .001M. The effect of including an activity for hydrogen and ammonium ions other than unity (these species it was felt would be the ones most likely to be of importance) was also tested). In particular the pH predicted for these solutions was compared with the measured values. The results are tabulated in Table 5.3 and shown graphically in Figure 5.9. It can be seen that the agreement was not particularly good. The main discrepancy was that the prediction indicated that the pH should increase with decreasing total nickel concentration, while the measured pH of the solutions prepared in fact were practically constant over the range of total nickel concentration in solutions tested.

Simulated Hydrogen Reduction at 25 and 200°C: The next exercise consisted of carrying out hydrogen reduction of ammoniacal solutions of composition similar to those reported by Benson and Colvin⁽⁸⁾ as being used in plant practice. The solutions were chosen such that the total nickel concen-

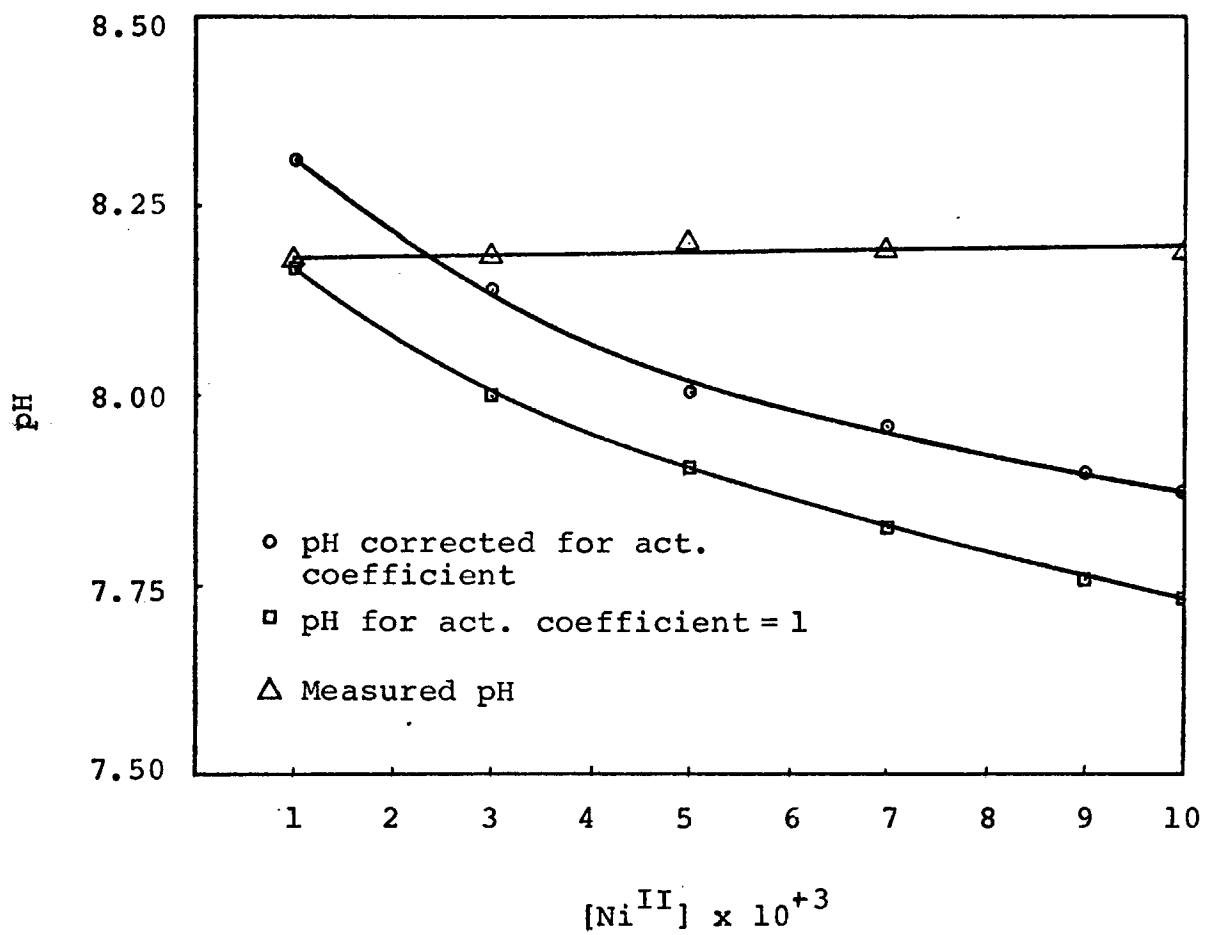


Figure 5.9. pH predicted and measured for concentrations between .01 M and .001 M.

tration was 1 M and the ratio of ammonia (from ammonium hydroxide) to total nickel was 2.2 and 1.2. The results are tabulated in Tables 5.4 to 5.7 where the total nickel concentration is shown in column 1 and the corresponding nickel ion concentration is shown in column 2. The pH and the ratio of ammonia (free ammonia plus ammonia complexed) to total nickel are shown in columns 3 and 4 respectively. The distribution of the other species has not been included in the tables. However, to aid in their determination, Figures 5.12 to 5.16 were constructed, which represent the inverse of the plots given previously in Figures 3.2 to 3.6. These additional plots show the effect of complexing for a fixed ratio of ammonia (free ammonia plus ammonia complexed) to total nickel as a function of total nickel concentration. The solution to the equations which describe the equilibria for these cases were also solved using a Newton-Raphson technique.

Figures 5.10 and 5.11 show the information contained in Tables 5.4 to 5.7 in graphical form. In Figure 5.10 it can be seen that the nickel ions in solution decrease as the total nickel decreases as a result of the reduction. At 200°C the asymptotic approach (large fractions of nickel as nickel ions) to the total nickel line is evident. At 25°C the equilibria is such that the pH (see inset) is almost constant with an increase occurring when the reduction is

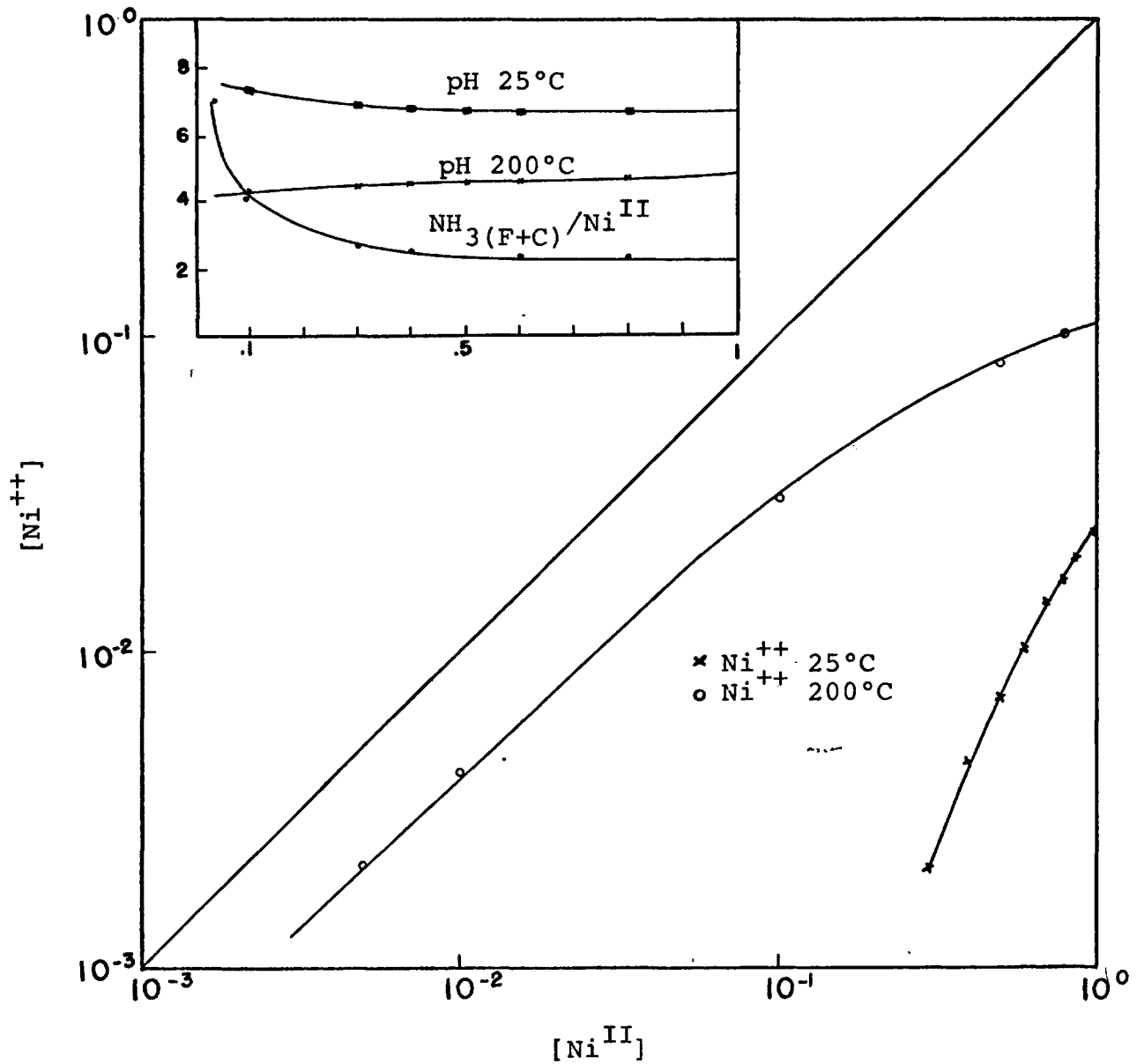


Figure 5.10. Nickel ion in solution as the total nickel decreases as a result of the reduction at 25°C, 200°C for a ratio of ammonia-to-nickel of 2.2.

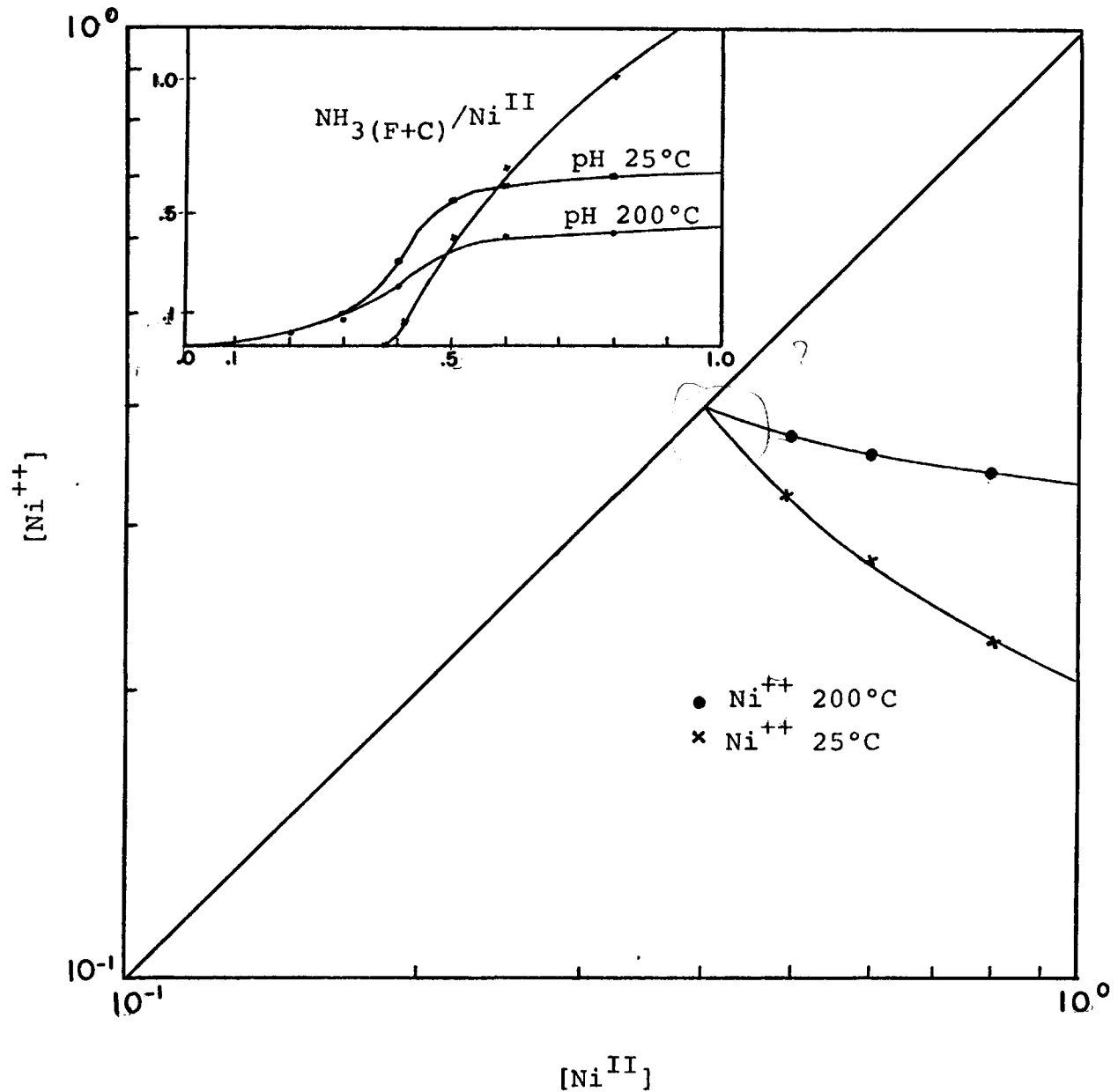


Figure 5.11. Nickel ion in solution as the total nickel decreases as a result of the reduction at 25°C and 200°C for an initial ammonia-to-nickel ratio of 1.2.

Table 5.4 Values of Nickel Ions Concentration, pH, and $\text{NH}_3(\text{F+C})/\text{Ni}^{\text{II}}$ Predicted as Reduction is Carried Out at 25°C and Initial Ratio of 1.2

Ni^{II}	Ni^{++}	pH	$\text{NH}_3(\text{F+C})/\text{Ni}^{\text{II}}$
1.0	0.205	6.15	1.2
0.8	0.228	5.98	1.0
0.6	0.277	5.65	0.66
0.55	0.297	5.57	0.545
0.50	0.323	5.39	0.40
0.45	0.357	5.09	0.222
0.40	0.399	3.04	$2.25 \cdot 10^{-3}$
0.30	0.299	0.69	$1.01 \cdot 10^{-5}$
0.20	0.191	0.398	$5.09 \cdot 10^{-6}$

Initial Solution: $\text{NiSO}_4 = 1\text{M}$, $\text{NH}_3 = 1.2\text{M}$, $(\text{NH}_4)_2\text{SO}_4 = 4\text{M}$.

Table 5.5 Values of Nickel Ions Concentration, pH, and $\text{NH}_3(\text{F+C})/\text{Ni}^{\text{II}}$ Predicted as Reduction is Carried Out at 25°C and Initial Ratio of 2.2

Ni^{II}	Ni^{++}	pH	$\text{NH}_3(\text{F+C})/\text{Ni}^{\text{II}}$
1.0	$2.39 \cdot 10^{-2}$	6.708	2.2
0.8	$1.69 \cdot 10^{-2}$	6.691	2.25
0.6	$1.03 \cdot 10^{-3}$	6.694	2.33
0.5	$5.21 \cdot 10^{-3}$	6.708	2.40
0.4	$4.46 \cdot 10^{-3}$	6.737	2.50
0.3	$2.16 \cdot 10^{-3}$	6.796	2.66
0.1	$3.16 \cdot 10^{-5}$	7.21	4.0
0.04	$6.64 \cdot 10^{-7}$	7.54	7.0
0.01	$2.78 \cdot 10^{-8}$	7.72	22.0

Initial Solution: $\text{NiSO}_4 = 1\text{M}$, $\text{NH}_3 = 2.2\text{M}$, $(\text{NH}_4)_2\text{SO}_4 = 4\text{M}$.

Table 5.6 Values of Nickel Ions Concentration, pH, and $\text{NH}_3(\text{F+C})/\text{Ni}^{\text{II}}$ Predicted as Reduction is Carried Out at 200°C and Initial Ratio of 1.2

Ni^{II}	Ni^{++}	pH	$\text{NH}_3(\text{F+C})/\text{Ni}^{\text{II}}$
1.0	0.332	4.36	1.2
0.8	0.341	4.16	1.0
0.6	0.359	3.88	0.666 $\frac{1.2 - 2 \times 0.4}{0.6}$
0.5	0.575	3.60	0.40
0.4	0.395	2.16	$1.72 \cdot 10^{-2}$
0.3	0.299	0.6985	$6.66 \cdot 10^{-4}$
0.2	0.199	0.398	$4.02 \cdot 10^{-4}$
0.1	0.099	0.222	$4.05 \cdot 10^{-4}$

Initial Solution: $\text{NiSO}_4 = 1\text{M}$, $\text{NH}_3 = 1.2\text{M}$, $(\text{NH}_4)_2\text{SO}_4 = 2\text{M}$

Table 5.7 Values of Nickel Ions Concentration, pH, and $\text{NH}_3(\text{F+C})/\text{Ni}^{\text{II}}$ Predicted as Reduction is Carried Out at 200°C and Initial Ratio of 2.2

Ni^{II}	Ni^{++}	pH	$\text{NH}_3(\text{F+C})/\text{Ni}^{\text{II}}$
1.0	0.114	4.74	2.2
0.8	0.102	4.64	2.25
0.5	$8.04 \cdot 10^{-2}$	4.51	2.4
0.1	$3.00 \cdot 10^{-2}$	4.22	4.0
0.05	$1.76 \cdot 10^{-2}$	4.14	6.0
0.01	$4.11 \cdot 10^{-3}$	4.05	22.01
0.005	$2.10 \cdot 10^{-3}$	4.04	42.01
0.003	$1.27 \cdot 10^{-3}$	4.03	68.69

Initial Solution: $\text{NiSO}_4 = 1\text{M}$, $\text{NH}_3 = 2.2\text{M}$, $(\text{NH}_4)_2\text{SO}_4 = 4\text{M}$.

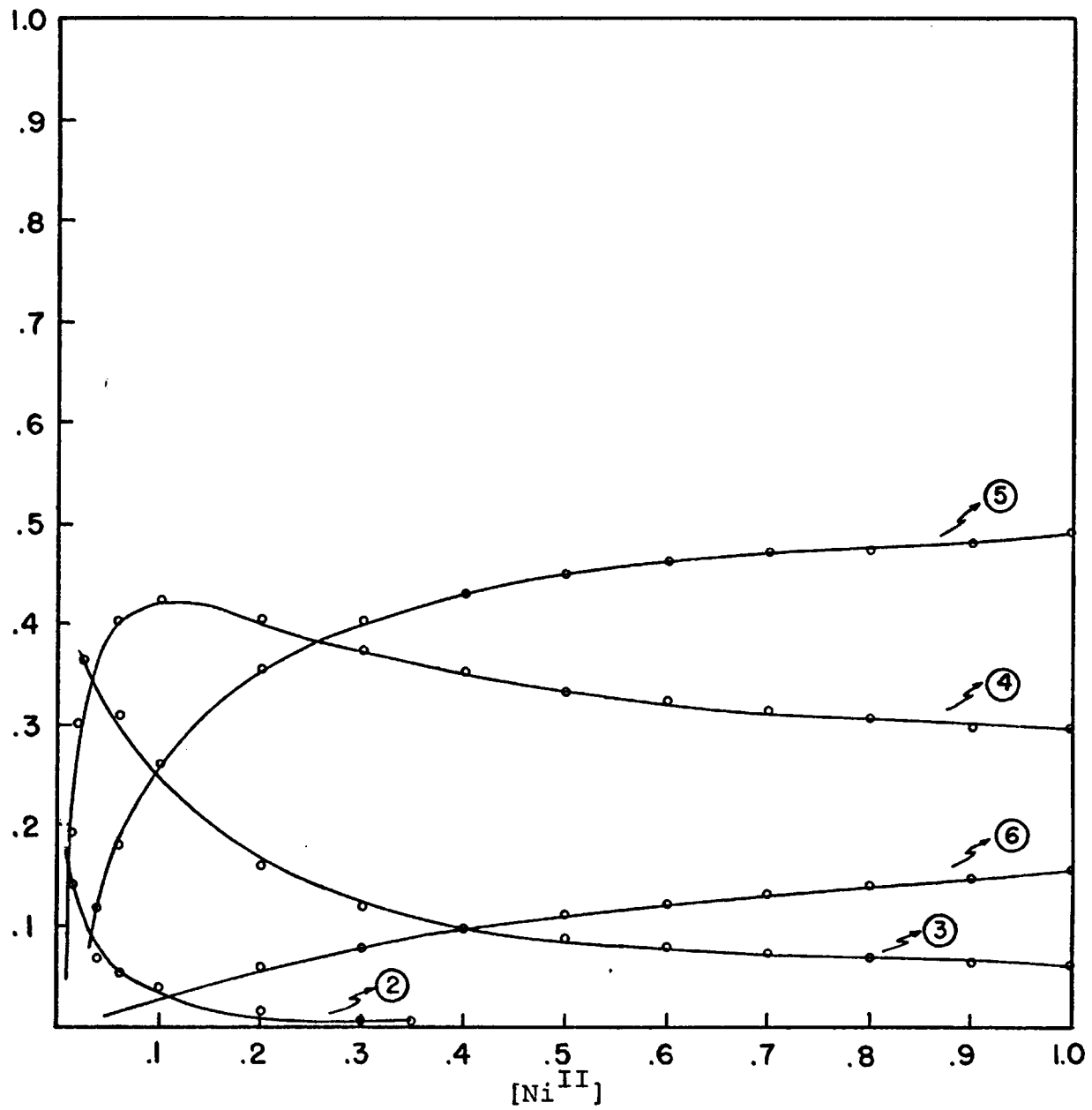


Figure 5.12 Fraction of nickel present in each form for an ammonia-nickel ratio of 5:1, at 25°C.

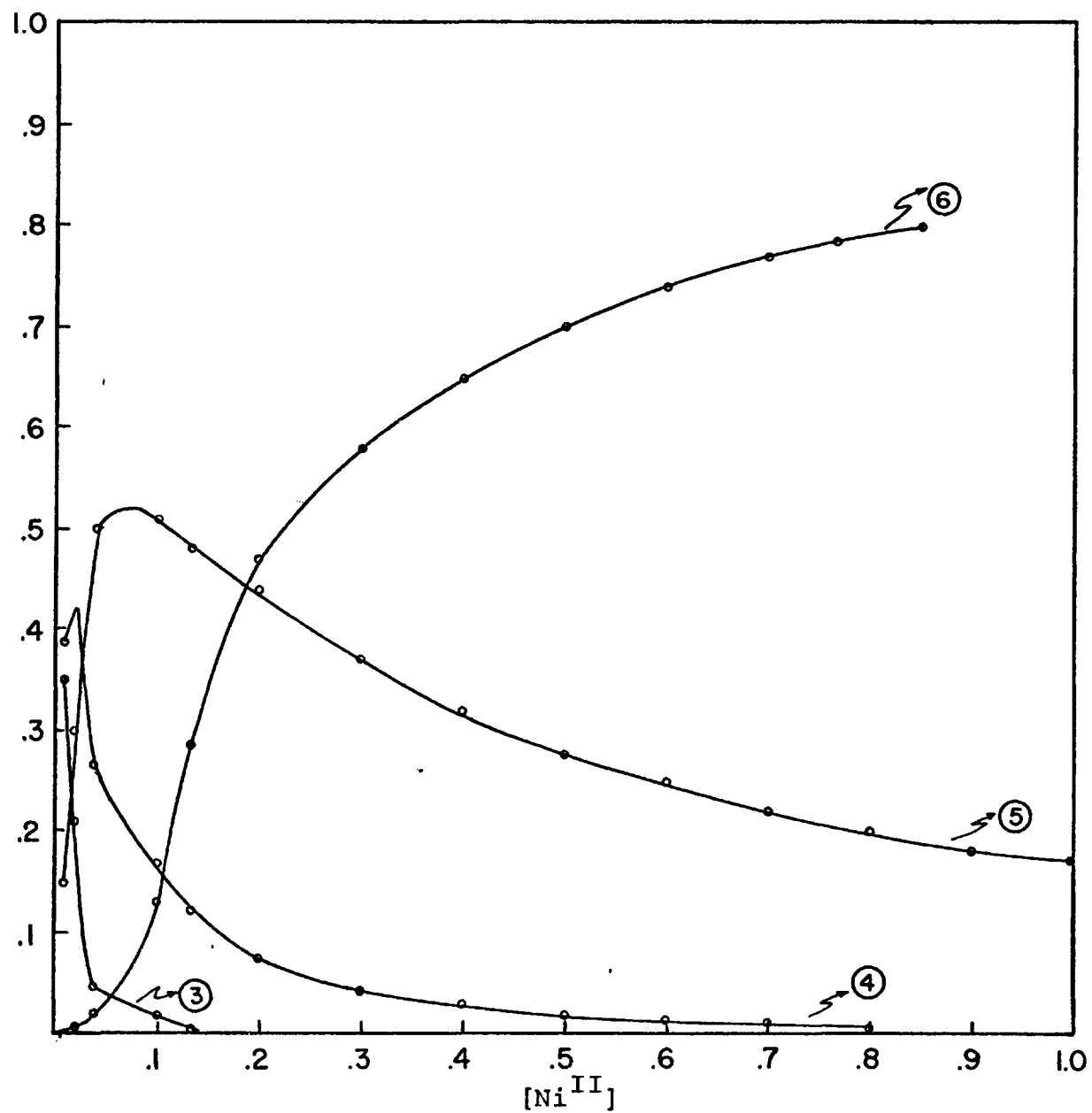


Figure 5.13 Fraction of nickel present in each form for an ammonia-nickel ratio of 10:1, at 25°C.

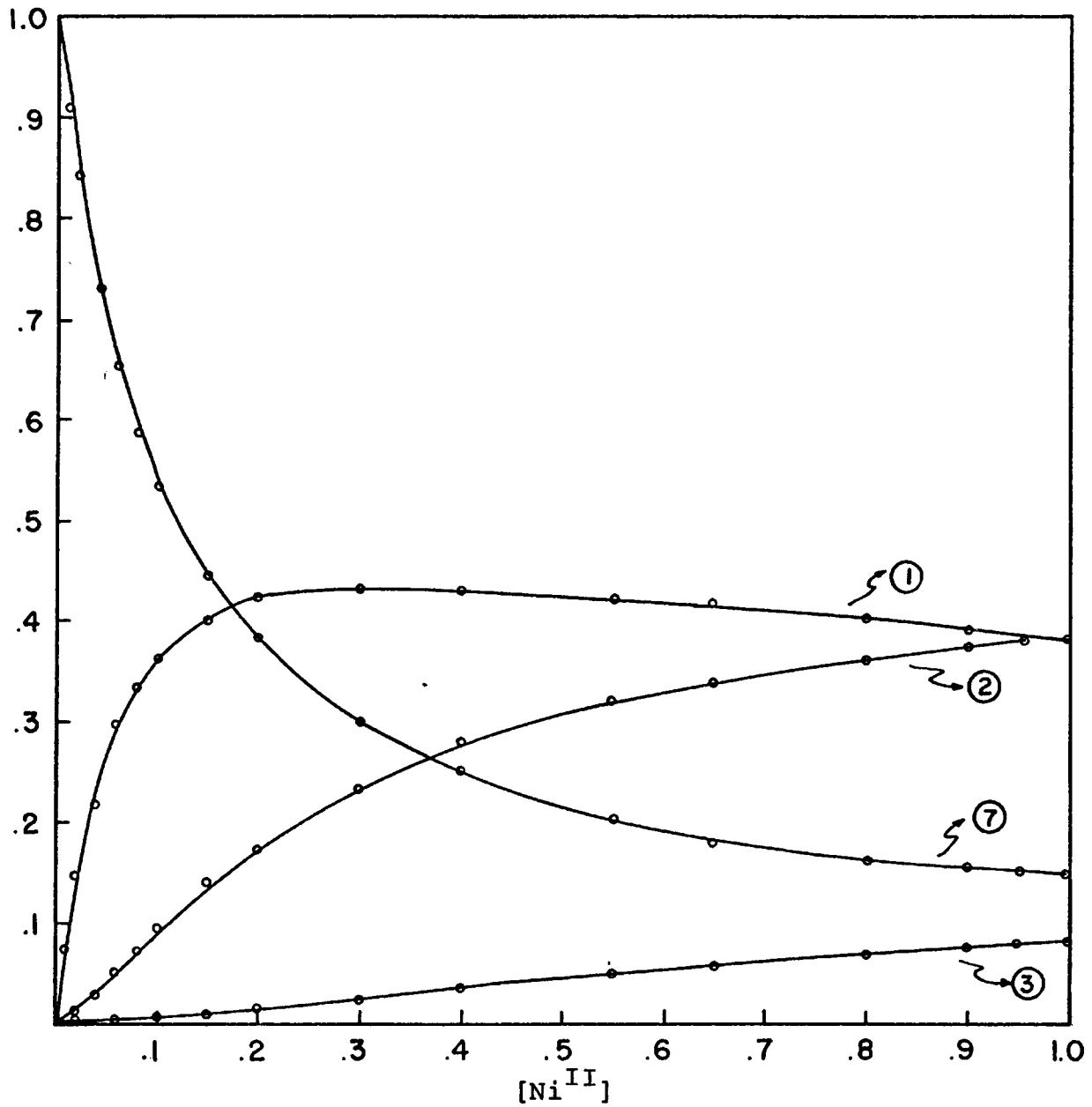


Figure 5.14 Fraction of nickel present in each form for an ammonia-nickel ratio of 2:1, at 200°C.

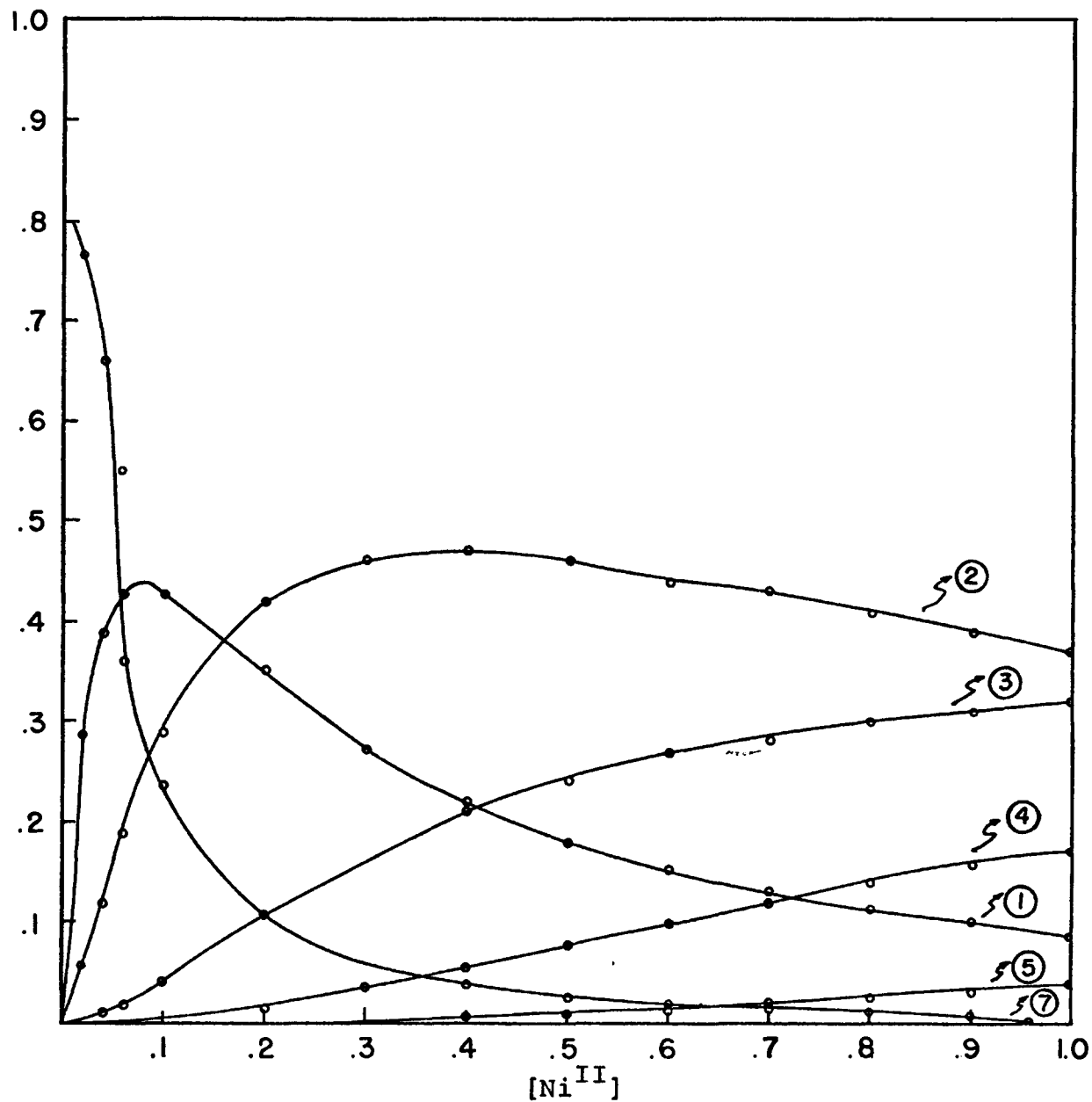


Figure 5.15 Fraction of nickel present in each form for an ammonia-nickel ratio of 5:1, at 200°C.

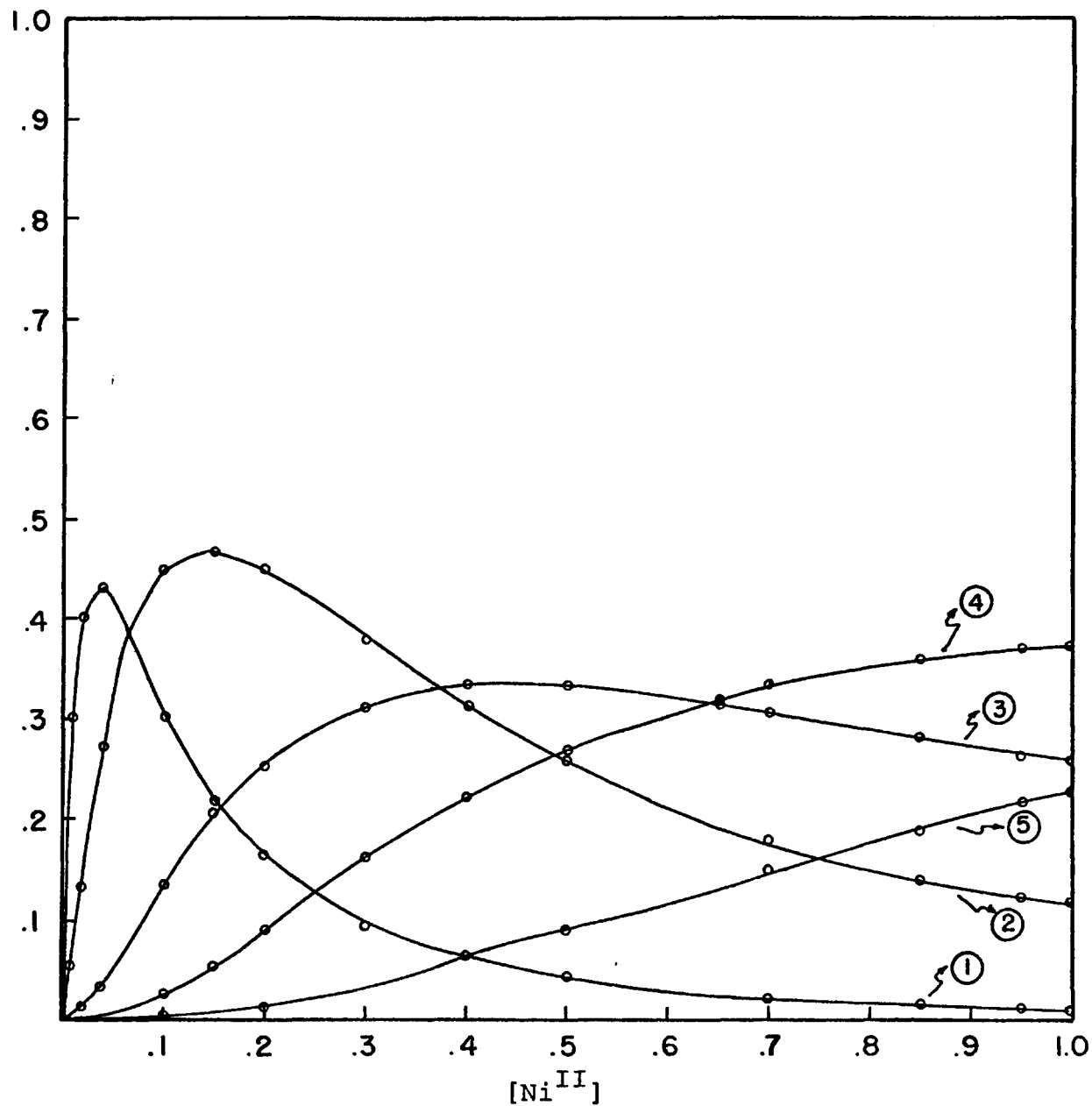


Figure 5.16 Fraction of nickel present in each form for an ammonia-nickel ratio of 10:1, at 200°C.

about 70% completed. However, at 200°C the pH is lower and there is a gradual decrease in pH as the reduction is taking place. The species distribution at 25°C was only included in order to be able to predict the pH of equivalent high temperature solutions at room temperature and of course is not intended to mean that reduction can occur at this temperature. It is also noted that in Figure 5.10 the $\text{NH}_3(\text{F+C})/\text{Ni}^{\text{II}}$ ratio increases drastically once the reduction is about 80% completed. The interesting feature is that this behavior is the same (within the accuracy of the calculations) regardless of the temperature.

In Figure 5.11 it can be seen that at the lower value of the ratio of ammonia (from ammonium hydroxide) to total nickel (1.2) the behavior is very different. At both temperatures the nickel ion concentration increases up to a point where the reduction is about 60% completed when the curves join the total nickel line (indicating that no nickel is complexed). At 200°C the nickel ion concentration is higher than for the 25°C up to the point where the two join the total nickel line. The interesting feature is that for both cases the point at which practically no complexing occurs is the same (60% reduction). In the inset can be seen the variation of pH. At both temperatures the pH decreases drastically once 60% of the nickel has been reduced. The pH at 200°C is lower than at 25°C, the two curves becoming asymptotic for reduction

greater than 70%). As for the previous case, the $\text{NH}_3(\text{F+C})/\text{Ni}^{\text{II}}$ ratio is identical at both temperatures.

The differences in the behavior between the predictions obtained for the two systems may be summarized as follows:

- a) The nickel ions start off higher in the case of the low ratio (1.2) system.
- b) The nickel ions decrease continuously as reduction occurs in the high ratio (2.2) system whereas for the low ratio system it starts off lower but increases up to a certain point overhauling the higher ratio system.
- c) The pH decreases at both temperatures investigated, in the low ratio system.
- d) The pH at 25°C increases as reduction proceeds in the 2.2 ratio system while at 200°C there is a gradual decrease in pH.

The behavior of the pH at 25°C for the two systems has been suggested by several authors

Simulation of Hydrogen Reduction Under Conditions Used in This Investigation: The species distribution for the conditions used in the experimental part of this thesis was now predicted. The results are shown in Figure 5.17 where the variation of nickel ion concentration at 200°C is plotted together with the pH at 25°C. It is evident that very little complexing

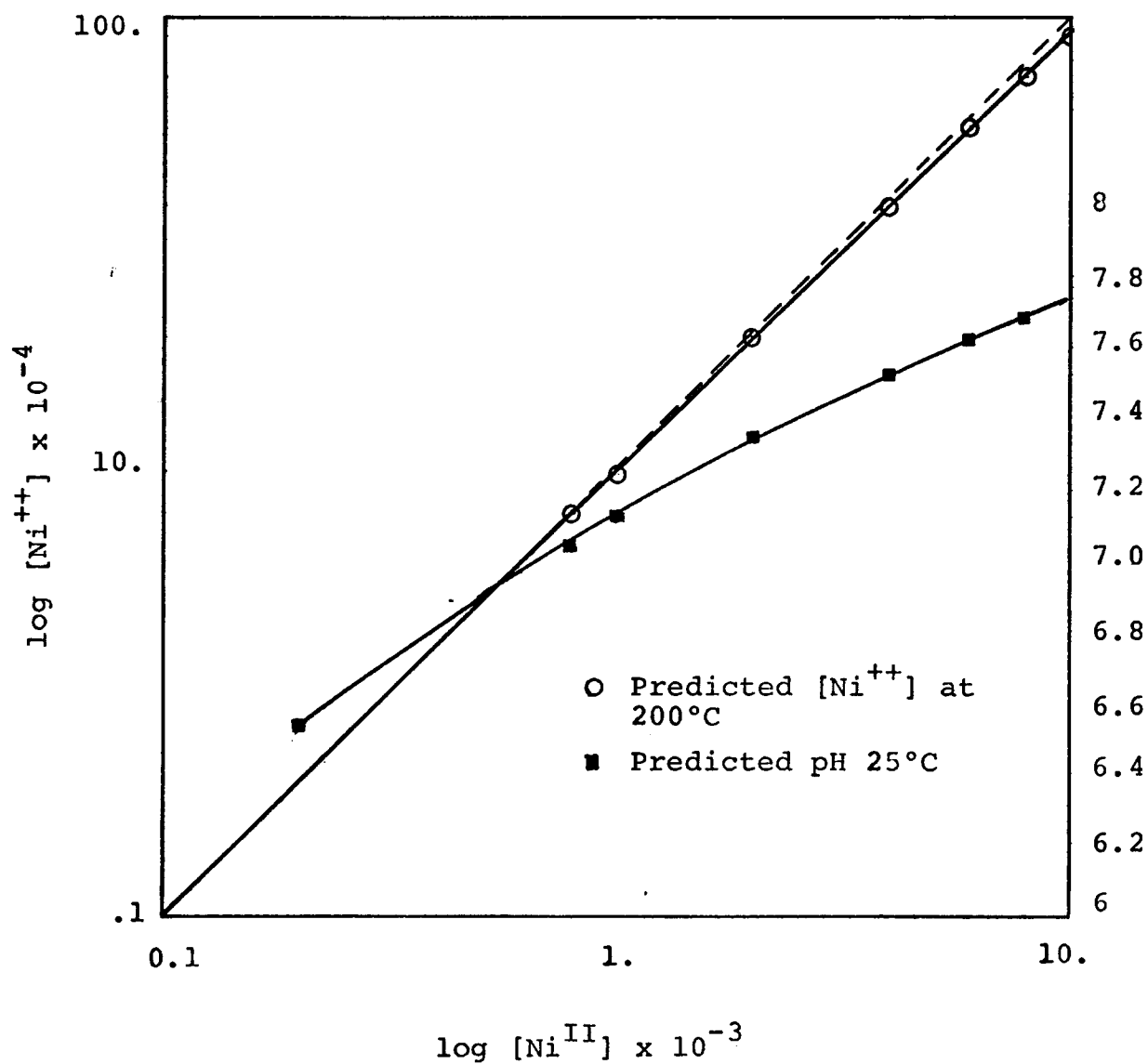
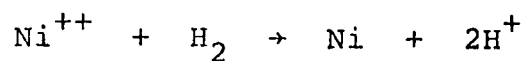


Figure 5.17. Variation of nickel ion concentration at 200°C as reduction proceeds

occurs and all the nickel is present as nickel ions. The pH decreases from a value of about 7.7 to 7.0 when the reduction is about 90% complete. Although the trend is the same as observed experimentally, the change in pH is very much smaller than that observed. Also the starting pH of the solution predicted is lower than the values measured. As a word of caution, it is worth pointing out that solutions of a certain nickel, total ammonium and sulphate concentration which are produced by hydrogen reduction do not have the same chemical characteristics as similar solutions prepared from neutral salts. This is of course due to the hydrogen ions produced by the reduction and the fact that the positive (or negative) charges in the system remain constant. Thus, it is impossible to "pick up" the reduction from some point during the reduction by starting with an artificial solution with the same total nickel, total ammonium and total sulphate concentration (the pH obviously will not be the same).

Equilibria Applied to Kinetic Behavior: The major objective of becoming familiar with the species equilibria of the system was to be able to apply the findings to the interpretation of the kinetic behavior of the experimental system. The equilibrium constant for the overall reaction:



is practically independent of temperature.

A mechanism for the reaction based on an active-site theory has been given in Chapter 3. However the equilibria predicted in Figure 5.17, does not allow an interpretation of the experimental results obtained. In order for the reduction rate to be constant, the nickel ion concentration in the solution should remain constant. This would mean that either the mechanism proposed is incorrect or that the prediction is not accurate. The latter is suspect at the moment.

The proposed mechanism that the hydrogen in solution saturates the active sites appears to be reasonable, since no effect of hydrogen partial pressure on the rate of the reaction could be discerned. Also, this is in line with the low activation energy, determined rather roughly, if one assumes that the chemisorption of hydrogen ion liquid/solid systems will be similar to that for gas/solid catalysis.

CHAPTER 6

CONCLUSIONS

6.1 Discussion and Summary

Due to the complexity of the system, the kinetics results do not permit detailed conclusions to be drawn concerning the mechanism of the precipitation reaction, or the order of the reaction. However, there seems to be a linear relationship between concentration of total nickel in solution and time, with an approximate estimate of the activation energy for the reaction of the order of 8 Kcal-mol^{-1} . The high activation energy of the reaction indicates that the reaction is chemical control. The disc preparation and the resulting deposit morphology plays an important role in the reaction rate. At 200°C the specific heterogeneous reaction rate (the nickel disc was approximately 1 cm^2) is approximated $10^{-4} \text{-mol-liter}^{-1}\text{-minute}^{-1}\text{-cm}^{-2}$ for the electrochemical-hydrogen-treated disc.

As long as some catalytic surface and hydrogen are present, the reaction seems to proceed to almost completion. However, it appears from the results obtained in this investigation that for any practical application the optimum temperature range lies above 200°C , and the optimum pressure range is

between 100 and 200 psi. The uses of higher partial pressures of hydrogen suggested by several authors seems unjustified because the finite active sites on the system will become saturated with hydrogen at much lower pressures.

Rotational speed proved to have no effect on the rate of the reaction, on the other hand material and surface preparation of the discs showed characteristic precipitation rate curves for each case. Nucleation and growth of hydrogen from the initially supersaturated solution seems to be responsible for the plateau appearing in the rate curves of nickel discs treated electrochemically.

Perhaps the most important contribution of the present work was the prediction of the species equilibrium behavior at high temperatures with and without hydrogen reduction. Previous workers have tried to relate room temperature data to behavior at high temperatures. The behavior of the system to changes in the experiments has been neglected.

The system is unique for each initial composition, a fact that has made the system impossible to generalize.

The room temperature predictions were attended so that it would be possible to relate the pH of samples taken from the autoclave and measured at room temperature. The trials with artificial solutions were not successful, however. The discrepancies could be due to the values of the equilibrium

constants calculated with 2 M ammonium nitrate as electrolyte or to the fact that activity coefficients for complex species were not taken into account due to the non-availability of this data. Although, it is realized that values obtained in the theoretical aspects of the present work with relation to reduction at high temperatures may not represent the real values a priori under the conditions at which they were applied.

It is believed that they nevertheless show the right trends of the process. It is also plausible that hydrogen reduction of nickel occurs by the reaction of just nickel ions, with the hydrogen adsorbed onto the catalytic surface. Measurement of pH at high pressures and temperatures should shed some light on the matter.

6.2 Suggestions for Future Work

It is evident from this study that there are several aspects of this work which warrant further investigation. It is the author's belief that these should be studied first as individual topics. The most important area is probably that of the species equilibrium distribution, since it is only by being able to predict this can any conclusions be drawn on the kinetic mechanism. As mentioned previously, the use of a high temperature pH electrode should help provide some answers. The adsorption of the species (especially hydrogen)

on the nickel surface is another area also of importance. In this connection it might be worthwhile to study the reduction under acidic conditions without ammonia, perhaps with ammonium acetate as a buffer.

APPENDIX ISpecies Distribution

The equations which have to be solved simultaneously are:

$$[\text{NH}_4^+] = K_0 [\text{NH}_3] [\text{H}^+] \quad \text{AI-1}$$

$$[\text{Ni}(\text{NH}_3)_2^{++}] = K_1 [\text{Ni}^{++}] [\text{NH}_3] \quad \text{AI-2}$$

$$[\text{Ni}(\text{NH}_3)_3^{++}] = K_2 [\text{Ni}^{++}] [\text{NH}_3]^2 \quad \text{AI-3}$$

$$[\text{Ni}(\text{NH}_3)_4^{++}] = K_3 [\text{Ni}^{++}] [\text{NH}_3]^3 \quad \text{AI-4}$$

$$[\text{Ni}(\text{NH}_3)_5^{++}] = K_4 [\text{Ni}^{++}] [\text{NH}_3]^4 \quad \text{AI-5}$$

$$[\text{Ni}(\text{NH}_3)_6^{++}] = K_5 [\text{Ni}^{++}] [\text{NH}_3]^5 \quad \text{AI-6}$$

$$[\text{Ni}(\text{NH}_3)_6^{++}] = K_6 [\text{Ni}^{++}] [\text{NH}_3]^6 \quad \text{AI-7}$$

Also, the mass balances in ammonia and nickel, as well as electroneutrality of the system, has to be satisfied. These are as follows:

For nickel --

$$Y_9 = Y_1 + Y_2 + Y_3 + Y_4 + Y_5 + Y_6 + Y_7 \quad \text{AI-8}$$

where Y_7 represents the nickel ions concentration, Y_1 to Y_5 are the concentrations of each of the amines respectively, and Y_9 is the total nickel in the system.

For ammonium --

$$Y_{10} = Y_1 + 2Y_2 + 3Y_3 + 4Y_4 + 5Y_5 + 6Y_6 + Y_8 + Y_{14} \quad \text{AI-9}$$

where Y_8 is equal to the concentration of free ammonia in the system, Y_{14} is the concentration of ammonium only, and Y_{10} is the ^{total} ammonium.

The electroneutrality equation is:

$$2Y_{12} + \frac{K_w}{Y_{11}} = Y_{11} + Y_{14} + 2[Y_1 + Y_2 + Y_3 + Y_4 + Y_5 + Y_6 + Y_7] \quad \text{AI-10}$$

where Y_{12} and Y_{11} are the concentrations of sulphate and hydrogen ions respectively and K_w is the equilibrium constant for water.

Equation AI-1 to AI-9 can be reduced to three equations and three unknowns:

$$F_1 = X_1 [1 + K_1 K_2 X_2^2 + \dots + K_1 K_2 K_3 K_4 K_5 K_6 X_2^6] - Y_9 = 0 \quad \text{AI-11}$$

$$F_2 = X_2 [1 + K_7 X_3] + X_1 [K_1 X_2 + K_1 K_2 X_2^2 + \dots + K_1 K_2 K_3 K_4 K_5 K_6 X_2^6] - Y_{10} = 0 \quad \text{AI-12}$$

$$F_3 = \frac{X_3}{2} [1 + K_7 X_2] + X_1 [1 + K_1 X_2 + K_1 K_2 X_2^2 + \dots + K_1 K_2 K_3 K_4 K_5 K_6 X_2^6] - \frac{K_w}{2X_3} - Y_{12} = 0 \quad \text{AI-13}$$

$$\begin{aligned} \text{where } X_1 &= Y_7 = [\text{Ni}^{++}] \\ X_2 &= Y_8 = [\text{NH}_3] \quad (\text{Free Ammonia}) \\ X_3 &= Y_{11} = [\text{H}^+] \end{aligned}$$

Simulated Hydrogen Reduction

For the case where the reduction scheme was carried out, the equation of electroneutrality was replaced by mass balance charge which accounted for the hydrogen ions produced as reduction proceeds, where two hydrogen ions are replaced for each nickel removed.

The additional equation is:

$$F_4 = 2Y_9 + Y_{11} + Y_{14} - S_3 - S_2 - 2 \cdot S_1 = 0 \quad \text{AI-14}$$

where the additional variable S_1 , S_2 and S_3 represents the original total nickel concentration in the solution, the original ammonium $[\text{NH}_4^+]$ and the original $[\text{H}^+]$ of the solution respectively.

Equation AI-14 as a function of the unknowns will take the form of:

$$F_4 = 2Y_9 + X_3 + K_7 X_2 X_3 - S_3 - S_2 - 2 \cdot S_1 = 0 \quad \text{AI-15}$$

APPENDIX IISpecies Distribution

The following derivations are required for the Newton-Raphson scheme:

$$\frac{\partial F_1}{\partial X_1} = 1 + K_1 K_2 + K_1 K_2 X_2^2 + \dots + K_1 K_2 K_3 K_4 K_5 K_6 X_2^6 \quad \text{AII-1}$$

$$\frac{\partial F_1}{\partial X_2} = X_1 [K_1 + 2K_1 K_2 X_2 + 3K_1 K_2 K_3 X_2^2 + \dots + 6K_1 K_2 K_3 K_4 K_5 K_6 X_2^5] \quad \text{AII-2}$$

$$\frac{\partial F_1}{\partial X_3} = 0 \quad \text{AII-3}$$

$$\frac{\partial F_2}{\partial X_1} = K_1 K_2 + K_1 K_2 X_2^2 + \dots + K_1 K_2 K_3 K_4 K_5 K_6 X_2^6 \quad \text{AII-4}$$

$$\frac{\partial F_2}{\partial X_2} = 1 + K_7 X_3 + X_1 [K_1 + 2K_1 K_2 X_2 + 3K_1 K_2 K_3 X_2^2 + \dots + 6K_1 K_2 K_3 K_4 K_5 K_6 X_2^5] \quad \text{AII-5}$$

$$\frac{\partial F_2}{\partial X_3} = K_7 X_2$$

$$\frac{\partial F_3}{\partial X_1} = 1 + K_1 X_2 + K_1 K_2 X_2^2 + \dots + K_1 K_2 K_3 K_4 K_5 K_6 X_2^6 \quad \text{AII-6}$$

$$\frac{\partial F_3}{\partial X_2} \frac{\partial F_3}{\partial X_1} = \frac{X_3 K_7}{2} + X_1 [K_1 + 2K_1 K_2 X_2 + 3K_1 K_2 K_3 X_2^2 + \dots + 6K_1 K_2 K_3 K_4 K_5 K_6 X_2^5] \quad \text{AII-7}$$

$$\frac{\partial F_3}{\partial X_3} = (1 + K_7 X_2)/2 + \frac{K_w}{2X_3^2} \quad \text{AII-8}$$

Simulated Hydrogen Reduction

The partial derivations of F_3 are now referred

$$\frac{F_4}{X_1} = 0 \quad \text{AII-9}$$

$$\frac{F_4}{X_2} = K_7 X_3 \quad \text{AII-10}$$

$$\frac{F_4}{X_3} = 1 + K_7 X_2 \quad \text{AII-11}$$

APPENDIX III

```

10 REM*****PROGRAM CALCULATES SPECIES DISTRIBUTION *****
20 DIM X(7),D(7,7),E(7,7),S(7,1),F(7,1),Y(25)
30 DATA 3          ' ***** NUMBER OF EQUATIONS *****
40 DATA 1E-4,1E-4,1E-8  '**GUESS  [NI++],[NH3]FREE, [H+] ****
50 DATA 2.84,2.29,1.78,1.24,.79,.07,9.25,-14  ' EQ. CONSTANTS *****
60 K9=1
70 P1=1
80 DATA 10E-3,17.91E-2,8.957E-2  ' ** [NI TOT],[NH4 TOT],[SO4 TOT]
90 READ N
100 MAT D=ZER(N,N)
110 MAT F=ZER(N,1)
120 MAT E=ZER(N,N)
130 MAT S=ZER(N,1)
140 FOR I= 1 TO N
150 READ X(I)
160 NEXT I
170 D(1,3)=0

180 FOR I= 1 TO 8
190 READ K(I)
200 K(I)=10*(K(I))
210 NEXT I
220 READ Y(9),Y(10),Y(12)
230 K1=0
240 REM *****SIMULTANEOUS EQS. --F(I,1); DERIVATIVES -- D(I,1)*****

250 K1=K1+1
260 F(1,1)=1
270 A=1
280 FOR I= 1 TO 6
290 A=A*K(I)*X(2)
300 F(1,1)=F(1,1)+A
310 NEXT I
320 D(1,1)=F(1,1)
330 F(1,1)=X(1)*F(1,1)-Y(9)
340 F(2,1)=0
350 D(2,2)=0
360 A=1
370 FOR I= 1 TO 6
380 A=A*K(I)*X(2)
390 F(2,1)=F(2,1)+I*A
400 D(2,2)=D(2,2)+I*I*A/(X(2))
410 NEXT I
420 D(2,2)=D(2,2)*X(1)+1+K(7)*P1*X(3)/K9
430 D(2,1)=F(2,1)
440 D(1,2)=D(2,1)*X(1)/X(2)

```

```

450 F(2,1)=X(2)*(1+K(7)*P1*X(3)/K9)+F(2,1)*X(1)-Y(10)
460 D(2,3)=K(7)*P1*X(2)/K9
470 F(3,1)=F(1,1)-K(8)/(2*P1*X(3))+X(3)/2*(1+K(7)*P1*X(2)/K9)-Y(12)+Y(9)

480 D(3,3)=K(8)/(2*(P1*X(3))^2)+.5+D(2,3)/2
490 D(3,1)=D(1,1)
500 D(3,2)=D(1,2)+X(3)*P1*K(7)/(2*K9)
510 REM *****MATRIX OPERATION *****
520 FOR I= 1 TO N
530 F(I,1)=-F(I,1)
540 NEXT I
550 MAT E= INV(D)
560 MAT S= E*F
570 REM *****UPDATED VALUES *****
580 J1=0
590 FOR I= 1 TO N
600 Y=X(I)
610 X(I)=X(I)+S(I,1)
620 IF ABS((X(I)-Y)/X(I))<1E-4 THEN 640
630 J1=J1+1
640 NEXT I
650 REM*****
660 IF K1= 50 THEN 700
670 IF J1=0 THEN 700
680 GO TO 250
690 GO TO 250
700 A= 1
710 FOR I= 1 TO 6
720 A= A*K(I)*X(2)
730 Y(I)=A*X(1)
740 NEXT I
750 Y(7)=X(1)
760 Y(8)=X(2)
770 Y(13)=Y(8)
780 FOR I=1 TO 6
790 Y(13)=Y(13)+I*Y(I)
800 NEXT I
810 Y(14)=Y(10)-Y(13)
820 Y(11)=-LOG(P1*X(3))/LOG(10)
830 PRINT" AMMINES ROWS 1 TO 6,NICKEL IONS-7,FREE AMMONIA- 8"
840 PRINT" TOTAL NICKEL-9,TOTAL AMMONIUM-10,PH-11,TOTALSULPHATE-12"
850 PRINT" AMMONIA FREE+COMPLEXED-13, AMMONIUM ONLY -14"
860 PRINT" POSITIVE AND NEGATIVE CHARGES - 15,16"
870 PRINT" MASS BALANCES CHECK ON NICKEL& AMMONIA -17,18 "
880 PRINT" CHARGE BALANCE CHECK - 19"
881 PRINT

```

890 PRINT

900 $Y(15) = 2 * (Y(1) + Y(2) + Y(3) + Y(4) + Y(5) + Y(6) + Y(7)) + X(3) + Y(14)$

910 $Y(16) = 2 * Y(12) + K(8) / (K9 * Y(11))$

920 $Y(17) = F(1,1)$

930 $Y(18) = F(2,1)$

940 $Y(19) = F(3,1)$

950 FOR I= 1 TO 19

960 PRINT I;Y(I)

970 NEXT I

980 REM*****CHARGE AND MASS BALANCES CHECK*****

990 PRINT

1000 PRINT

1010 IF J1= 0 THEN 1030

1020 PRINT " NO CONVERGENCE" ,K1

1030 END

APPENDIX IV

```

10  REM ***** PROGRAM SIMULATES HYDROGEN REDUCTION *****
20  DIM X(7),D(7,7),E(7,7),S(7,1),F(7,1),Y(25)
30  DATA 3      ' ***** NUMBER OF EQUATIONS *****
40  DATA 1E-3,1.7E-1,1E-5  '** GUESS [NI++],[NH3]FREE,[H+]****
50  DATA .68,.25,-.43,-.63,-1.01,-2.02,5.5,-11.19 ' EQ. CONST. 200 C**
60  K9=1
70  P1=1
80  DATA .0008,.1791,.08957  ' ** [NI TOT],[NH4 TOT],[SO4 TOT] ***
90  DATA 10E-3,.159114,4.57918  ' [NI INIT],[NH4 INIT], PH INIT.**
100 READ N
110 MAT D=ZER(N,N)
120 MAT F=ZER(N,1)
130 MAT E=ZER(N,N)
140 MAT S=ZER(N,1)
150 FOR I= 1 TO N
160 READ X(I)
170 NEXT I
180 D(1,3)=0
190 FOR I= 1 TO 8
200 READ K(I)
210 K(I)=10*(K(I))
220 NEXT I
230 READ Y(9),Y(10),Y(12)
240 READ S1,S2,S3  '***** VALUES FOR ACCOUNT. ELECTRONEUTRALITY**
250 S3=10*(-S3)
260 KI=0
270 REM *****SIMULTANEOUS EQUATIONS *****
280 K1=K1+1
290 F(1,1)=1
300 A=1
310 FOR I= 1 TO 6
320 A=A*K(I)*X(2)
330 F(1,1)=F(1,1)+A
340 NEXT I
350 D(1,1)=F(1,1)
360 F(1,1)=X(1)*F(1,1)-Y(9)
370 F(2,1)=0
380 D(2,2)=0
390 A=1
400 FOR I= 1 TO 6
410 A=A*K(I)*X(2)
420 F(2,1)=F(2,1)+I*A
430 D(2,2)=D(2,2)+I*2*A/(X(2))

```

$$[D] \cdot [S] = [E]$$

$$S = E * F$$

```

440 NEXT I
450 D(2,2)=D(2,2)*X(1)+1+K(7)*P1*X(3)/K9
460 D(2,1)=F(2,1)
470 D(1,2)=D(2,1)*X(1)/X(2)
480 F(2,1)=X(2)*(1+K(7)*P1*X(3)/K9)+F(2,1)*X(1)-Y(10)
490 D(2,3)=K(7)*P1*X(2)/K9
500 F(3,1)=2*Y(9)+X(3)+K(7)*P1/K9*X(2)*X(3)-S3-S2-2*S1
510 D(3,1)=0
520 D(3,2)=K(7)*P1/K9*X(3)
530 D(3,3)=1+K(7)*P1/K9*X(2)
540 REM ***** MATRIX OPERATION*****
550 FOR I= 1 TO N
560 F(I,1)=-F(I,1)
570 NEXT I
580 MAT E= INV(D)
590 MAT S= E*F
600 REM ***** UPDATED VALUES *****
610 J1=0
620 FOR I= 1 TO N
630 Y=X(I)
640 X(I)=X(I)+S(I,1)
650 IF ABS((X(I)-Y)/X(I))<1E-4 THEN 670
660 J1=J1+1
670 NEXT I
680 REM *****
690 IF K1= 50 THEN 720
700 IF J1=0 THEN 720
710 GO TO 280
720 A= 1
730 FOR I= 1 TO 6

740 A= A*K(I)*X(2)
750 Y(I)=A*X(1)
760 NEXT I
770 Y(7)=X(1)
780 Y(8)=X(2)
790 Y(13)=Y(8)
800 FOR I= 1 TO 6
810 Y(13)=Y(13)+I*Y(I)
820 NEXT I
830 Y(14)=Y(10)-Y(13)
840 Y(11)=-LOG(P1*X(3))/LOG(10)
850 PRINT" AMMINES ROWS 1 TO 6, NICKEL IONS -7,FREE AMMONIA -8"
860 PRINT" TOTAL NICKEL -9,TOTAL AMMONIUM -10,PH -11 "
870 PRINT" TOTAL SULPHATE -12, AMMONIA FREE + COMPLEXED -13"
880 PRINT" AMMONIUM ONLY -14, POSITIVE AND NEGATIVE CHARGES -15,16"

```

```
890 PRINT" MASS BALANCE CHECK ON NICKEL & AMMONIA -17,18"
900 PRINT" CHARGE BALANCE CHECK -19, RATIO -20 "
910 PRINT
920 Y(15)=2*(Y(1)+Y(2)+Y(3)+Y(4)+Y(5)+Y(6)+Y(7))+X(3)+Y(14)
930 Y(16)=2*Y(12)+K(8)/(K9*Y(11))
940 Y(17)=F(1,1)
950 Y(18)=F(2,1)
960 Y(19)=F(3,1)
970 Y(20)=Y(13)/Y(9)
980 FOR I= 1 TO 20
990 PRINT I; Y(I)
1000 NEXT I
1010 REM *****CHARGE AND MASS BALANCE *****
1020 PRINT
1030 PRINT
1050 PRINT
1060 PRINT
1070 IF J1= 0 THEN 1090
1080 PRINT " NO CONVERGENCE" ,K1
1090 END
```

REFERENCES

1. Boldt, Joseph R. Jr., 1967, The winning of nickel, in Queneau, Paul, ed., Princeton, New Jersey, D. Van Nostrand Company, p. 141-493.
2. Queneau, Paul, ed., 1961, Extractive Metallurgy of Copper, Nickel, and Cobalt, p. 3-547.
3. Bush, P.D., Engle, L.F., Gates, E.H., and Vijayaraghavan, M.D., 1972, The pressure leaching-concentration-in-pulp process for nickel laterites and sulphides, in Evans, D.J.I., and Shoemaker, R.S., eds., International Symposium On Hydrometallurgy: New York, Am. Inst. Mining Metall. Petroleum Engineers Trans., p. 63-93.
4. Wadsworth, M.E., 1969, Reduction of metals in solution: Trans. Met. Soc. AIME, v. 245, p. 1381-1394.
5. Meddings, B. and Mackiw. V.N., 1964, The gaseous reduction of metals from aqueous solutions, in Wadsworth, M.E. and Davis, F.T., eds., Unit Process in Hydrometallurgy: New York, Gordon and Breach, p. 345-384.
6. Burkin, A.R., 1966, The Chemistry of Hydrometallurgical Processes, E. and F.N. Spon Ltd. London, p. 114-150.
7. Evans, D.J.I., 1968, Production of metals by gaseous reduction from solution-process and chemistry, in Advances in Extractive Metallurgy, The Institute of Mining and Metallurgy, London, p. 832-901.
8. Benson, B. and Colvin, N., 1964, Plant practice in the production of nickel by hydrogen reduction, in Wadsworth, M.E. and Davis, F.T., eds., Unit Process in Hydrometallurgy: New York, Gordon and Breach, p. 735-752.
9. Beketow: Comptes Rendus, 1859, vol. 48, p. 442.
10. Ipatiew, V.N., 1926, Precipitation de l'iridium de ses solutions par l'hydrogene sous pression: C.R. Acad. Sc., Paris, v. 183, p. 51-53.

11. Muller, Schlecht, Schubardt: U.S. Patent 2734821.
12. Tronev, V.G. and Bondin, S.M., 1948, Reduction of silver from nitrate solutions and reduction of solids from chloride and cyanide solutions with hydrogen under pressure: *Izv. Sekt. Platiny drug. blagor. Metall. Inst. Obshcheineorg. Khim*, n. 22, p. 187-193.
13. Forward, F.A., 1953, Ammonia pressure leach process for recovering nickel, copper, and cobalt from Sherrit Gordon nickel sulphide concentrate: *Canadian Inst. Mining Metallurgy Trans.*, v. 86, p. 363-370.
14. -----, 1954, Production and properties of high purity nickel powder: *Bull. Inst. Metals*, v. 2, p. 113-116.
15. Schaufelberger, F.A. and Roy, T.K., 1955, Separation of copper, nickel, and cobalt by selective reduction from aqueous solution: *Bull. Inst. Mining Metall.*, p. 375-381.
16. Schaufelberger, F.A., 1956, Precipitation of metals from salt solutions by reduction with hydrogen: *Mining Engineering*, v. 8, n. 5, p. 539-548.
17. Courtney, W.G. and Schaufelberger, F.A., 1961, Observations of the kinetics of the reduction of NiSO_4 in aqueous solutions, in St. Pierre, G.R., ed., *Physical Chemistry of Process Metallurgy*, New York, Intersciences, p. 1277-1290.
18. Mackiw, V.N., Lin, W.E., and Kunda, W., 1957, Reduction of nickel by hydrogen from ammoniacal nickel sulphate solution: *J. Metals*, v. 209, p. 787-793.
19. Peters, Ernest, 1972, Hydrometallurgy theory and practice, in *Colorado School of Mines: Symposium on Extractive Metallurgy*, Golden, Colorado, section V.
20. Wimber, R.T. and Wadsworth, M.E., *Trans. Met. Soc. AIME*, v. 221, p. 1141, (1961).
21. Kunda, W., Evans, D.J.I., and Mackiw, V.N., 1966, Effect of addition agents on the properties of nickel powders produced by hydrogen reduction, in Mansuer, H.R. and Roll, K.H., eds., *Modern Developments in Powder Metallurgy*: New York, Plenum Press, v. 11, p. 15-49.

22. Habashi, Fathi, 1970, Principle of extractive metallurgy, Gordon-Breach, New York, v. 2, p. 648.
23. Dobrokhotov, G.N. and Onuchkina, G.N., 1966, Reduction of metals in solution with hydrogen under pressure: Tsvet. Metall., v. 5, p. 72-78. }
24. Sicar, S.C. and Wiles, D.R., 1960, Hydrogen precipitation of nickel from buffered acid solutions: Am. Inst. Mining Metall. Petroleum Engineers Trans., v. 218, p. 891-893.
25. Nagai, Tadao, and Sato, Alasao 1972, An electrochemical aspect on pressure precipitation of nickel, in Evans, D.J.I., and Shoemaker, R.S., eds, International Symposium on Hydrometallurgy: New York, Am. Inst. Mining Metall. Petroleum Engineers Trans., p. 16-41.
26. Letowski, F. and Niemiec, J., 1966, Diagrams of electrochemical equilibria, E-pH at 25°C, Part II. Ni-H₂O-NH₃-H₂SO₄ systems, Roczniki Chemii Ann Soc. Chim. Pol., v. 40, p. 1149-1157.
27. Malmstrom, Rolf, 1969, Investigations of selective pressure precipitation of nickel and cobalt from aqueous solutions, Doctor Thesis, Bergsaw and Huttenwesen of the Rheinisch-Westfalischen Technischen Hochschule Aachen.
28. Latimer, W.M., 1952, Oxidation potentials, Second Edition, Prentice Hall. Inc., p. 185.
29. Bjerrum, J., 1957, Metal ammine formation in aqueous solution, Haase, Copenhagen.
30. Yatsimirskii, K.B. and Grafora, Z.M., 1952, Zh. Obshch. Khim., v. 22, p. 17-26.
31. Schultz, J.L., 1959, Thesis, Univ. Minnesota.
32. Criss, C.M. and Cobble, J.M., 1964, The thermodynamic properties of high temperature aqueous solutions, IV: Entropies of the ions up to 200°C and the correspondence principle, J. Am. Chem. Soc., v. 86, p. 5385-5390.
33. Robbins, R.G., 1968, The application of potentials - pH diagrams to the prediction of reactions in pressure hydrothermal processes, Stevenage: Warren Spring Laboratory, LR80(MS7).

34. Butler, James Newton, 1964, Ionic equilibrium - a mathematical approach, Addison-Wesley Publishing Co, Reading, Mass., p. 471.
35. Levich, V.G., 1962, Physiochemical Hydrodynamics, Prentice-Hall, Englewood Cliffs, New Jersey.
36. Smith, J.M., 1970, Chemical Engineering Kinetics, McGraw-Hill, New York, p. 273-399.
37. Levenspiel, Octave, 1967, Chemical Reaction Engineering: John Wiley and Son, New York, p. 384-476.
38. Blurton, K.F. and Riddiford, A.C., 1956, Shapes of practical rotating disc electrodes, J. Electroanal. Chem., v. 10, p. 457-464.
39. Pray, H.A., Schweickert, C.E., and Minnich, B.H., 1950, Solubility of hydrogen, oxygen, nitrogen, and helium in water, Indust. and Eng. Chem., v. 44, n. 3, p. 1146-1151.
40. LeGorrec, Bernard and Guitton, Jacques, 1971, Utilization de l'electrode tournante pour l'etude du mecanizme de l'electrodeposition du nickel: C.R. Acad. Sc., Paris, v. 272, p. 1784-1787.